Universidade de Aveiro
2020

ALEXANDRE MIGUEL MENDES PORTUGAL DA ROCHA

EFEITOS E APLICAÇÕES DE NANOMATERIAIS EM REMEDIAÇÃO AMBIENTAL

EFFECTS AND APPLICATIONS OF NANOMATERIALS IN ENVIRONMENTAL REMEDIATION

Universidade de Aveiro
2020

ALEXANDRE MIGUEL MENDES PORTUGAL DA ROCHA

EFEITOS E APLICAÇÕES DE NANOMATERIAIS EM REMEDIAÇÃO AMBIENTAL

EFFECTS AND APPLICATIONS OF NANOMATERIALS IN ENVIRONMENTAL REMEDIATION

Dissertação apresentada à Universidade de Aveiro para cumprimento dos requisitos necessários à obtenção do grau de Mestre em Eco-toxicologia e Análise de Risco, realizada sob a orientação científica do Doutor Marcelino Miguel Oliveira, Investigador Auxiliar do Departamento de Biologia da Universidade de Aveiro, e da Doutora Filipa Lourosa Sousa Investigadora auxiliar do Departamento de Química da Universidade de Aveiro

Dedico este trabalho à minha família, à Ana Sofia Joaquinito e à Snu.

o júri

presidente	Doutor Carlos Miguel Miguez Barroso Professor Auxiliar, Universidade de Aveiro
arguente	Doutor Nuno Gonçalo de Carvalho Ferreira Investigador Associado, Cardiff University
orientador	Doutor Marcelino Miguel Guedes de Jesus Oliveira Investigador Auxiliar da Universidade de Aveiro.

Agradecimentos

Quero expressar o meu profundo agradecimento a todas as pessoas que, com o seu altruísmo e notável conhecimento, me ajudaram a realizar este trabalho.

O meu primeiro agradecimento é dirigido ao meu orientador. Um especial e sentido agradecimento ao Dr. Miguel Oliveira, pela sua orientação, disponibilidade, pelos conselhos, pelo conhecimento e experiência que me transmitiu e por acreditar sempre em mim e nas minhas capacidades. Agradecer ainda a ajuda prestada no decorrer dos ensaios e por me ter ajudado a ultrapassar os obstáculos que, de uma maneira inevitável, se colocaram no nosso caminho. Muito obrigado Miguel!

Um agradecimento também à minha coorientadora Filipa Sousa pela cooperação e comentários feitos ao meu trabalho que certamente me ajudaram a melhorar o resultado final. Ainda agradecer por me ter recibo no seu laboratório de braços abertos a fim de se obter as nanopartículas usadas neste trabalho. Obrigado Filipa!

Um agradecimento também à Niedja Santos e à Gabriela Guedes. Obrigado Niedja por toda a ajuda, conhecimento e experiência transmitidos e disponibilidade nos ensaios de comportamento e desenvolvimento, sem ti não teria sido possível serem realizados com a brevidade e rigor como foram!
Obrigado Gabriela por toda a disponibilidade e auxílio na síntese e caracterização das nanopartículas e por me teres recebido no vosso grupo!

Agradecer ainda a todos aqueles que se cruzaram comigo e que de forma altruísta me ajudaram e aconselharam no decorrer dos ensaios e me transmitiram experiência e conhecimento. A todos um muito obrigado!

Agradecer ainda à minha família e amigos que com o seu apoio e presença assídua me ajudaram a encontrar as forças necessárias para a realização deste trabalho. Obrigado a todos!

Palavras-Chave

Nanotecnologia, Nanopartículas de SiO_2, Remediação ambiental, Comportamento, Desenvolvimento embrionário

Resumo

Apesar de muitas restrições e limites terem sido estabelecidos por várias entidades competentes, a contaminação e poluição de compartimentos aquáticos por metais de transição e poluentes orgânicos continua a ser um grande problema que está longe de estar resolvido. A verdade é que para além de se impedir a contaminação é necessário que haja um tratamento de locais já contaminados, tendo sido já proposta a remediação ambiental desses contaminantes como medida complementar às restrições já em vigor. À medida que o interesse e o progresso no campo da nanotecnologia se aprofundam, novos nanomateriais são lançados como parte integrante de produtos comerciais ou métodos industriais inovadores. Nanopartículas de sílica (SiO_2 NPs) e nanopartículas magnéticas (MNP) são exemplos de nanomateriais que têm sido empregados em inúmeras aplicações ao longo dos anos, que vão desde aplicações biomédicas a aplicações ambientais como adsorventes de poluentes orgânicos e iões metálicos em meio aquoso. Desse modo, as SiO_2 NPs e MNPs surgem como potenciais soluções altamente eficazes e especificas para os contaminantes alvo, sendo ainda de baixo custo, reutilizáveis e, com o devido tratamento, biocompatíveis. No entanto, apesar de ser já reportado o potencial de adsorventes à base de MNP e SiO_2 NPs, existe o risco e preocupação de poluição secundária nos vários compartimentos, colocando em perigo espécies aquáticas que neles habitem. Dessa forma, é de suma importância avaliar os efeitos desse tipo de nanomateriais nos organismos aquáticos e avaliar os potenciais riscos para os ecossistemas aquáticos. Este estudo teve como objetivo avaliar a toxicidade de acordo com o tamanho (80 e 150 nm) e concentração (0, 0.1, 1, 10, 100, 1000 $\mu g.L^{-1}$) de SiO_2 NPs em embriões de *Danio rerio* com foco em parâmetros de desenvolvimento embrionário e comportamentais. As SiO_2 NPs foram preparadas utilizando o método de Stöber, e caracterizadas através de microscopia eletrónica de varredura (SEM) e dynamic light scattering (DLS). O teste de embriotoxicidade foi feito com embriões de *D.rerio* em placas de 24 poços cobertas à temperatura de 26 ± 1.0 °C durante 96 h e com uma fase de luz entre 16–8 h. Às 24, 48, 72 e 96 hpf, foram medidos parâmetros como a taxa de sobrevivência, o tempo de eclosão e alterações morfológicas, através de um estereomicroscópio. A atividade locomotora foi medida colocando as placas individualmente no ZebraBox usando a configuração de monitorização durante períodos de 3 min de luz / 3 min de escuridão, e a avaliação dos efeitos comportamentais subletais foi realizada monitorizando o movimento de cada larva durante períodos alternados de luz, usados como estímulo (iluminação LED) e escuro (iluminação infravermelha) e registando distâncias e tempo de movimento para cada integração de 60 s durante ambos os períodos escuros e claros. Os resultados indicam que existem algumas tendências para as SiO_2 NPs com 80 nm de afetarem o desenvolvimento embrionário na concentração de 10 $\mu g.L^{-1}$, os efeitos incluindo eclosão precoce e perda de equilíbrio. A mesma concentração das SiO_2 NPs com 80 nm provocou também efeitos em termos comportamentais, diminuindo a atividade locomotora no escuro, aumentando os movimentos erráticos e aumentando a natação em zonas exteriores dos poços, constituindo um perfil de ansiedade dos peixes semelhante aos encontrados nos compostos ansiogénicos.

Keywords

Nanotechnology, SiO_2 Nanoparticles, Environmental Remediation, Behavior, Embryonic Development

Abstract

Although many restrictions and limits have been established by several competent entities, contamination and pollution of aquatic compartments by transition metals and organic pollutants remains a major problem that is far from being resolved. The truth is that, in addition to preventing contamination, there must be a treatment of already contaminated sites, and the environmental remediation of these contaminants has been proposed as a complementary measure to the restrictions already in force. As interest and progress in the field of nanotechnology deepens, new nanomaterials are launched as an integral part of commercial products or innovative industrial methods. Silica nanoparticles (SiO_2 NPs) and magnetic nanoparticles (MNP) are examples of nanomaterials that have been used in numerous applications over the years, ranging from biomedical to environmental applications such as in the adsorption of organic pollutants and metal ions in aqueous media. This way, SiO_2 NPs and MNPs emerge as potential highly effective and specific solutions for target contaminants, being still low cost, reusable and, with due treatment, biocompatible. Although the potential for adsorbents based on MNP and SiO_2 NPs has already been reported, there is a risk and concern of secondary pollution in the various compartments, endangering aquatic species that inhabit them. Thus, it is extremely important to evaluate the effects of this type of nanomaterials on aquatic organisms and to assess the potential risks to aquatic ecosystems. This study aimed to evaluate toxicity according to the size (80 and 150 nm) and concentration (0, 0.1, 1, 10, 100, 1000 $\mu g.L^{-1}$) of SiO_2 NPs in *Danio rerio* embryos with a focus in embryonic development and behavioural parameters. The SiO_2 NPs were prepared using the Stöber method, and characterized by scanning electron microscopy (SEM) and dynamic light scattering (DLS). The embryotoxicity test was performed with *D.rerio* embryos in covered 24-well plates at 26 ± 1.0 ° C for 96 h and with a light phase between 16 - 8 h. At 24, 48, 72 and 96 hpf, parameters such as survival rate, time to hatch and morphological changes were measured using a stereomicroscope. Locomotor activity was measured by placing the plates individually in the ZebraBox using the monitoring setting during periods of 3 min of light / 3 min of dark, and the assessment of sublethal behavioural effects was performed by monitoring the movement of each larvae during alternating periods of light, used as a stimulus (LED lighting) and dark (infrared lighting) and recording distances and movement time for each 60 s integration during both dark and light periods. The results indicate that there are some tendencies for SiO_2 NPs with 80 nm to affect embryonic development at a concentration of 10 $\mu g.L^{-1}$, the effects including early hatching and loss of balance. The same concentration of nanoparticles with 80 nm also caused effects in behavioural terms, decreasing locomotor activity in the dark, increasing erratic movements and increasing swimming in the outer areas of the wells, constituting an anxiety profile in fish, similar to those found after exposure to anxiogenic compounds.

Table of Contents

Chapter 1 – Environmental Pollution and Remediation

Chapter 2 – Toxicity of Silica and Magnetic Nanoparticles

Chapter 3 – Behavioural Effects of SiO_2 NPs in *Danio rerio* Embryos

Chapter 4 – Final Considerations and Future Directions

List of Tables

Chapter 1 – Environmental Pollution and Remediation

Chapter 2 – Toxicity of Silica and Magnetic Nanoparticles

Chapter 3 – Behavioural effects of SiO_2 NPs in *Danio rerio* embryos

List of Figures

Chapter 1 – Environmental Pollution and Remediation

Chapter 3 – Behavioural effects of SiO_2 NPs in *Danio rerio* embryos

List of Abbreviatures

AB25 Anionic dye acid blue 25
AR Aspect ratio
APTES 3-aminopropyltrimethoxy-silane
SOCl2 Thionyl dichloride
EDTA Ethylenediaminetetraacetic acid
BaP Benzo[a]pyrene
BC Biochar
BCA Activated biochar
CAT Catalase
CR Congo Red
CV Crystal violet
DDT Dichlorodiphenyltrichloroethane
DHA Dehydrogenase
Dpf Days post fertilization
EE2 17α-ethinylestradiol
EMA European Medicines Agency
EPA The United States Environmental Protection Agency
FCS Magnetic lignosulfonate
FeS NPs Biogenic iron sulphide nanoparticles
FMNP Fluorescein-loaded magnetic nanoparticles
FSNPs Fluorescent silica NPs
GPX Glutathione peroxidase
Hpf Hour post fertilization
HUVEC Human umbilical vein endothelial cells
LS Lignosulate
MAlgHT Magnetic-alginate-assisted hydrotalcite
MB Methylene blue
MCBB Magnetic chitosan beads
MCSHT Magnetic-chitosan-assisted hydrotalcite
MeHg Methylmercury
MG Malachite green
MNP Magnetic nanoparticle
Mpf Month post fertilization
MPPs Magnetic porous polymers
MPS (trimethoxysilyl) propyl methacrylate
MV Methyl violet
NFNCs Nickel ferrite nanocomposites
NM Nanomaterial
NP Nanoparticle
NW Nanoworms
OA Oleic acid
OCPs Organochlorine pesticides
OP Organic pollutants
PAEC Porcine aortic endothelial cells
PAH Poly-aromatic hydrocarbons
PAMAM Polyamide-amine
PCBs Polychlorinated biphenyls
PCDD Polychlorinated dibenzo-p-dioxins
PCDD/Fs Dibenzo-p-dioxins and furans
PCDF Polychlorinated dibenzofurans
PD Pharmaceutical drugs
PEG Polyethylene glycol
PEI Polyethyleneimine
PEO Polyethylene oxide
PF Phenosafranine
PHC Petroleum hydrocarbons
PLA Poly-L-lactic acid
PLGA Poly(lactic-co-glycolic acid)
PLL Ferumoxides–poly-L-lysine
PMA-g-PVA Poly(maleic anhydride)-graft-poly(vinyl alcohol)
POPs Persistent Organic Pollutants
PTME Potentially toxic metallic elements
PVA Polyvinyl alcohol
PVP Poly(vinylpyrrolidone)
QD Quantum dots
RhB Rhodamine B
RITC Rhodamine B isothiocyanate
ROS Reactive oxygen species
SA sodium alginate

SC Stockholm Convention

Si Silica
SiO_2 NP Silica Nanoparticle

SiO_2 Silica/Silicon dioxide
SiO_4 Silicate
SOD Superoxide Dismutase

SP Serpentine mineral

SPION Superparamagnetic iron oxide nanoparticle

STPs Sewage treatment plants

TAFLD Fatty liver disease

TASH Toxicant-associated steatohepatitis

TCC Triclocarban

TY Titan Yellow

TCS Triclosan

UNEP United Nations Environment Programme

VOC volatile organic compounds

WHO World Health Organization

WWTPs Wastewater treatment plants

Chapter 1 - Environmental Pollution and Remediation

1. Environmental pollution: A Review of The Most Problematic Pollutants

Environmental pollution is undoubtedly one of the biggest problems humans are currently facing, with soil and water masses receiving daily massive quantities of pollutants from diverse sources, potentially leading to their degradation. Pollutants may end up in environmental compartments from a point source (single and identifiable source), and from a non-point source, (many unidentifiable sources). Notwithstanding pollution raises serious ecological problems regardless the source as it can affect biota in their diversity and functionality and the ecosystem integrity [1–6]. Among the most problematic and ubiquitous pollutants in nature are the group of transition and post transition metals, hereby defined as potentially toxic metallic elements (PTME, based on the designation suggested by Pourret *et al.* (2019) [7]*),* including elements like cadmium, mercury or lead, and organic pollutants, such as pesticides, herbicides, fertilizers, products resulting from oil spills, industrial effluents, sewage, among others.

1.1. Potentially Toxic Metallic Elements

PTME can be defined here as the group of transition and post transition metals and metalloids with an atomic density above 4 g/cm^3 [8], [9], in which are included non-essential toxic elements, such as arsenic (As), cadmium (Cd), chromium (Cr), cobalt (Co), lead (Pb), mercury (Hg), nickel (Ni), and vanadium (V), as well as essential ones, such as copper (Cu), iron (Fe), manganese (Mn), and zinc (Zn). These metallic elements are known to be ubiquitous and capable of producing adverse effects in the environment and in living organisms, being that some are listed as priority pollutants to control by the USA Environmental Protection Agency (EPA) [9-11].

1.1.1. Pollution Sources and Environmental Behaviour

In almost all of the existent countries, surface and ground water may have been somehow contaminated or affected by PTME pollution, with the severity of contamination varying from site to site and being essentially controlled by local activities [11]. The main sources for PTME contamination are presented in Table 1, being that they enter in environmental compartments mainly through natural rock weathering, as many geological sites are natural reservoirs of these metallic elements, and anthropogenic sources, in which all man-made emissions or effluents derived from the extraction or production of metal containing products are included [11], [12]. Thus, it comes as no surprise that urban waterbodies usually possess higher levels of PTME than less urbanized areas that have fewer anthropogenic activities, even though PTME end up being present in points far from the source of pollution [11]. Furthermore, environmental conditions of deposition such as acidity, alkalinity, pH, adsorption, speciation and temperature also influence metals' solubility, mobility, availability, and accessibility. PTME exhibit a great tendency to deposit in sediments, a potential source of environmental contaminants, especially in limnology. In fact, lake sediments can hold up to 90% of metals in the lake ecosystem, that once engrossed and settled can desorb from sediments and get dissolved into the water column due to some physiochemical and biological processes. Thus, these sediments can serve as repositories and pose a threat of secondary source of pollutants [13].

Table 1. List of sources of environmental PTME contamination.

PTME	Sources
As	Semiconductors, petroleum refining, wood preservatives, animal food additives, coal power plants, herbicides, volcanic eruptions, mining, smelting
Cd	Geogenic sources, anthropogenic activities, metal smelting and refining, fossil fuel burning, application of phosphate fertilizers, sewage sludge
Cr	Electroplating industry, sludge, solid waste, tanneries, road traffic
Cu	Electroplating industry, smelting, refining, mining, biosolids, road traffic
Hg	Volcanic eruptions, forest fire, emissions from industries producing caustic soda, coal, peat, wood burning
Ni	Volcanic eruptions, land fill, forest fire, bubble bursting and gas exchange in ocean, weathering of soils and geological materials
Pb	Mining and smelting of metalliferous ores, burning of leaded gasoline, municipal sewage, industrial wastes enriched in Pb, paints
Zn	Electroplating industry, smelting, refining, mining, biosolids, road traffic

Source: [10], [12], [185]

1.1.2. Toxicity to Humans and Living Organisms

Increasing levels of PTME in water bodies increase the risks to the integrity of the ecosystems, as PTME can not only affect ecological functions of water including recycling and primary production of nutrients, but also the health of many species [11]. Moreover, when referring to PTME's toxicity, one must consider the bioaccumulation (accumulation of toxic substances in living beings) and biomagnification (build-up of concentration at higher trophic levels).

Effects of PTME in aquatic animals have been reported in organisms like fish exposed to waterborne PTME or contaminated food items. Among the reported effects are structural changes in the organs at cellular level, disruption of DNA, growth inhibition, reduced breeding potential in adult fish and even death. Furthermore, the accumulation of PTME in fish has been reported in the kidney, liver, gills, and muscle tissue [11]. For example, in the Copperbelt mining region (Zambia), stunted growth and changes in the taste of fish from polluted streams were attributed to heavy metal pollution, while multiple pathological changes in tilapia fish in the Kafue River have also been found [14]. Other organisms, such as species present in benthic environments, like worms, crustaceans and insects are greatly affected by contaminated sediments (e.g. alterations in their feeding habits and ultimately death), reducing the food availability for larger animals such as fish [11].

In plants, high concentrations of PTME may also provoke toxic effects, interfering with metabolic functions, leading to oxidative stress, inhibition of photosynthesis and respiration, growth reduction, chlorosis, degeneration of main cell organelles and leaf necrosis, which eventually may lead to death [9], [11].

There is also the concern that these pollutants have toxic effects in humans, especially through the most direct exposure pathway: oral ingestion. When inside an organism, they tend to bind to cellular structures and thus to damage the performance of essential biological functions. For instance, many of these PTME can easily bind to the sulfhydryl groups of several enzymes that take part in metabolic reactions, being that the “new” metal-enzyme complex usually leads to the loss of the catalytic activity of the enzyme. In the case of antioxidant enzymes, the loss of function leads inevitably to an increasing level of reactive oxygen species (ROS) and oxidative stress [9]. As part of the group of highly toxic metals are lead, mercury, cadmium, nickel, arsenic and chromium.

Table 2. Compilation of highly toxic PTME according to their exposure pathway, mode of action and overall toxicity.

PTME	Exposure pathway	Mechanism	Toxicity
Lead	Inhalation of contaminated dust particles and aerosols; ingestion of contaminated food and water	Disturbance of haemoglobin synthesis; inhibition of the activity of d-aminolaevulinic dehydratase; Interference with calcium and vitamin D metabolism and with the normal maturation of erythroid elements in the bone marrow	Mental retardation; attention deficit hyperactivity disorder; developmental disabilities; damage to the kidneys, liver, heart and skeleton
Mercury	**MeHg** ingestion of fish and seafood **Inorganic Hg** inhalation of air containing elemental mercury vapors; ingestion of inorganic mercury compounds	**MeHg Thus** Formation of stable complexes with proteins; oxidative stress; increase in the formation of ROS; damage to mitochondria; compromised nucleic acid and lipids integrity **Inorganic Hg** Affinity for sulfhydryl groups; bonding to sulphur-containing amino acids.	**MeHg** Blurred vision; hearing impairment; olfactory and gustatory disturbances; ataxic gait; clumsiness of the hands; dysarthria; somatosensory and psychiatric disorders; spongiosis of the cerebral cortex **Inorganic Hg** Carcinogenicity; damage to lungs and kidneys; high blood pressure; vomiting;

			diarrhea; skin rashes; eye irritation
Cadmium	Ingestion of contaminated food items	Oxidative stress; formation of reactive oxygen species, lipid peroxidation; increased production of inflammatory cytokines; disturbed phosphorus and calcium metabolism	Damages of respiratory, renal, skeletal and cardiovascular systems; carcinogenicity
Chromium	Occupational exposure (inhalation and dermal contact); ingestion of chromium contaminated food and water	Reduction of Cr(VI) by hydrogen peroxide (H_2O_2), glutathione (GSH) reductase, ascorbic acid, and GSH to produce reactive intermediates. Disruption of DNA, proteins, and membrane lipids	Carcinogenicity; slow healing ulcers; allergic dermatitis; damages of respiratory, renal, skeletal, reproduction, nervous and cardiovascular systems
Arsenic	ingestion of contaminated food and water	**As(V)** phosphate replacement in several reactions **As(III)** reaction with thiol groups in proteins and inhibition of their activity; binding to haemoglobin and leukocytes	Neurotoxicity; carcinogenicity; hyperpigmentation; hyperkeratosis; Blackfoot disease
Nickel	Inhalation; ingestion of contaminated food and water	Replacement of essential metal of metalloproteins, binding to catalytic residues of non-metalloenzymes; oxidative stress.	Allergic contact dermatitis; fibrosis, chronic bronchitis, impaired pulmonary function, and emphysema

Source: [15]–[21]

1.1.3. Potentially Toxic Metallic Elements in the Environment

In the last decades, devastating consequences for humans due to the presence of PTMEs in the environment have been reported. For instance, the first well-documented case of acute MeHg poisoning by consumption of highly contaminated fish and shellfish occurred in the Minamata bay (Japan, in 1953), because of the production of MeHg chloride as a by-product in the acetaldehyde plant of the chemical factory located there. This exposure resulted in acute adult cases of MeHg poisoning, inducing blurred vision, hearing impairment, olfactory and gustatory disturbances, ataxic gait, clumsiness of the hands, dysarthria, and somatosensory and psychiatric disorders, and in acute cases in children, with children born to mothers exposed to MeHg showing extensive spongiosis of the cerebral cortex [18]. Furthermore, in the Juzu River basin region in Toyama prefecture in central Japan, in the 1930s, was first noted a cadmium poisoning disease, known as itai-itai disease, being only identified as such in the 1960s.

The exposure resulted from the pollution of rice fields with the liquid wastes of the Kamioka mine, owned by the Mitsui Mining & Smelting Company Ltd (Mitsui Kinzoku). Many patients with itai-itai disease suffered from pneumonia, renal diseases and gastrointestinal diseases that contributed to increased mortality risk [20], [21].

To limit the risks for living species, humans and the environment, many countries have legislated limits regarding the PTME concentrations in drinking, waste, and surface waters (lakes, rivers, seas), food and animal food [9], [23–25]. EPA established regulatory limits for Hg, Cd, and Pb in drinking water, this being 2 ppb, 5 ppb and 15 ppb, respectively, whereas the WHO recommended the safe limits for Hg, Cd, Pb, Cr and Ni in wastewater to be 0.0019, 0.003, 0.01, 0.05, 0.02 ppm, respectively, and in soils for agriculture are 0.05, 0.003, 0.1, 0.1, 0.05 ppm, respectively [9], [16], [23–25]. Nevertheless, contaminated waters with PTME exist all over the world, in particular in countries like Turkey, China, India, and Bangladesh where the concentrations in surface water exceed established limits in many regions [25]. In a recent study, it was found that in the Edku lagoon, one of the northern coastal lagoons in Egypt, PTME such as Fe, Mn, Zn, Cu, Pb, Cd and Hg are present at concentrations that violate the maximum established limits by the WHO [26], while in another study in Nairobi industrial area the levels of Hg in wastewater are a clear public health concern [16]. Nkwunonwo *et al*. (2020), state that, in Nigeria, PTME concentrations found in some varieties of fish, fruits, and vegetables in different regions of the country show significant potential health risk as the PTME may be above the permitted limits [17]. In addition, Abdeldayem (2020) performed a research in Dakahlia region using water, urine, and blood samples of 50 individuals (aged between 29 and 63), reporting levels of Fe, Mn, Pb, and Cd, higher than the permissible limits established by the WHO for the water. A positive correlation was found between the metals for both water and urine samples and the high levels of serum creatinine, aspartate transaminase, and haemoglobin, supporting the idea that the water may represent a public health risk and the existence of a source of pollution that increases these PTME’s concentration, probably anthropogenic [27]. In Pakistan, a qualitative and quantitative study on lead contamination in soil along two major roadsides (Motorway M-2 and National Highway N-5) of Thokar Niaz Baaig (TNB) in Lahore, and adjoining areas of the Hudiara drain was performed, revealing that the amount of Pb was within the permissible limits of the WHO. However, a serious health issue may exist for the people consuming the crops of this contaminated area, due to the biomagnification effect of lead through the food chain [28]. A research, focused on soil contamination and the health risks around a mining area in Henan Province of China, showed that the local inhabitants face high potential health risks due to intake of Cd and Pb via consumption of leafy vegetables and other agricultural products [29]. A high ecotoxicological risk was reported for the Keenjhar Lake, in Sindh, Pakistan, due to high contamination of PTME's [13] while in a study performed in Meghna Ghat industrial area, in Bangladesh, only 10% of the samples presented acceptable levels, according to water quality index [30].

1.2. Organic Pollutants

Organic pollutants, defined as pollutants containing carbon covalently bonded with other compounds, are of considerable environmental concern known for their potential toxic or carcinogenic nature [11]. Among these organic pollutants are detergents, disinfection by-products, food processing waste, insecticides and herbicides, petroleum hydrocarbons and lubricants, fuel combustion by-products, volatile organic compounds, chlorinated solvents, dyes, perchlorate (from personal care products) and pharmaceutical drugs and their metabolites [11], most of these substances are of anthropogenic origin [31].

1.2.1. Persistent Organic Pollutants (POPs)

Some of the organic pollutants (OP) are persistent in nature thus classified as persistent organic pollutants (POPs). POPs are mostly man-made chemical products intended to be used in agriculture (e.g. pesticides) and in industry (e.g. polychlorinated biphenyls, hexachlorobenzene, brominated compounds, perfluorinated compounds), but can also be unintentional by-products resulting from industrial processes, or from waste incineration (e.g. dioxins and furans) [31], [32].

Table 3. Stockholm convention list of POPs marked for elimination, restriction and to stop unintentional production

Elimination	Restriction	Unintentional Production
Aldrin* Alpha hexachlorocyclohexane Beta hexachlorocyclohexane Chlordane* Chlordecone Decabromodiphenyl ether* Dieldrin* Endrin Heptachlor* Hexabromobiphenyl	dichlorodiphenyltrichloroethane (DDT)* Perfluorooctane sulfonic acid, its salts* Perfluorooctane sulfonyl fluoride*	Hexachlorobenzene Hexachlorobutadiene Pentachlorobenzene Polychlorinated biphenyls Polychlorinated dibenzo-p-dioxins and dibenzofurans Polychlorinated naphthalenes

Hexabromocyclododecane*
Hexabromodiphenyl ether*
Heptabromodiphenyl ether*
Hexachlorobenzene*
Hexachlorobutadiene
Lindane*
Mirex*
Pentachlorobenzene
Pentachlorophenol and its salts and esters*
Polychlorinated Biphenyls*
Polychlorinated naphthalenes*
Short-chain chlorinated paraffins*
Technical endosulfan*
Tetrabromodiphenyl ether*
Pentabromodiphenyl ether*
Toxaphene

*possess exemption regarding their application
Source: [34]

In response to the environmental challenge posed by these pollutants, the United Nations Environment Programme (UNEP) Stockholm Convention (SC) on POPs that was adopted and opened for signature in May 2001 and entered into force on 17 May 2004, prohibited the use of some of the most dangerous ones, listed in Table 4. Initially, the list included the Dirty Dozen [polychlorinated biphenyls (PCBs), polychlorinated dibenzo-p-dioxins (PCDD), polychlorinated dibenzofurans (PCDF), dichlorodiphenyltrichloroethane (DDT), hexachlorobenzene, mirex, toxaphene, aldrin, dieldrin, endrin, chlordane, heptachlor], but additional chemicals were included in the SC, that currently include 26 chemicals listed under global control, even though some exemptions were made for some compounds regarding certain applications. For example, the use of nine organochlorine pesticides was banned in agriculture in most countries worldwide but an exception was made for the use of DDT in disease vector control [34–36].

However, despite the efforts made in the SC to mitigate the sources and contamination by these OP, even banned POPs, remain in the environment. This is not only due to their persistence nature but also to inappropriate management of decommissioned products, like old electrical equipment containing polychlorinated biphenyls (PCBs). In fact, some better-known examples of POPs, including DDT and PCBs, are often referred to as ‘legacy’ POPs because present-day contamination is mainly a ‘legacy’ of past emissions.

Notwithstanding, there are still direct emissions of some POPs, such as polycyclic aromatic hydrocarbons (PAHs) that are released into the atmosphere through vehicle exhaust fumes [36], [37].

One of the main concerns is that POPs can be transported through long distances by natural atmospheric and oceanic processes, reaching and contaminating regions where they have never been used or produced [37], [38]. As volatile substances, POPs evaporate into the air in warm regions of the globe, being then transported by air currents up to cold regions and in mountainous regions where they condense, turning the polar regions areas where the concentration of POPs is expected to be high [31]. Thus, they can exert effects in organisms and humans in regions far away from their source. Like PTME, POPs can, in aquatic ecosystems, be adsorbed to sediments and suspended particles in the water column, and bioaccumulate in organisms and throughout the food web. Since POPs, and particularly PCBs, polychlorinated dibenzo-p-dioxins and furans (PCDD/Fs) and organochlorine pesticides (OCPs) can be stored in fatty tissue, there is the risk of reaching exposure concentrations above threshold health effect levels in many species, posing a risk to not only wild animals but also humans [32], [37–39]. Some of the known effects of POPs in wild species include smaller brain size and neurotoxicity, behaviour changes, endocrine disruption, carcinogenesis, cell and tissue damage and reproductive problems [37]. POPs are also known as potential endocrine disruptors compounds and there are evidences that correlate the development and manifestation of chronic diseases to exposure to these organic pollutants. In addition, available oxygen in water can be reduced by the presence of organic pollutants, which in turn affects water organisms by causing reduced fitness or even death from asphyxiation. The effects may also include increased water turbidity (especially by petroleum-related wastes), which reduces the available light for photosynthetic organisms. The presence of OP in the soil is also problematic as it can serve as reservoirs of these POPs which may lead to significant secondary emissions from soil. Studying the extent of the contamination in soil worldwide is, thus, of great importance [33]. Human exposure to POPs may thus occur through various means, that include air, water and soil, through contact with consumer products and also through diet [37]. Many toxic effects like hormone-dependent cancers, ovarian disfunction in women, reproductive disorders in metabolic disorders (including type 2 diabetes), obesity, blood poisoning, eyes and skin irritation, increased susceptibility to infectious diseases and effects in IQ or autism have been linked to exposure to POPs [11], [37]. They are also known to cause teratogenic effects leading to neurodevelopmental disorders and subclinical brain dysfunction [39].

As part of POPs, oil spills, defined as unintentional or deliberate release of crude liquid petroleum oil and other derived oils into the marine ecosystem, are the cause of widespread environmental damage impacting fauna and flora, raising life-threatening concerns to marine biodiversity, compromising the growth and development of organisms living in the water body and causing economic destruction. It has been estimated that more that 5.7 million tons of crude oil have been spilled between 1970 and 2017 [40]. These oil spills have a negative impact on tourism and recreational activities of the affected areas. In addition, the mixture of petroleum hydrocarbons (PHCs), volatile organic compounds (VOCs), poly-aromatic hydrocarbons (PAHs) and other combustible products in petroleum can cause serious health impacts in humans such as asthma, inflammation, irritation, dizziness, headache, cardiovascular disorders, kidney and liver damage, nervous and immune effects and reproductive and developmental deformities [40].

1.2.2. Pharmaceutical Drugs

Another group of organic pollutants that raises concern regarding their presence in the environment is the group of pharmaceutical drugs (PD). Pharmaceuticals can be classified into numerous therapeutic groups, including anti-inflammatories, antibiotics, antipsychotics, antihypertensives, antidiabetics, antihistamines, lipid regulators, anticonvulsant, β-blockers, stimulants and statins. The environmental impact of these substances is nowadays recognized worldwide, as they are designed to be robust and stable, having a polar and non-volatile nature, which make their degradation in the aquatic environment difficult [41]. Notwithstanding, its use and manufacture cannot be avoided and, therefore, a sound risk assessment of their presence in the environment is a highly needed key issue. Environmental contamination in aquatic media by these drugs usually occurs due to patient use, drug production and formulation, and improper disposal, being typically found at concentrations from sub-ng/l to a few µg/L and even in the order of mg/L [42]. Even though some of these pharmaceuticals are eliminated or transformed via biological or chemical pathways during the wastewater treatment processes, others remain relatively unchanged, being introduced into surface water and resulting in the exposure of aquatic organisms to these compounds [43]. A compilation of some PD already found in the environment is presented in Table 4. PDs like diclofenac, sulfamethoxazole, metoprolol, β-estradiol, carbamazepine, clofibric acid, erythromycin, norfloxacin, ciprofloxacin, propylphenazone, paracetamol, diazepams, Ibuprofen, methyl 2-(4-isobutylphenyl)propanoate, 17α-ethinylestradiol (EE2), antimicrobial agents like triclosan (TCS) and triclocarban (TCC), have already been found in wastewater treatment plants (WWTPs), surface water, groundwater, sewage treatment plants (STPs), rivers and lakes across the world [44], [45]. Drugs are also found in the soil media, which happens mainly through the application of sewage sludge to land, leaching from landfills, or irrigation of arable land with treated or untreated wastewaters [42]. In India, the Environment Ministry classifies pharmaceutical manufacturing as a "red category" activity due to its hazardous waste [46].

Table 4. List of some PDs contaminants in the environment according to their therapeutic group

Therapeutic Group	**Compounds**		
Anxiolytics	Alprazolam	Lorazepam	Zolpidem
	Diazepam		
Analgesics	Propylphenazone		
Antibiotics	Azithromycin	Ciprofloxacin	Clarithromycin
	Erythromycin	Sulfamethoxazole	Norfloxacin
	triclosan	triclocarban	
Lipid Regulators	Bezafibrate	Gemfibrozil	Simvastatin
	Clofibric Acid		
Antiepileptic	Carbamazepine		
Selective Serotonin Reuptake Inhibitors	Citalopram	Desmethylcitalopram	Desmethylsertraline
	Escitalopram	Fluoxetine	Norfluoxetine
	Paroxetine	Sertraline	
B-Blockers	Metoprolol		
Anti-Inflammatories	Diclofenac	4-Hydroxydiclofenac	Ibuprofen
	Naproxen	Paracetamol	4-Aminophenol
	Methyl 2-(4-isobutylphenyl) propanoate		
Hormones	Estrone	17β-Estradiol	17α-Ethinylestradiol

Sources: [44], [45], [47]

According to the European Medicines Agency (EMA) legislation, before a PD approval for commercialization, the lack of ecotoxicological risk must be demonstrated. However, PDs still possess the potential to cause adverse ecotoxicological effects, even at sublethal concentrations, with the risk, emphasized by their biologically active nature and ubiquitous occurrence, being far from being fully understood [47]. The major concern is that PD can potentially exert toxicity in non-target organisms, when present at concentrations on the ng.L^{-1} level. In addition, most PDs exist as a complex mixture which can interact synergistically or through antagonism. Furthermore, there may also be toxic effects of transformed products or metabolites resulting from the metabolization of certain drugs.

The design of pharmaceuticals must allow the release of the active ingredient in the target site to give the required pharmacological effect, and, thus, they must possess lipophilic properties to pass through the cell membranes of the body. While for some drugs metabolism is considered as a deactivating process for drugs, for others, known as 'prodrugs', metabolism is required to release the active parent compound and produce a pharmacological effect. This leads to the creation of metabolites that are often more persistent, have more tendency to bioaccumulate, and can even be more toxic than the parent compounds, as in the cases of paracetamol and amitriptyline, which are partly metabolised to highly reactive compounds [41], [44]. Adsorption to sediments is also for PD a factor influencing toxicity. Higher sorption to sediments may result in an apparent reduction of bioavailability and toxicity to organisms present in the water column, but increases the risks for benthic invertebrates present in those sediments, creating a reservoir that may later be released into the water column [47]. Thus, the assessment of the potential adverse effects in aquatic biota must take these aspects in consideration. Among the reported toxic effects of pharmaceuticals are inhibition of ATP-dependent Na/K-ATPase activity, increased oxidative stress, alterations to kidney, gills, liver and intestines and behavioural changes [41]. The majority of the available studies address sublethal or lethal effects, mainly measuring the levels of specific biomarkers. Angeles *et al*. (2020), suggests that measuring variations in animal behaviour, is also very important, as it can serve as a sensitive indicator of toxicity, providing a more complete ecological assessment, particularly for contaminants known to influence behaviour at low concentrations such as antidepressants [43].

1.2.3. Dyes

In addition to the concern regarding contamination by PDs and POPs, dyes are also being contaminants of environmental concern. Dyes are complex unsaturated aromatic compounds with characteristics like intense colour, solubility, substantivity and fastness [48]. Synthetic organic dyes form a large group of compounds differentiated by their chromogen structure, solubility or stability in fabrics. There are two main dye classification systems. One, ranks dyes based on their chromogens (acridine, anthraquinone, azo, azine, diphenylmethane, indigoid, methine, nitro, nitroso, oxazine, phthalocyanine, thiazine, triphenylmethane and xanthene dyes whereas the other regarding their application purposes (acid, basic, direct, disperse, fibre, reactive, vat, and mordant) [49].

In fact, and due to their wide applicability, the global consumption of dyes and pigments reaches values close to 7×10^5 tons per year, with the textile industry demanding around two-thirds of all the world production [50]. According to the Confederation of Indian Textile Industry, textile mills are discharging approximately 1.2×10^3 million litres per day of coloured wastewater without proper treatment into the environment [48]. The release of dyes to environmental compartments is mainly related with the cleaning of the dye tank following the preparation of the dye bath and draining of the dye bath after the dyeing process is complete. Also, the inefficiency in the colouring generates large amounts of dyes residues, which are directly released into water bodies [48],[50]. Wastewaters from industries of paint and varnishes, plastics, ink and cosmetics industries are also a great contamination source as they use a large number of organic dyes and their intermediates in industrial processes [50]. Furthermore, the tendency of dyes to be recalcitrant in aerobic environments leads to their bioaccumulation in sediments and soil and transportation to public water supply systems [51]. Thus, the release of effluents without proper treatment into water systems (e.g. river, lakes) can pose an ecotoxicological risk to aquatic fauna and flora, affect the aesthetic nature of the surroundings and alter odour and taste of water [48].

Adverse effects have been reported associated with a decrease of light and water re-oxygenation capacity and physiological effects of these substances, some of which carcinogenic. In fact, these pollutants have been associated with changes in protozoan colonization rate, phytoplankton species composition and primary productivity as well as with alterations in macroinvertebrates' behaviour and community systems. Dyes can also interact with other contaminants for example altering the availability and toxicity of PTME to fishes [48],[52]. In humans they can cause allergies, dermatitis, skin irritations, cancers, mutations, disorders of the central nervous system and inactivation of enzymatic activities [53]. Usually, acute toxicity of dyes occurs through oral ingestion and inhalation, especially by exposure to dust. Notwithstanding, the greatest concern and potential long-term hazard to human health is their genotoxicity. This is especially true for the class of complexed metal dyes, which are widely used in textile industry, have up to 13 years of half-life and present in their composition nickel, copper, cobalt and chromium [51]. However, almost every class of dyes can cause adverse effects, being some listed in Table 5.

Table 5. Description of some dyes and their toxicity according to their chromophore-based class

Dyes	Description	Class
Congo Red	Very toxic and carcinogenic; difficult to biodegrade	Azo
Brilliant Cresyl Blue	Cationic dye; scientific and industrial applications; adverse effects on human beings and microorganisms	Oxazine
Rhodamine 6G	High fluorescent; biotechnology applications; water-soluble; photostability; undesirable effects on microorganisms and humans	Xanthene
Rhodamine B	Water-soluble; used in textiles and food industry; toxic if ingested; Irritation to the skin, eyes, respiratory tract	Xanthene
Phenol red	Water-soluble; stable in weak acid and air; pH indicator; carcinogenic; inhibits the growth of renal epithelial cells; provokes skin, eyes and respiratory tract irritation; mutagenic and lethal to muscle fibers	Triphenylmethane
Alizarin Red S	Water-soluble; textile industries; inhibits the activity of cytochrome p450 isozymes in humans	Anthraquinone
Methylene blue	Used to dye cotton, paper, wools, silk leather, and coating of paper stock; causes cyanosis, vomiting, increase in heartbeat, quadriplegia, shock, jaundice, and tissue necrosis in humans	Thiazine
Crystal violet	Recalcitrant dye; used in textile processing; biological stain in veterinary and human medicine; persistent; carcinogen and mutagenic; causes tumour growth in some fishes; hepatocarcinoma, reticular cell sarcoma in various organs, such as the vagina, uterus, ovary and bladder, hardened gland adenoma and ovarian atrophy in rats; chemical cystitis, irritation of the skin and digestive tract, respiratory and renal failure in humans	Diphenylmethanes
Malachite green	Used in fish farms to prevent fungal infections; carcinogen for human urinary bladder; tumorigenic in laboratory animals; converted into leucomalachite green, persisting in tissues of edible fish; contact with eye and skin causes irritation with pain and redness	Triphenylmethane
Azure-B	Textile industry; able to intercalate with the helical structure of DNA and duplex RNA; inhibitor of monoamine oxidase A	Thiazine

Disperse Red 1	Textile industry; mutagenic potential; increases the frequency of micronuclei in human lymphocyte and human hepatoma (hepg2) cells; induces DNA adducts	Azo
Disperse Orange 1	Induces DNA damage; cytotoxic effect in hepg2 cells	Azo
The Sudan I dye (Solvent Yellow 14)	Used in many industrial segments; enzymatically transformed into carcinogenic aromatic amines;	Azo
Basic Red 9	Textile, leather, paper and ink industries; carcinogenic potential in humans; high environmental toxicity; potential for allergic dermatitis, skin irritation, mutations; local sarcomas and tumours in the liver, bladder, mammary glands and hematopoietic system in rats	Triphenylmethane

Source: [49], [51]–[54]

1.2.4. Organic Solvents

Organic solvents are also contaminants of great concern. Organic solvents are widely used in many industries such as in manufacturing paints, glues, resins, varnishes, dyes, adhesives, shoes, plastics, rubber, synthetic fibres, pesticides, cosmetics, degreasers, polyurethane foam, and others, being also widely applied as liquid media in multiphase bioprocess operations [55], [56]. The common organic solvents are generally classified as aliphatic hydrocarbons, aromatic hydrocarbons, cyclic hydrocarbons, halogenated hydrocarbons, amines, ketones, esters, ethers, aldehydes and alcohols [56], [57] and the main concern regarding them, associated with their volatility, lipophilicity/hydrophobicity and flammable nature, is their toxicity towards process operators and the environment [55], [57], [58]. Lipophilicity is an issue as it influences the distribution of solvents to various body parts, entering easily in the brain. Since organic solvents are highly volatile, the air is an effective exposure pathway making the lungs a primary organ to be affected [57]. Furthermore, lipophilic compounds need to be converted to a water-soluble form, which in some cases might result in a metabolite more toxic than the original compound [57]. Acute poisoning by organic solvents can eventually lead to the death of the individual, being a higher exposure associated with inflammation of the respiratory tract and haemorrhage in the lungs. In addition, these pollutants may interfere in the process of red blood cells proliferation and cause significant damage to red blood cells causing aplastic anaemia [59]. Furthermore, effects of organic solvents in humans also include toxicant-associated fatty liver disease (TAFLD), toxicant-associated steatohepatitis (TASH), hepatic cirrhosis and cancer (mainly hepatocellular carcinoma and acute myeloid leukemia/exposure to benzene) [56]. Also of concern are the solvent mixtures as they may potentiate the individual effect of the solvents. An example of that is the mixture of toluene with xylene, where that the latter inhibits the toluene metabolism and increases its toxicity [56].

Adverse effects in bacteria have also been reported, provoking progressive damage to cell walls and membranes of bacteria, compromising the structural and functional integrity of the cell [55], [58].

2. Environmental Remediation

Many efforts have been made in the past years to reduce the emission to the environment of many pollutants, especially those mentioned above. However, it is becoming clear that an additional effort is required to remove the contaminants that are already present in many waterbodies and soil. Thus, in order to maintain good quality of soils and waters and meet the requirements of living organisms regarding their quality, efforts have been made to develop technologies that are easy to use, sustainable and economically feasible [60]. Approaches involving photooxidation, phytoextraction, electrocoagulation, electrodialysis, irradiation, membrane separation, ultrafiltration, forward osmosis, ion exchange, precipitation, coagulation/flocculation, microorganisms and plants have been applied to remove different water pollutants from aquatic systems [11], [61]. However, many of the strategies developed so far possess several limitations and drawbacks such as high costs, inefficiency in low pollutants concentrations, long cycle times, reagents and energy consumption and chemical sewage sludge formation, making critical research of new technologies to be applied in the remediation of these contaminants [61].

The capture and degradation of contaminants are processes needed but challenging. Thus, remediation through adsorption using nanoparticles began to arise as a very promising method [62]. Adsorption can be described as a physicochemical phenomenon by which an adsorbate, gas or liquid molecule, concentrate on the surface of another substance (the adsorbent). However, both bioabsorption and bioadsorption dimensions are involved in terms of sorption mechanism. While absorption is the incorporation (integration) of a material in one state into a material with another state, adsorption is a physical bonding in which sorbate interacts with a surface of a sorbent resulting in sorbent-sorbate interface [61]. The great value of this approach is that it is an eco-friendly, economic and efficient technique for minimizing the levels of different contaminants in water resources to the acceptable limits, recommended by different regulations globally [61]. In addition, it permits the recycling of the biowastes, being that their utilization in their native and/or modified forms can directly participate in wastes minimization [61]. Therefore, the adsorption method might be an effective approach to remove several types of pollutants in water and soil. Carbon-rich materials such as activated carbons, carbon nanotubes, biochar, carbon fibres and graphene oxides, but also zeolites, silica, magnetic nanoparticles, clay-based nanocomposites, among others, have already been used in water purification (Figure 1) [61]. Nanomaterials have the greatest potential in remediation, supporting the research nanotechnology in remediation.

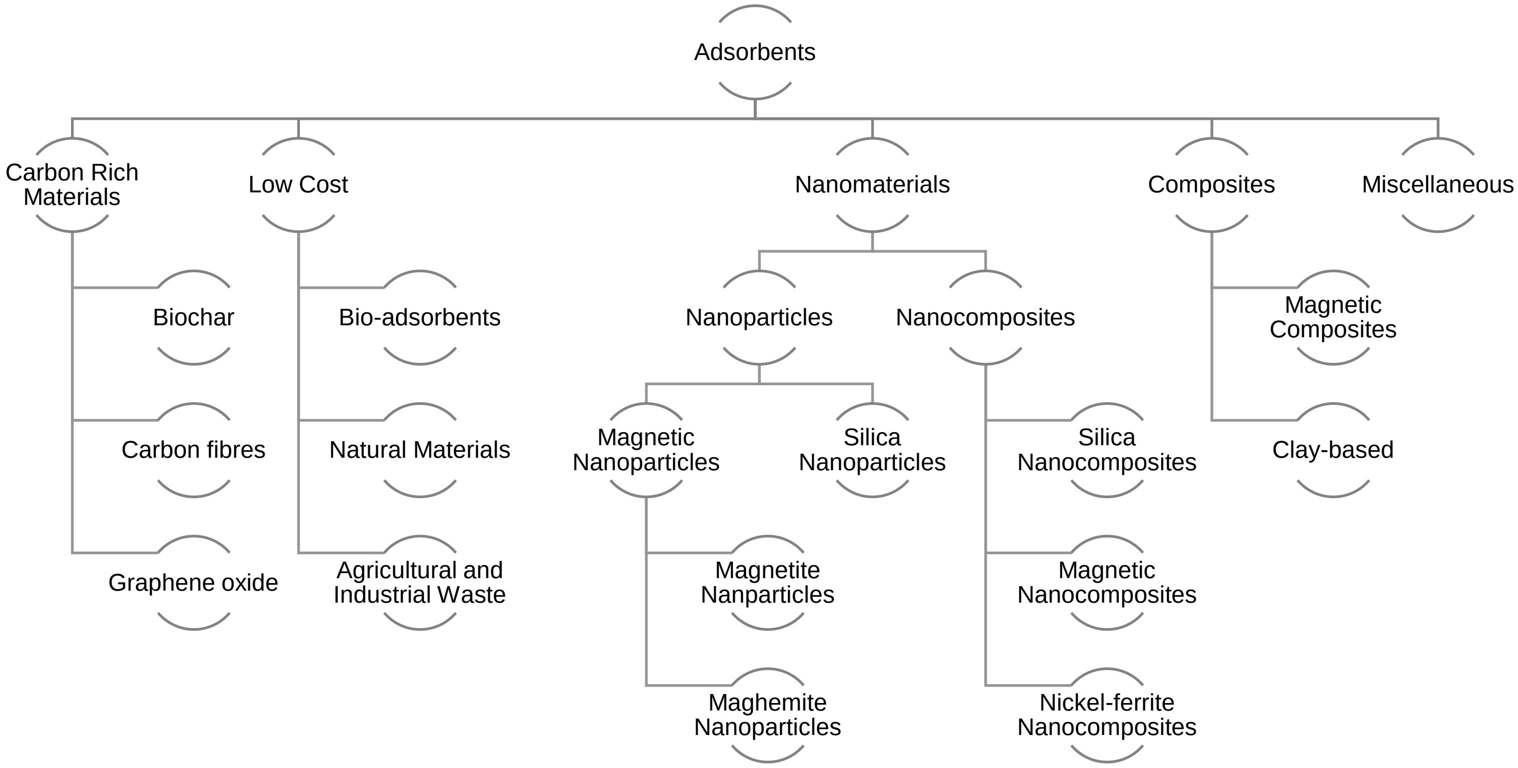

Figure 1. Classes of some adsorbents already reported in the literature for environmental remediation.

3. Nanotechnology

Nanomaterials (NM) are at the leading edge of the intriguing and rapidly developing field of nanotechnology, a field that has been considered to be the "next industrial revolution" by some authors, already exerting a great impact on society, industry, economy, and life in general [64–66]. Nanotechnology is a field referring to every technology and science operating on a nanoscale range and to scientific principles and new properties that are found when operating in this range. In its turn, NM can be defined as a material having one or more external dimensions in the nanoscale or which is nanostructured [66] while a nanoparticle (NP) can be described as a small elemental ensemble having at least one dimension below 100 nm, that behaves as a whole unit and presents novel electrical, chemical, structural, optoelectronic and magnetic properties, not exhibited in the characteristic bulk material, attributed to quantum effects, larger surface area, and self-assembly [65], [68–71].

3.1. General Applications of Nanomaterials

An important class of NPs comprises those made of inorganic materials. Nowadays, thanks to the progresses in nanocrystal synthesis, most NP can be generated with great control over their size, shape, and composition. Because of this, and due to their physicochemical properties, NP have been increasingly utilized not only in areas like biomedical research for purposes of diagnosis, imaging, and drug delivery, but also in environmental solutions for water and soil remediation. In addition, several types of inorganic NP are multifunctional by nature, this being NPs that are capable of accomplishing multiple objectives such as imaging and therapy or performing a single advanced function through incorporation of multiple functional units [71], which raises their value even further. Nanotechnology and NM's have already been applied in commercially available products (e.g. textile industry to make clothing stain and odour resistant, and in the electronic industry in several products like the LCD screens) [63].

3.2. Nanomaterials in Environmental Remediation

Following the wide application of nanotechnology in various fields in recent decades, the NPs potential to be applied in the removal of pollutants are gaining recognition. NPs possess unique surface chemistry, can be functionalized with functional groups and thus used to target specific pollutants for efficient remediation, but can confer, through tuning of their physical properties (such as size, morphology, porosity, and chemical composition) additional advantageous characteristics that directly affect the performance of a material for contaminant remediation [63], [73–75]. Another very important feature is the high mobility of NPs in solution, an advantage as the whole solution volume can be quickly scanned with small amounts of NPs [5]. It is very important that the NPs used for remediation are not pollutants themselves, which makes biodegradable materials preferable [62]. For this matter, NPs such as magnetic nanoparticles (MNPs) and silica nanoparticles (SiO_2 NPs) are promising adsorbents of organic and inorganic pollutants because of their advantageous magnetic properties and adsorption capabilities. Some methods have even been developed as a combination of several different NPs, gathering specific desired properties from each of its components [62].

3.3. Magnetic Nanoparticles

As an integral part of the promising group of NPs, the MNPs have gained a major role in various fields. The term ‘magnetic nanoparticle’ refers to magnetically responsive spherical nanocrystals of 10–20 nm of size, usually with a Fe^{2+} and Fe^{3+} core typically surrounded by dextran or polyethylene glycol (PEG) molecules [65], [75]. MNPs exhibit magnetic properties very different from the ones of bulk materials, determined by many factors like the chemical composition, type and the degree of defectiveness of the crystal lattice, particle size and shape, morphology, interaction of the particle with the surrounding matrix, and the neighbouring particles [70]. By changing the NP size, shape, composition, and structure, it is possible to control, to a certain extent, the magnetic characteristics of the material [70]. However, even though MNPs possess several virtues, that also include their low operating cost, rapid separation and convenient recycling, it is critical that their biological effects are studied in depth [71], [77–79]. In order for them to be effective and biocompatible in their applications, an elaborate and crucial design process is required [79].

3.3.1. Design of Magnetic Nanoparticles

The NP design is a complex process stated as crucial for their successful application requiring several steps such as (1) depositing of metal layers onto a supporting NP core, (2) modification of the biocompatible polymer used to stabilise the NP and (3) use of different linkers [65], [80]. Thus, a successful design requires careful selection of the magnetic core and surface coating material, as the first mainly determines the MNPs abilities related with application efficiency, and the second modulates the interaction of these NPs with the surrounding environment [80], [82–84].

3.3.1.1. Size and Shape

The size and shape of a MNP are other aspects to take in consideration, and, even though size control is difficult to achieve, numerous MNPs shapes, such as spheres, quasi-spheres, octahedrons, and cubes, have already been reported [84].

The role of the size and shape has been studied in more extent for biomedical applications, but they are also crucial features that may influence the toxicity to living beings and efficiency in remediation processes. Thus, it has already been reported that smaller MNPs possess an advantage in degradation of water contaminants [85]. Magnetite suspensions with 9 nm of diameter size reacted more towards carbon tetrachloride than those with 80 nm of size [85]. Regarding shape, it has been reported that spherically shaped MNPs circulate *in vivo* for a few hours and can usually enter the cells [86], that anisotropic NPs can avoid bioelimination better than spherical NPs [79], [87], [88], but have dimensions too big to exhibit any effect, being also extensively agglomerated [87]. In addition, nanostructures circulation time in mice blood seems to increase with an increase in the length-to-width aspect ratio of the nanostructures [86], as Park *et al*. (2008), enlightened with nanoworms (NW), better able to evade the organism's elimination processes [88]. Spherical MNPs may not be easily subjected to differential functionalization of the surface, causing changes in the surface properties of the NP [89] unlike nanotube shaped structures which appear an attractive alternative as their inner and outer surfaces can be modified differently [90–92].

3.3.1.2. Core Material

The selection of the core material of a MNP must take into account that all the magnetic cores in a sample should have uniform shapes (monodispersed), the core should be crystalline and smaller than a critical size to consist of only one magnetic domain ensuring the superparamagnetic behaviour with zero remnant magnetization. This phenomenon is the key requirement for all biomedical and environmental applications, allowing the particles to be dispersed and concentrated in water samples, solutions *in vitro* or in blood circulation *in vivo*, without forming clusters and to respond to an applied magnetic field [92]. Materials with highly saturated magnetization, such as transition metals or metal oxides, are usually considered to enhance the effectiveness of many applications [93]. Thus, several materials including iron oxides, cobalt, nickel and manganese ferrites, metals and metal alloys such as Fe and FePt, have been developed. Even though pure metals, such as cobalt, possess the highest saturation magnetization, they are extremely toxic and sensitive to oxidation, being unlikely to be used as biomedical or environmental agents without appropriate surface treatment [78], [93], [94]. In its turn, iron oxide-based materials such as magnetite (Fe_3O_4) and maghemite (γ-Fe_2O_3), which are not as sensitive to oxidation as pure metals, can also give a stable magnetic response, posing as valuable options [93]. Superparamagnetic iron oxide nanoparticles (SPIONs) are a class of MNPs generally composed of γ-Fe_2O_3 or Fe_3O_4, biocompatible and able to suffer biodegradation [95]. They do not retain any magnetism after removal of magnetic field [96] which, in addition to the characteristics mentioned before, have made SPIONs prominent candidates for *in vivo* applications in the biomedical context and in remediation of contaminated environmental samples [93]. Magnetic alloy NPs composed of two or three different kind of metals like FeCo, FePt and NiCu, are another class of materials that can be used as magnetic cores, being the FePt the most prominent due to its chemical stability and high magnetic anisotropy [92].

3.3.1.3. Surface Modification

The surface of the NPs mentioned above usually needs to be coated/modified, a crucial process for several reasons: On the one hand, surface coatings are important to prevent the leaching of toxic components of NPs [94], and to improve their biocompatibility properties [97]. On the other hand, they are used to disperse the MNPs into suitable solvents, forming homogeneous suspensions, called ferrofluids [96] and to counter the great tendency for NPs with hydrophobic surfaces to agglomerate [80], [93], [94], [96]. In fact, without surface coatings, MNPs that have hydrophobic surfaces and large surface area to volume ratio, due to hydrophobic interactions between the particles, will almost certainly lead to the formation of large clusters. These clusters, in its turn, exhibit strong magnetic dipole–dipole attractions between them and show ferromagnetic behaviour leading to further aggregation of the NPs [96]. Thus, surface modification not only increases the stability of MNPs by preventing agglomeration and oxidation but also provides the possibility for further functionalization [98].

Coating with Inorganic Metal Oxides

The coating of the surface of MNPs can be performed using inorganic metal oxides, for example, SiO_2. The choice of SiO_2, to coat MNPs arises from the fact that it is an acidic oxide with stable chemical properties, good biocompatibility, low toxicity, acid resistance, and high temperature resistance. In addition, SiO_2 can also shield the electrostatic repulsion of MNPs and is rich in hydroxyl groups, which will take part in the formation of covalent bridges between MNPs and targeting molecules or ions [92], [98], [99]. Besides silica, the use of noble metals like Gold (Au) and silver (Ag) to coat MNPs have already been reported [92], [99] as they possess stable chemical properties, biocompatibility, resistance to oxidation, and corrosion, and can prevent the formation of free radicals [92], [98].

Coating with Organic Molecules

Organic molecules, such as oleic acid (OA) or citric acid, can also be found in the literature as coating agents for the MNPs [98]. OA is nontoxic in blood and high soluble in organic solvents, and MNPs modified with OA usually exhibit good biocompatibility, dispersibility, and stability as a result of the reduction in the surface energy by OA [98]. Coating the MNPs with citric acid, on the other hand, benefits from the fact that electrostatic repulsive forces among citric acids can protect the NPs from aggregation, resulting in increased dispersibility [98]. Carbon-based materials are another example of surface coatings that can be employed, known to enhance stability in contact with air, solvents and in a wide pH range, biocompatibility and dispersion in aqueous media [95], [99]. However, their ferromagnetic behaviour usually grants them a higher tendency to aggregate [95].

Coating with Polymers

Polymers (including natural polymers) can also be used as coating agents for MNPs. Among these are: (1) carbohydrates, such as chitosan and dextran [82], [92], [93], [100], [101], (2) proteins, such as albumin and RGD (Arg–Gly–Asp) [82], [102], [103], and (3) lipids, such as polymeric micelles, the latter forming MNPs-embebbed polymeric micelles (MNP-PMs), an important sustained-release carrier for hydrophobic drugs [104], [105]. Chitosan coatings are widely used in the fields of waste treatment, health care, and food hygiene because they give the MNPs many advantageous properties which include nontoxic, hydrophilic, biocompatible, and biodegradable nature [92], [98]. The number of amino groups promotes the attachment of MNPs with targeting molecules, thus expanding their potential applications [98]. Dextran coatings, in its turn, can prevent aggregation and are reported to possess good biocompatibility [92], [98].

Some of these natural polymer coating materials, however, are water soluble and lack mechanical strength, besides tending to be porous and to show non-selective adsorption. Therefore, many synthetic polymers have been designed to face some of the limitations of the natural ones. Poly(vinylpyrrolidone) - PVP, polyethylene glycol (PEG), polyethylene oxide (PEO), polyvinyl alcohol (PVA), poly(lactic-co-glycolic acid) (PLGA), polyethyleneimine (PEI), and poly-L-lactic acid (PLA) are some examples of synthetic polymers that have been synthesized. For example, PEI is a common non-viral vector for gene delivery as it can electrostatically bind to DNA to form a PEI/DNA complex. PEI-coated MNPs can also be applied in targeted drug delivery, magnetic hyperthermia and environmental remediation [98]. PEG, on the other hand, is a hydrophilic, nontoxic polymer, with a long linear chain that can be prepared with a wide range of terminal functional groups. Also, PEG coated MNPs have excellent stability and solubility in aqueous dispersions and in physiological media, increasing the blood circulation time of MNPs [92]. In its turn, coating of MNPs surface with PVA has been suggested to enhance the colloidal stability of ferrofluids. However, it has been reported that PVA irreversibly binds on MNPs surface which can influence different properties of NPs such as particle size, zeta potential and surface hydrophobicity [92]. Nonetheless, even though synthetic polymers have better mechanical strength than many natural polymers, possessing characteristics like being hydrophilic, nontoxic, some coatings cannot fully prevent the corrosion of the magnetic core and are difficult to further functionalize [94], [98].

3.3.2. Environmental Remediation using Magnetic Nanoparticles

In the past years, efforts have been made to remove PTME and organic pollutants from water and soil. However, many adsorbents, even though highly efficient in water treatment, are not easy to separate from wastewater streams during treatment processes. Therefore, the application of magnetic adsorbents in water treatment could come as an effective, safe, and low-cost way to separate these suspended adsorbents in wastewater. Magnetic nanoparticle possess magnetic properties that makes them interesting, such as the fact that they are superparamagnetic and thus, can be easily separated from the aqueous media by an external magnetic field. However, the fact that they possess high adsorption capacity to many analytes due to their large specific surface area is no less important. In recent studies, MNPs coated with hydrophobic materials, have been successfully applied to detect and remove metal ions as well as organic compounds [61], [76], [106].

3.3.2.1. Potentially Toxic Metallic Elements

In the past years, the need to develop techniques for the continuous removal/immobilization of PTME from contaminated soils and water bodies became clear. Accordingly, the use of MNPs to perform environmental remediation of these contaminants has been studied. This process usually depends on the physical and chemical properties of adsorbents including surface area, porosity, and sorption parameter including pH, initial concentration, adsorbent dose, and contact time. Wang *et al*. (2018) used recyclable multifunctional magnetic mesoporous silica nanocomposite encapsulated with CdTe QDs (QDs-MMS) to detect, adsorb and efficiently remove Hg(II) from aquatic media. The nanocomposites not only recognized Hg(II) through ratiometric fluorescence but also showed good separability and reusability, superparamagnetic properties and a great adsorption capacity. The authors were able to recover up to 97.6 % of mercury at pH values between 5.0 and 9.0 and were able to reuse the adsorbent in up to 8 cycles. However, the use of CdTe quantum dots (QD) in a shell of magnetic mesoporous silica nanocomposites is far from ideal as cadmium containing QDs have been reported to exert toxicity *in vitro* and *in vivo* [65], [67], [107–113]. In another study, Zhu *et al*. (2018), studies the adsorption performance of magnetic porous polymers (MPPs) with poly(styrene-divinylbenzene), stabilized by amine-functionalized Fe_3O_4 NPs (Fe_3O_4-NH_2), towards Pb^{2+} and Cd^{2+} from aqueous solutions. The study reported that the adsorption of Pb^{2+} and Cd^{2+} relies on ionic strength and solution pH, with best results at pH 5.5. The adsorption mechanism of Pb(II) and Cd(II) is mainly associated with electrostatic attraction and cation-π (aromatic ring) interactions in a spontaneous endothermic process. The MPPs maintained a high degree of structural stability after 5 cycles of regeneration [113]. Nicola *et al.* (2020) assessing the efficiency of silica-coated magnetic nanocomposites ($MNPs35@SiO_2$) for Pb(II) removal from aqueous solution found that they can be good adsorbents towards Pb(II) especially at values between pH 4 and 6 and that adsorption occurs at the surface of the material, in a spontaneous and endothermic process. The authors theorized that hydrogen bonding or electrostatic attraction is involved in the adsorption process in a process mainly governed by chemisorption. This adsorbent may be reutilized maintaining good efficiency [114]. In another study, Plohl *et al.* (2019), analysed the efficiency of a derived-polyethyleneimine linked to silica magnetic nanocomposites ($MNPs@SiO_2@GOPTS$-bPEI) nano adsorbent on Cu^{2+} removal from an aqueous environment, highlighting the importance of surface modification and pH in the adsorption process. At pH 6 that the primary groups of bPEI are deprotonated, which is an important feature for the adsorption of Cu^{2+} by this nano adsorbent. In fact, the author's proposed adsorption mechanism involved NH/NH_2 functional groups, adsorbing Cu^{2+} by reducing its electronic state through donation of free electron pairs. In addition, this adsorbent maintained its efficiency even after several cycles [115]. Bao *et al*. (2017), also studied the influence of amino groups in the removal of Hg^{2+} and Pb^{2+} from aqueous samples by employing mercaptoamine-functionalised silica-coated MNPs (MAF-SCMNPs) adsorption. The study revealed that adsorption of the metals is likely to occur by chelation through the amine group and ion exchange between metal ions and thiol functional groups on the surface of the adsorbent. The maximum adsorptions were observed at pH 5–6 for Hg(II) and 6–7 and Pb(II). In line with previous reports already mentioned, the adsorption process was endothermic, spontaneous at high temperatures and effective even after 5 cycles [116]. In their turn, Villa *et al*. (2019) used thiol-functionalized ($Fe_3O_4@MPTMS$) MNPs for remediation of Pb(II) ions from water samples. The authors not only removed more than 91% of Pb(II) ions, but were also able to recollect more than 99% of the MNPs from the sample media, with the adsorbent still efficient after 5 cycles [117]. Using poly(vinylbenzyl chloride) grafted Fe_3O_4 NPs (Fe3O4@PVBC), Yilmaz *et al*. (2019), obtained a high removal efficiency of Pb(II) (97.07%) at pH 5.88, in a process that remained efficient after 5 cycles [118].

Yu *et al*. (2020), used biogenic iron sulphide nanoparticles (FeS NPs) for aqueous Cr(VI) removal demonstrating that the 30–40 nm in size, displayed a high removal rate, 94.6 ± 1.3%, and large removal capacity at pH 3 making them promising candidates for the removal of these metal ions [119]. Also working in Cr(VI) remediation from water, Verma *et al*. (2020) used nickel ferrite nanocomposites (NFNCs) to treat the effluent of the electroplating industry. Their results showed that within 1 hour it is possible to adsorb up to 91.6% of Cr(VI), with maximum uptake obtained at pH of 2 and 40 °C, due to electrostatic attraction and chemisorption. Also, the adsorbents can be employed repeatedly in the wastewater treatment, being observed an efficiency loss of less than 30% after 7 reutilization cycles. The authors suggested that these adsorbents are also capable of removing Cu, Zn, and Ni from the electroplating effluent, and thus possessing a tremendous potential for remediation of metals ions in wastewater effluents [120]. In another work related to Cr (VI) removal from water, Gallo-Cordova *et al*. (2019) used three MNPs with different surface charges, namely MNP, TEOS@MNP (negative charge) and APTES@TEOS@MNP (positive charge), to that purpose. The MNPs without functionalization and the APTES@TEOS@MNP, at pH~2.5, obtained an efficacy of almost 100% whereas TEOS@MNP barely removed the metal ions, showing that the adsorption increases with increasing the NPs' positive surface charge. The efficacy of the adsorbents was not significantly altered after 7 cycles, which goes in favour of their reusability [121].

Alchouron *et al*. (2020), aimed to develop an economic, viable, and sustainable adsorbent for arsenic-free water, for biochar remediation of aqueous As(V), raw biochar (BC), activated biochar (BCA), raw Fe_3O_4 nanoparticle-covered biochar (BC-Fe), and activated biochar covered with Fe_3O_4 nanoparticles (BCA-Fe). BC-Fe proved efficient allowing a complete removal of arsenate, at concentrations found in the environment which was not significantly affected by pH between 5 and 9. This adsorbent also displayed a good adsorption performance in the presence of competing ions (nitrates, sulphates, chlorides, fluorides). The adsorption process was endothermic for the four adsorbents and the capacities rose with the increase of temperature which in the case of the BC-Fe and BCA-Fe adsorbents might be due to iron leaching followed by precipitation of iron arsenate insoluble products [122]. Ayub *et al*. (2020), reported the use of magnetic chitosan beads (MCBB), with chitosan as matrix and magnetite (Fe_3O_4) nanoparticles as reinforcement, to remove As(III) and As(V) species from water systems, obtaining at pH 6.7 99.5 and 99% efficiency in the removal of As(V) and As(III), respectively. The impregnation of Fe_3O_4 NPs increased the adsorption capacity by exposing the -OH and -NH2 functional groups, important in arsenic binding. However, despite the promising results, the regeneration and recycling of this adsorbent still needs to be improved as the regenerated composite loses efficiency after some cycles and might cause secondary pollution [123]. Also working in the remediation of As(V) were Zeng *et al*. (2020), studying the use of two types of MNPs prepared with iron-containing water treatment residues, cMNP and iMNP, in the removal of As(V) from water reporting that at pH 6.6 over 90% of As(V) could be easily removed with efficacy maintained during consecutive cycles of regeneration [124].

Liu *et al*. (2020), an innovative study, proposed a novel type of poly(maleic anhydride)-graft-poly(vinyl alcohol) comb polymer functionalized magnetic nanoparticles as an efficient adsorbent with stimuli-responsive reversible adsorption/desorption behaviour for the removal of metal ions, namely Ag(I), Ni(II), Cd(II), Pb(II) and Co(II). Two novel nanocomposites, namely comb-shaped poly(maleic anhydride)-graft-poly(vinyl alcohol) (PMA-g-PVA) functionalized MNPs (Fe_3O_4/PMA-g-PVA) and linear poly(vinyl alcohol) (PVA) functionalized MNPs (Fe_3O_4/PVA) were synthesized. The adsorption rates of Fe_3O_4/PMA-g-PVA towards Ag(I), Ni(II), Cd(II), Pb(II) and Co(II) reached 92.15%, 89.2%, 90.16%, 83.56% and 84.52% respectively, being 5.1, 6.2, 5.4, 6.1 and 6.0 times respectively higher than those of Fe_3O_4/PVA. An increase of the solution pH from 4 to 7 increases in the adsorption which shows a pH-responsive mechanism. A good sustainability and facile reusability was also reported as even after 5 consecutive cycles there was over 80% uptake efficiency [125]. A novel magnetic calcium-rich biochar (MCRB) obtained by loading Fe_3O_4 NPs on crab shell-derived biochar was synthesized and characterized by Chen *et al*. (2020), for remediation of waters contaminated with metal like As(III) and Pb(II). The removal of the metal ions had an optimal pH of 6 with a strong ability for removing arsenic and lead, and competitive and synergistic effects on the simultaneous removal of the metal ions (i.e. As(III) addition enhanced Pb(II) removal due to the formation of the Pb(II)-As(III)-FeO ternary surface complex with As(III) as the bridging molecule, while the presence of Pb(II) suppressed As(III) removal, being the competitive complexation of the two metals with biochar responsible for that [126]). In another study, Wang *et al*. (2020), studied the simultaneous removal of Pb (II), Cd(II) and Cu(II) by a functionalized magnetic mesoporous NM (Fe_3O_4-HBPAASA) with high density of amino, imine and salicylic acid groups, to explore the use of different functional groups simultaneously to remove metal ions in a mixture. The authors observed that the adsorbent showed good adsorption towards the metal ions at pH 8 and 25ºC, and adsorption capacity could be ranked as Cu(II)>Cd(II)>Pb(II). The adsorption process was an exothermic reaction and, for each metal, a different adsorption mechanism was involved. Thus, while the main mechanism for Cd(II) adsorption involved to the complexation of amino salicylic acid, the Pb (II) removal was mainly related to the amino groups remaining on the surface of the adsorbent and the adsorption of Cu(II) because of the amino salicylic acid and terminal amino groups. This and the fact that this adsorbent exhibits good regeneration performance after 5 cycles, are arguments supporting the potential of these multifunctional adsorbents to adsorb various components in a mixture [127]. In their turn, Tetteh *et al*. (2020), presented the effects of MNPs on an inorganic coagulant (alum) and their coagulation performance for the removal of turbidity, colour, and metal ions from a textile effluent. Upon 50 minutes of magnetic exposure, at pH 4 and a concentration of coagulant of 45 mg.L^{-1}, a removal percentage of 85% in terms of turbidity and colour, and above 75% for Al, Cu, Zn, Fe and Mg was obtained [128].

Wang *et al*. (2020), applied flower-like molybdenum disulphide decorated with iron oxide NPs (MoS_2/Fe_3O_4) for the removal of Hg(II) and Pb(II) ions from aqueous environment, observing not only a good adsorption capacity towards the metal ions at pH 5, but also that the favourable adsorption capacity, selectivity and recyclability mainly originates from the strong Hg^{2+}/Pb^{2+} - S^{2+} bonding interactions. The practical application of the adsorbent in realistic lead-acid battery industry wastewater and Pb(II)-contaminated soil was also studied, and a removal efficiency of 99.63% for wastewater and 57.15% for soil was obtained, unveiling some of the potential of the MoS_2/Fe_3O_4 NPs in PTME removal from real water and soil samples [129].

Even though studies in soil media can be considered scarce, this media has already attracted research. Lin *et al*. (2019), worked on the immobilization of cadmium in polluted soils by phytogenic iron oxide NPs, which proved efficient specially with an increase in the concentrations of iron oxides, soil pH and dissolved organic carbon (DOC) under both oxic and anoxic conditions. The mechanisms of Cd immobilization may involve the formation of insoluble hydroxides at elevated pH, ligand complexation with Cd by biomolecules released from PION and co-precipitation of Cd during iron oxides formation [130]. The ability of nano-magnetic $MnFe_2O_4$ to immobilize Cr(VI) in the soil, was tested by Eyvazi *et al.* (2019) who reported that the leachability of Cr(VI) was reduced from 70.95% to 4.22%, chromium bioavailability to humans was reduced from 86.76% to 4.42% and the plant bioavailability reduced from 83.72% to 5.53% [131]. The feasibility of using MNPs coated with PEI to remediate radioactive contaminated soil by separating Cs-contaminated clay from the soil was evaluated by Kim *et al.* (2020). The study reported that MNPs provide an efficient way to remediate Cs from the soil, with PEI coating enhancing the adsorption of charged clay minerals, by increasing the quantity of functional amino groups available for adsorption. The process resulted in a Cs soil removal efficiency of 81.7% and, thus, in a satisfactory reduction of radioactivity and waste volume in the soil [132].

In another relevant study in this matter, Baragaño *et al*. (2020), employed commercial magnetite NPs to immobilize As and organic pollutants, mainly PAHs, from a polluted soil. This co-contamination remediation study showed that by using MNPs, depending on the MNPs concentration, it is possible to reach As immobilization (42.5% - 92.3%). Furthermore, a decrease up to 89% of PAH content in soil can be observed. The use of these adsorbents does not appear to compromise soil integrity as no negative effects on soil parameters (soil pH, electrical conductivity) nor increase on Fe availability were found [133].

Table 6. Efficacy of MNPs based adsorbents towards heavy metal ions in aqueous and soil media based on their adsorption capacity, % of metal ions removal, sample pH and reusability.

Adsorbent	Pollutant	Sample Media	Adsorption Capacity (mg/g)	% Removal	pH	Reusability (Cycle Nº)	Reference
QDs-MMS-Rh6G	Hg(II)	Aqueous media	17.7	97.6 - 102.3	6.0 - 9.0	8	[51]
Fe3O4-NH2	Pb(II)	Aqueous media	257	-	5.5	5	[58]
	Cd(II)		129				
MNPs35@SiO2	Pb(II)	Aqueous media	14.9	-	4.0 - 6.0	-	[59]
MNPs@SiO2@GOPTS-bPEI	Cu(II)	Aqueous media	143	-	6.0	>4	[60]
MAF-SCMNPs	Hg(II)	Aqueous media	355	-	5–6	5	[61]
	Pb(II)		292		6–7		
FeS MNPs	Cr(VI)	Aqueous media	565.6	94.6 ± 1.3	3.0	-	[62]
NFNCs	Cr(VI)	Aqueous media	129.87	91.6	2.0	7	[63]
BC	As(V)	Aqueous media	256	~40	5.0 - 9.0	-	[64]
BCA			217	~40			
BC-Fe			457	~100			
BCA-Fe			868	~25			
MCBB	As(III)	Aqueous media	73.69	99.0	6.7	5	[65]
	As(V)		79.49	99.5			
Fe3O4/PVA (1)	Ag(I)	Aqueous media	5.4	18.1	4.0 - 7.0	5	[66]
	Ni(II)		3.48	14.4			
	Cd(II)		5.69	16.7			
	Pb(II)		13.59	13.7			
	Co(II)		3.15	14.1			
Fe3O4/PMA-g-PVA (2)	Ag(I)		16.83	92.2			
	Ni(II)		13.62	89.2			
	Cd(II)		21.52	90.2			
	Pb(II)		30.77	83.6			
	Co(II)		8.82	84.5			
MCRB	As(III)	Aqueous media	15.8	93.0	6.0	6	[67]
	Pb(II)		62.4	86.0			

Fe3O4-HBPAASA	Pb(II)	Aqueous media	165.46	~90	8.0	5	[68]
	Cd(II)		88.36				
	Cu(II)		136.66				
CMC	Al(II)	Aqueous media	-	>75	4.0	-	[69]
	Cu(II)						
	Zn(II)						
	Fe(II)						
	Mg(II)						
MoS2/Fe3O4	Hg(II)	Aqueous media	428.9	~99	5.0	5	[70]
	Pb(II)		263.6				
PION	Cd(II)	Soil media	-	22.0	>8	-	[71]
MnFe2O4	Cr(VI)	Soil Media	-	87.9 - 96.8	-	-	[72]
MNPs@PEI	Cs	Soil media	-	81.7	<6	-	[73]
Fe3O4	As	Soil media	-	42.5 - 92.3	<7	-	[74]
	PAHs			89			

3.3.2.2. Organic Pollutants

As many studies confirmed, MNPs are great candidates to perform remediation of organic compounds. For instance, Fu *et al.* (2020) synthesized and applied a novel polyethyleneimine (PEI)-grafted chitosan (CS) core-shell (called as Fe_3O_4/CS/PEI) MNPs in phosphate adsorption in water. The study reported that the maximum adsorption was obtained at 25ºC and pH 3, involving as main mechanism of adsorption electrostatic attraction. A preferential adsorption of phosphate in the presence of other excess anions including chloride, nitrate, carbonate, and sulphate was found. More than 90% of phosphate was desorbed after the use of a NaOH solution and the adsorption remained efficient after 5 cycles [134]. In another study, performed by Karthikeyan *et al.* (2020), MNPs decorated GO-CMC (Fe3O4@GO-CMC) composite beads were used for the remediation of phosphate and nitrate from aqueous medium. The best removal efficiency was obtained at pH 6, within 40 minutes, in a process that involved electrostatic interaction, ion-exchange and surface complexation between the pollutants and the adsorbent. These MNPs showed good reusability maintaining their efficacy even after 6 cycles [135].

Recyclable $CoFe_2O_4$/sawdust composites able to remove oils from water surface (up to 11.5 times of the sawdust weight) under magnetic field were developed by Gan *et al.* (2016). The obtained oil-absorption composites could be cleared up and re-used for water–oil separation at least 10 times [136]. Iron oxide NPs coated by silica and 3- (trimethoxysilyl) propyl methacrylate, (Fe3O4@SiO_2@MPS), were assessed by Kamgar *et al*. (2020), as an oil absorbent of two crude oils (with 19.6 and 35 degree of API) with magnetic properties, was performed testing two different. Both oils were completely adsorbed, with NP adsorption capacity up to 48.5 times its weight, specially at higher pH values [137]. Chitosan (CS)-grafted MNP (Fe_3O_4@APFS-G-CS MNPs) were tested to treat addition emulsified oil wastewaters to treat (Lü *et al*. (2020)). The study showed that, while synthetic Fe_3O_4 MNPs show negligible demulsification effect, under both acidic and neutral conditions, APFS coated MNPs and further functionalized MNPs with CS exhibit good demulsification effect via electrostatic attraction. Under alkaline conditions and under a magnetic field, MNPs could overcome electrostatic repulsion and exhibit certain demulsification effect whereas. Under both acidic and neutral conditions, these MNPs could be recycled up to 7 cycles without showing significant loss in demulsification efficiency [138]. In another study, Soares *et al.* (2017), as proof-of-concept as potential adsorbents for oil remediation, used a magnetic nanosorbent composed of magnetite NPs functionalized with chitosan hybrid siliceous shells in a magnetically assisted removal of non-polar organic solvents, namely toluene, cyclohexane, chlorophorm and n-heptane. They found that the MNPs removed quickly and efficiently the non-polar organic solvents, from water. Their efficiency is related to the chitosan macromolecules grafted onto the surface of the particles, along with reduced particle dimensions and high surface-to-volume ratio. There was no significant variation of the chemical composition of particles surface and on their performance after 4 cycles. Thus, the authors suggest the use of MNPs in oil remediation in saline waters [139]. In a different approach, Mirshahghassemi *et al*. (2017) reported the use of polyvinylpyrrolidone (PVP)-coated MNPs with a high gradient magnetic separation (HGMS) technique for the rapid removal of oil from oil-water mixtures in a continuous flow system. By employing this technique, the authors achieved 85–95% oil and NP removal and stated that HGMS may be a promising technique for oil remediation using PVP-coated MNPs, in a process probably based on the hydrophobic effect forcing oil from the aqueous phase onto the PVP layer. Nevertheless, that the procedure can be improved as only a fraction of MNPs, more precisely the aromatic fraction, seems to be involved in the oil removal [140]. In an innovative way, Atta *et al*. (2020) assessed the ability of *Eichhornia crassipes* combined with MNPs capped with natural products based on Myrrh, to treat freshwater contaminated by crude oil, obtaining removal levels up to 95%. Notwithstanding, the crude oil phytotoxicity can affect *E. crassipes* biomass and, thus, to threat its success in phytoremediation [141].

Liao *et al*. (2015) in a study with water-based MNPs coated with midchain fatty acids (C6-C11) obtained promising results in terms of benzo[a]pyrene (BaP) removal as 93% of BaP was removed from contaminated water samples. The adsorption behaviour was not affected by pH nor ionic strength of the test solution but the chain length of fatty acids had a significant influence on the adsorption.

This influence, as the authors theorized, may be due to either accommodation of BaP and/or the fatty acid chain providing enough Van der Waals interactions. BaP can later easily be removed from MNPs, which showed good desorption capabilities [142]. In another study addressing the removal of BaP from water, Yang *et al*. (2019) proposed the functionalization of MNPs with carbon dots (CDs), CDs/C_{11}-Fe_3O_4, as a novel reusable adsorbent. These particles, well dispersed in water and re-collected completely from the solution without leaving any traces of material, can reach an efficiency of up to 93.9%, showing a decline with temperature increase [76].

The removal of dyes has also been the subject of research. Hu *et al*. (2020), used magnetic lignosulfonate (FCS) to adsorb two types of dye, Congo Red (CR) and Titan Yellow (TY), reaching highest adsorption capacity at pH 7 in a spontaneous endothermic process, and achieving adsorption results after 5 re-uses of 83% for CR and 80% for TY [143]. In another study, Seliem *et al.* (2020), proposed a novel nanocomposite of activated serpentine mineral decorated with MNPs (MNP/SP) to be used in the adsorption of the hazardous cationic dyes methylene blue (MB) and malachite green (MG). The adsorbent, at pH 8, exhibited removal levels higher than 95%, being easily regenerated and reutilized with almost the same efficacy, even after 5 adsorption cycles [144].

In another interesting approach, Liyanage *et al*. (2020), modified commercially available Douglas fir biochar (BC) with MNPs to remediate three common emerging aqueous contaminants, a stimulant (caffeine) and two anti-inflammatory drugs (ibuprofen and acetylsalicylic acid). Fe_3O_4 NPs were dispersed on the biochar surface to provide magnetization and create new adsorption sites for the contaminant uptake. This hybrid material had enhanced adsorption of the contaminants when compared to the biochar alone and provided a high removal capacity of these contaminants at 35ºC, being also able to be reused up to 5 cycles [145].

Table 7. Efficacy of MNPs based adsorbents towards organic pollutants, in aqueous media based on their adsorption capacity, % of metal ions removal, sample pH and reusability.

Adsorbent	**Pollutant**	**Sample Media**	**Adsorption Capacity (mg.g^{-1})**	**Removal (%)**	**pH**	**Reusability (Cycle Nº)**	**Reference**
Fe_3O_4/CS/PEI	Phosphate	Aqueous media	48.2	-	3.0 - 4.0	5	[134]
Fe_3O_4@GO-CMC	Phosphate	Aqueous media	84.9	84.7	6.0	6	[135]
	Nitrate		76.01	62.3			
MAlgHT	Phosphate	Aqueous media	29.71	-	6.0 - 8.0	4	[146]
MCSHT			35.98				
$CoFe_2O_4$/sawdust	Lubrification Oil	Aqueous media	11500	-	-	10	[136]

Fe_3O_4@SiO_2@MPS	Crude Oil 19.6 API	Aqueous media	48500	100	>pH*	-	[137]
	Crude Oil 35 API						
Fe_3O_4@APFS-G-CS	Diesel	Aqueous media	-	-	7.0	7	[138]
Fe_3O_4@SiO_2/SiChitosan	Toluene	Aqueous media	6300 ± 1200	-	-	4	[139]
	Cyclohexane		5300 ± 800				
	n-Heptane		4100 ± 900				
	Chloroform		6200 ± 500				
PVP-MNPs	Crude oil	Aqueous media	-	85-95	-	-	[140]
MNP-Myrrh	Crude oil	Aqueous media	-	95	-	-	[141]
MNPs coated with midchain fatty acids (C6-C11)	BaP	Aqueous media	63.9	93.5	-	3	[142]
CDs/C11-Fe_3O_4	BaP	Aqueous media	76.23	93.9	-	6	[76]
FCS	CR	Aqueous media	198.24	83	7	5	[143]
	TY		192.51	80			
MNP/SP	MB	Aqueous media	162	>95	8	5	[144]
	MG		176				
Biochar-Fe_3O_4	Caffeine	Aqueous media	75.1 ± 1.8	95	8	5	[145]
	Ibuprofen		39.9 ± 1.2	90			
	acetylsalicylic acid		149.9 ± 4.5	70			

Table 8. Compilation of the adsorption mechanisms of some MNPs based adsorbents towards heavy metal ions and organic pollutants according to their functional groups.

Adsorbent	Functionalization	Pollutant	Adsorption mechanism	Reference
Fe_3O_4-NH_2	Amino groups	Pb(II)	Electrostatic attraction Cation-π (aromatic ring) interactions	[113]
		Cd(II)		
MNPs@SiO_2@GOPTS-bPEI		Cu(II)	Reduction of eletronic state	[115]

MCBB		As(III)	Binding to -OH and -NH2 functional groups	[123]
		As(V)		
MAF-SCMNPs	Amino groups	Hg(II) and Pb(II)	Chelation	[116]
	Thiol groups	Hg(II) and Pb(II)	Ion Exchange	
FeS MNPs		Cr(VI)	Reduction	[119]
MNPs35@SiO_2	Silanol groups	Pb(II)	Hydrogen bonding Electrostatic attraction Chemisorption	[114]
NFNCs	-	Cr(VI)	Electrostatic attraction (<pH)	[120]
			Ion Exchange (>pH)	
			Chemisorption	
Fe_3O_4/PVA (1)	Hydrocarbon, Alcohol, carbonyl, carboxylate groups	Ag(I)	Electrostatic attraction	[125]
		Ni(II)		
Fe_3O_4/PMA-g-PVA (2)		Cd(II)		
		Pb(II)		
		Co(II)		
MCRB	Calcite	As(III) and	Cation exchange Complexation with hydroxyls	[126]
	Hydroxyl groups	Pb(II)		
Fe_3O_4-HBPAASA	Amino groups	Pb(II)	Complexation	[127]
	Salicylic acid groups	Cd(II)		
	Both	Cu(II)		
CMC	Hydroxyl groups	Al(II)	Cationic exchange Formation of hydroxide on the surface	[128]
		Cu(II)		
		Zn(II)		
		Fe(II)		
		Mg(II)		
MoS_2/Fe_3O_4	Thiol groups	Hg(II)	Chemisorption	[129]
		Pb(II)		
PION	Hydroxyl groups	Cd(II)	Complexation	[130]
$MnFe_2O_4$		Cr(VI)	Chemisorption	[131]
Fe_3O_4		As	Complexation	[133]
Fe_3O_4/CS/PEI	amino groups	Phosphate	Electrostatic attraction	[134]
Fe_3O_4@GO-CMC			Electrostatic interaction	[135]

	Carboxyl, Epoxy, Ketone, and Hydroxyl groups	Phosphate and	Ion-exchange	
		Nitrate	Surface complexation	
Fe_3O_4@APFS-G-CS	Carboxylate groups Amino groups	Diesel	Electrostatic attraction	[138]
PVP-MNPs	Alkyl groups	Crude oil	Hydrophobic effect	[140]
MNPs coated with midchain fatty acids (C6-C11)	Carboxyl groups	BaP	Electrostatic attraction	[142]
CDs/C_{11}-Fe_3O_4	Carbonyl groups	BaP	Chemisorption	[76]
FCS	Hydroxyl groups	CR	Hydrogen bonding	[143]
		TY		
Biochar-Fe_3O_4	Carbonyl groups	Caffeine	Electrostatic attraction Cation-π (aromatic ring) interactions	[145]
		Ibuprofen		
		acetylsalicylic acid		

3.4. Silica Nanoparticles

Among the manufactured NMs, metalbearing NPs are attracting great interest from many industries and thus been applied in many applications. Metal oxide NPs can be synthesized from many metals. Silicon (Si) is one of the most abundant chemical elements on Earth’s crust. Even though it is chemically inert, it has a strong affinity towards oxygen which results in its oxide forms: silicate (SiO_4) and silica (silicon dioxide, SiO_2) [147], [148]. While Si is often used in industry, SiO_4 and SiO_2, with special relevance for their nanoparticulate forms, are used mainly in biomedical and biological applications, such as in agriculture, in gene carrier, drug delivery and molecular imaging [145–147]. In fact, Silica NPs possess very different physio-chemical characteristics compared to its bulk form and are these advantageous features that increase their attractiveness. Among their attractive properties, are their easy synthesis, modifiable surface, chemically inert composition, large surface to volume ratio and tolerable biodegradability [148], [149], [151]. Furthermore, silica can be divided into crystalline or amorphous, being that both have the same basic molecular formula, but different structural arrangements [148], [152]. Crystalline silica, presents the silicon and oxygen atoms arranged in a geometric pattern, while the amorphous silica has no spatial ordering of the atoms [153].

3.4.1. Design of Silica Nanoparticles

Similar to the above mentioned MNPs, the design of the SiO_2 NPs is also a complex process, crucial for their application in various fields. However, the key features that need to be addressed may differ a bit from the MNPs, as this time there are aspects like NPs porosity.

3.4.1.1. Porosity

Porosity is an important parameter, especially in the design of SiO_2 NPs to apply them in their vast applications. According to the pore diameter (Table 8), the SiO_2 NPs may be classified as nanoporous, mesoporous and microporous. In the absence of pores, the SiO_2 NPs are classified as nonporous [72].

Table 9. A classification of pores based on the average pore diameter, adopted by the International Union of Pure and Applied Chemistry [79].

Type of Pores	Pore Diameter (nm)
Nanopore	2 >
Mesopore	2-50
Micropore	100 <

Mesoporous Silica Nanoparticles

Among the porous SiO_2 NPs, the mesoporous maybe the most important and studied. These NPs are comprised of a honeycomb-like porous structure with hundreds of empty channels (mesopores) that can encapsulate large amounts of bioactive molecules, which combined with the high surface area and their good chemical and thermal stability, make them attractive to be used in several applications [148], [154], [155]. Furthermore, the pore size and structure of mesoporous SiO_2 NPs can be easily controlled by tuning the composition and concentration of surfactants during synthesis [156]. Silicon-based ordered mesoporous materials, however, tend to have a low catalytic and reactive activity due to the lack of lattice defects, protonic acid and Lewis acid centers in the framework network, which is why further functionalization is important for their effectiveness in many applications [157].

Nonporous Silica Nanoparticles

Nonporous SiO_2 NPs, while possessing no pores, are also of great interest in various applications like controlled release applications. While the mesoporous SiO_2 NPs use the pores to adsorb the bioactive molecules, the nonporous SiO_2 NPs deliver cargos through encapsulation or conjugation, being the release profile controlled by means of chemical linkers or the degradation of silica matrix. The size and shape of nonporous SiO_2 NPs can be easily controlled, which is an advantageous feature of this type of SiO_2 NPs [156].

3.4.1.2. Size

Size is another crucial feature to have in mind regarding the synthesis and use of NPs, affecting their efficiency in various biomedical and environmental applications and potential toxicity to biota. A strong connection between different sizes of NPs and their consequent cellular uptake has been reported (Li *et al*. (2019)). Smaller sized NPs enter the cells more easily, fact that can be promoted by bigger NPs. However, smaller NPs inhibit the uptake of the bigger ones [158]. Slowing *et al*. (2008), consider that mesoporous silica microspheres may not be suitable for many important biotechnological and biomedical applications because of their size, due to the fact that the mammalian cells are not capable to engulf large particles via endocytosis and being within the size window of bacteria, pose the risk to trigger an acute immune response *in vivo* [154]. Yu *et al*. (2016), observed that SiO_2 NPs in the range of 175 to 570 nm have better results in gene transfection than 330 nm particles [159]. Thus, as observed for other NPs, the ideal size of SiO_2 NPs may vary for each application, which is why it is important to study the effect of the size of the NPs beforehand.

3.4.1.3. Shape

The role of shape of the SiO_2 NPs in the toxicity to biota and their efficiency regarding their applications is an important feature in need of increased understanding, as it can modulate their toxicity. It has been reported shape can affect the agglomeration tendency of these particles [154], [160]. Worm-like micelles have shown higher circulation times when compared to spherical ones, which may be due to enhanced evasion of phagocytosis, and nanorods able to penetrate tumor tissues more efficiently than nanospheres because of the improved transport through pores [160]. In addition, Huang *et al*. (2010), in their study on the effect of different shaped SiO_2 NPs (spheres, and short and long rods) observed a relation between the shape of the NPs and particle uptake, cell viability, early apoptosis, adhesion, migration and cytoskeleton formation [161]. NPs with a smaller aspect ratio (AR) like spheres generally affect cells to a minor degree compared to NPs with a larger AR, such as rods [161]. Furthermore, in another study, it was not only shown that long-rod shaped NPs have higher intracellular retention amount in HeLa cells than short-rod- or sphere-shaped NPs over the same period of time but also that the cellular entry pathway in those cells was regulated by particle shape [162]. Huang *et al*. (2011), found that after internalization SiO_2 NPs become mainly present in the liver, spleen and lung [163].

3.4.1.4. Surface Modification

The surface characteristics/functionalization of NPs appear as a major factor governing their efficiency. Due to the versatile silane chemistry, many functional moieties can be conjugated to the SiO_2 NPs surface either by physical adsorption or covalent conjugation. SiO_2 NPs allow a great variety of moieties to be functionalized with ease in different regions of the particle, namely: the pore walls, entrance to the pores and the interior/exterior surfaces of the particles [164]. Functionalization can reduce NP aggregation and non-specific binding, two crucial features for environmental and biomedical applications [165]. An example can be provided by the study of Bagwe *et al*. (2006), that demonstrated that by conjugating octadecyl and carboxylate groups in dye-doped SiO_2 NPs minimal non-specific binding can be obtained, whereas surface modification with amino and thiol functional groups increases adsorption capacity and selectivity. Amino groups have also been widely used to adsorb anionic pollutants by electrostatic attraction at low pH, and PTME and other cationic pollutants at high pH [166], [167]. Additionally, the surface properties of NPs are also known to influence the interactions between NPs and biological systems including cellular internalization and trafficking, biodistribution and tumour penetration [160]. Therefore, one must carefully think and design the NP surface before employing it in any application, as it might influence their efficacy and potential toxicity when applied in environmental samples for remediation. However, this process is not without challenges. As He *et al*. (2013), stated in their study, a major challenge is the surface modification of colloidal SiO_2 NPs without disrupting the electric double layer of the NPs [168].

3.4.2. Environmental remediation by Silica NPs and NMs

In adsorption technology, inorganic materials are extensively used because of their chemical and thermal stabilities and because they can be regenerated and reused. Silica-based adsorbents, for instance, are used for the elimination of many pollutants due to their porosity, greater surface area, and good mechanical thermal stabilities. The hydroxyl groups make the silica polar and consequently the polar groups of the organic analytes make a strong bond with the surface of SiO_2 NPs, however, non-polar pollutants tend to interact weakly [169]. Notwithstanding, even though silica is an inorganic polymer that does not establish good interactions with nonpolar organic compounds, with the adequate coating, generally with an organic modifier, and by employing mesoporous structures instead of nonporous ones they can be effective to remove them as well [70]. Furthermore, silica-based materials have strong and sometimes irreversible non-selective adsorption because their surface consists of acidic silanol. By using modified silica one might achieve better capability for the adsorption of many pollutants including acidic dyes effluents and metal ions [169].

3.4.2.1. Potentially Toxic Metallic Elements

As one of the main pollutants in many environmental compartments nowadays, PTME are a great ecological hazard. Thus, many authors have been trying to introduce innovative ways to solve this issue by removing them from water masses, soils or even air by employing SiO_2 NPs and materials (Table 9), which has been described as a potential solution for that matter.

For instance, the efficiency of functionalized porous adsorbents, more specifically, thiol-functionalized silicas, in the uptake of Hg(II) from aqueous media was studied by Walcarius *et al*., (2005) which reported higher binding capacity and selectivity at pH>4 when using mesoporous structures instead of amorphous ones. At pH<4, however, the formation of positively charged complexes, which may compromise their efficiency in the mesoporous materials, could be observed. The adsorbent removed 100% the contaminant, maintaining efficient contaminant removal for up to 3 cycles [170]. Notwithstanding, and regarding thiol functionalization, Arencibia *et al*. (2010), stated that the successful effectiveness of thiol-functionalized silicas is due to high affinity of sulphur towards mercury [171]. Rostamian *et al*. (2011), also found that thiol functionalized SiO_2 NPs are good adsorbents for Hg(II) having adsorption levels higher than those obtained for other metal ions [172]. However, some difficulties in the regeneration or reutilization process of these adsorbents were reported, as mercury is not easily desorbed unless chemical species capable of forming stable complexes with Hg(II) are used or unless protons exist in the aqueous medium to stabilize the thiol groups of the adsorbent [171].

Mesoporous silica SBA-15 materials functionalized with up to three amino functional groups were used by Aguado *et al*. (2009), for Cu(II), Ni(II), Pb(II), Cd(II), and Zn(II) removal from aqueous solutions. These adsorbents displayed have excellent performances in the removal of the metal ions, particularly true for Pb(II) which had almost 100% removal. The metal loading of the modified SBA-15 samples might be almost exclusively due to the presence of the active amino groups anchored to the silica walls [173]. Similar results were achieved by Da'na *et al*. (2011), when investigating the use of SBA-15 functionalized with 3-aminopropyltrimethoxy-silane for the removal of Cu(II) ions but, in this case, the adsorbent was more efficient at a pH below 6.5 and could be reused 10 times without losing efficiency [174]. The importance of amino groups in functionalization was also highlighted by Heidari *et al*. (2009), that investigated the application of mesoporous silica materials, such as MCM-41, nano MCM-41,

NH_2-MCM-41 (amino functionalized MCM-41) and nano NH_2-MCM-41, for the removal of Ni(II), Cd(II) and Pb(II) ions from aqueous solution and found that those functionalized with the amino groups had the highest uptake for metal ions [175]. Jiang *et al*. (2020), in their turn, worked on a novel adsorbent by immobilizing amino-functionalized mesoporous silica (aMSP) into sodium alginate (SA) to potentially remove low concentration hexavalent Uranium from wastewater masses. Having into account several parameters of the adsorbent like pH, initial concentration, time, temperature, coexisting ions, and regeneration on the removal efficiency of U(VI), the best results were obtained at pH 4.0 and 313 K, with an efficiency of uranium removal from mine water of 99.41%. Ion exchange with Ca^{2+} on carboxyl and coordination with hydroxyl and amino groups were the reported main mechanism of adsorption [176].

The viability of applying mesoporous silica SBA-15 with abundant carboxyl groups for Pb (II) removal from water samples was studied by Huang *et al.* (2012) The adsorbent consisted of an organic–inorganic hybrid mesoporous silica with 3-aminopropyltrimethoxy-silane (APTES) and thionyl dichloride (SOCl2) activated ethylenediaminetetraacetic acid (EDTA), as the authors aimed to join the advantages of the SBA-15, a mesoporous silica material, and the chelating and ion exchanging properties of EDTA towards metal ions. The authors found that pH value of 5.0 was the optimum for Pb adsorption, achieving 92% of removal, and the adsorption mechanism was mainly due to ion-exchange and carboxyl group surface complexation [177]. In another work, where metal ion adsorption from aqueous solutions of different organo-functionalized SiO_2 NPs (i.e., -EDTA, -COOH, -SO_3H, -SH and -NH_2) was compared, it was shown that functionalization with EDTA made the adsorption of Pb(II), Cu(II), Ni(II), Zn(II) and Cd(II) ions much greater than when COOH-, SO_3H-, SH- and NH_2-functionalized SiO_2 NPs were used [178].

Barik *et al*. (2020), in another study, addressed the adsorption of Pb(II) and As(III) ions by graphene oxide-silica composites from aqueous solutions. Overall, graphene oxide-silica composite was found a highly effective adsorbent towards both Pb (II) and As (III) metal ions. At pH values around 5 there was an enhancement of arsenic anions adsorption, because of the positive surface charge, while at values near 6.8 the adsorption of Pb increased due to domination of negative surface charge. The adsorption capacity increased with the increase of the initial metal ion concentration, with temperature and over time [179]. Chatterjee *et al*. (2020), also studied the adsorption efficiency towards Pb (II), but this time of a mesoporous alumina–silica nanosorbent synthesized from coal fly ash and a waste aluminium foil. They found that the Pb(II) adsorption capacities were 193.6, 291.5 and 326.2 mg g^{-1} at 283, 303 and 313 K, respectively, but also that in a case of binary mixture and consequently binary adsorption, these capacities reach higher values, being those 231.27, 521.87 and 615.86 mg g^{-1} at 283, 303 and 313 K, respectively. In this case, the presence of another pollutant, malachite green (MG), had a synergistic effect on the adsorption of Pb [180]. Maiti *et al*. (2020), in their turned, used spherical shaped SiO_2 NPs to prepare nano dimensioned cubical shaped Faujasite silica-based NMs for PTME and carcinogenic dye degradation in aqueous solutions. The efficiency of the nanomaterial in adsorption of Pb, Co and Cr from aqueous solutions at pH 5 within 120 minutes was 85, 84 and 74%, respectively, [181]. A novel composite synthesized through the modification of mesoporous SiO_2 NPs with dibenzoylmethane was presented by Khalifa *et al*. (2020), and used it for Cu (II), Hg (II), and Cd (II) ions removal from aqueous media. The reported maximum adsorption capacity was 35.37, 25.17, and 31.76 mg g^{-1} in the case of Cd (II), Hg (II), and Cu (II) ions, respectively, at pH 6, being the adsorption processes based on chemisorption. Excellent percentages of desorption for Cd (II), Hg (II), and Cu (II) ions were obtained (99.12, 99.07, and 98.37%, respectively), meaning that these NPs can be reusable and, thus, can participate in many cycles of remediation without compromising their efficacy [182]. SiO_2 NPs produced from white sandstone to remove Cd(II) from various aqueous matrixes, yielded a maximum efficiency of 98.74% at 25 ºC and pH of 6.14 and could be employed in 8 cycles without significantly losing efficiency [183].

However, while there are some studies on the potential of silica materials and NPs in PTME remediation in water masses, little has been done on the remediation of soils. Wang *et al*. (2020), studied the potential of mercapto-functionalized SiO_2 NPs (MPTS/nano-silica) to stabilize Cd in contaminated agricultural soil, reporting that the application of MPTS/nano-silica can reduce the soil aggregate stability significantly increase the soil dehydrogenase (DHA), yield of wheat grains, Si content in wheat tissues, while decreasing the leachability and bioavailability of Cd in the soil in 36% and 54.3% [184]. Similar results were obtained by Khan *et al*. (2020), in their study on the effects of silicon NPs on growth and physiology of wheat in cadmium contaminated soil [185] and by Wang *et al*. (2020), in their study on the stabilization of Cd in contaminated soils by surface-modified nano-silica (SMNS) and its phyto-availability to corn and wheat [186]. Cao *et al*. (2020), also used SiO_2 NPs, more specifically mercapto propyltrimethoxysilane- and ferrous sulfate-modified SiO_2 NPs (RNS-SFe), to immobilize Pb, Cd and As in a contaminated soil, reporting that it could immobilize Pb, Cd, and As by 97.1%, 85.0%, and 80.1%, respectively, and transform bioavailable Pb, Cd, and As into insoluble mercapto-metal compounds [187].

Zarandi *et al*. (2020), in their turn, reported the use of nano sorbents based on functionalized bimodal mesoporous SiO_2 NPs (HS-UVM7 and NH2-UVM7) for the removal of Pb aerosols from air by solid liquid gas phase extraction method reaching a 95% adsorption efficiency [188].

Table 10. Efficacy of SiO_2 NPs based adsorbents towards potentially toxic metallic elements, in aqueous media based on their adsorption capacity, % of metal ions removal, sample pH and reusability.

Adsorbent	Pollutant	Sample	Adsorption Capacity (mg. g $^{-1}$)	Removal (%)	pH	Reusability (Cycle nº)	Reference
K40-SH	Hg (II)	Aqueous media	176.52	100	4	3	[165]
G60-SH			194.57				
MCM41-SH			156.46				
MPS-10%			184.54				
MPS-20%			290.86				
MPS-40%			481.42				
SBA-15-SH10	Hg (II)	Aqueous media	244.72	-	4.5	-	[166]
Thiol-SNHS	Hg (II)	Aqueous media	186.4019	-	-	-	[172]
	Pb (II)		17.1541				
	Cd (II)		15.4566				
G-SBA-15-N-C	Ni (II)	Aqueous media	-	>20	-	-	[173]
	Zn (II)		-	~30			
	Cu (II)		15.89	>20			
	Cd (II)		-	>40			
	Pb (II)		-	~100			
G-SBA-15-N-C-H	Ni (II)		-	>40			
	Zn (II)		-	>30			
	Cu (II)		24.78	~40			
	Cd (II)		-	>70			
	Pb (II)		-	~100			
G-SBA-15-N-E	Ni (II)		-	>30			
	Zn (II)		-	>30			
	Cu (II)		22.24	>30			
	Cd (II)		-	>70			
	Pb (II)		-	~100			
G-SBA-15-NN-E	Ni (II)		-	~20			
	Zn (II)		-	~40			
	Cu (II)		52.11	>30			
	Cd (II)		-	~30			
	Pb (II)		-	~100			
G-SBA-15-NNN-E	Ni (II)		-	>20			
	Zn (II)		-	~60			
	Cu (II)		-	~50			
	Cd (II)		-	>50			
	Pb (II)		-	>80			

APTS-SBA15	Cu (II)	Aqueous media	3.18	100	< 6.5	10	[174]
APTS-SBA-15-AB			13.34				
MCM-41	Ni (II)	Aqueous media	-	8.2	5-6	5	[175]
	Cd (II)		-	2.8			
	Pb (II)		-	29			
MCM-41 NPs	Ni (II)		-	15			
	Cd (II)		-	47			
	Pb (II)		-	75			
NH_2-MCM-41	Ni (II)		12.36	92			
	Cd (II)		18.25	93			
	Pb (II)		57.74	95			
NH_2-MCM-41 NPs	Ni (II)		-	92			
	Cd (II)		-	93			
	Pb (II)		-	95			
EDTA-SBA-15	Pb (II)	Aqueous media	273.2	92	5	4	[177]
EDTA-SiO_2	Pb (II)	Aqueous media	27.14	95	6-7	-	[178]
	Cu (II)		21.73	-			
	Ni (II)		5.81	-			
	Zn (II)		1.57	-			
	Cd (II)		2.92	-			
GO-SiO_2	Pb (II)	Aqueous media	527	-	6.8	4	[179]
	As (III)		30	-			
Faujasite Si-based nanomaterial	Pb (II)	Aqueous media	-	>85	>5	-	[181]
	Co (II)		-	>84			
	Cr (III)		-	>74			
SiA-2	Pb (II)	Aqueous media	193.6 (283 K) 291.5 (303 K) 326.2 (303 K)	-	5-6	5	[180]
SiO_2/(3-aminopropyl) trimethoxysilane composite	Cu (II)	Aqueous media	35.37	68.11	6	5	[182]
	Hg (II)		25.17	52.49			
	Cd (II)		31.76	73.65			
SiO_2	Cd (II)	Aqueous media	55.13	98.74	6.14	8	[183]
aMSP/SA	U (VI)	Aqueous media	210	99.41	4	4	[176]
MPTS/nano-silica	Cd (II)	Soil	-	53.9 - 61.9	8.12	-	[184]
Si NPs	Cd (II)	Soil	-	-	-	-	[185]

SMNS	Cd (II)	Soil	-	61.14	8.82		[186]
RNS-SFe	Cd (II)	Soil	-	85	3	-	[187]
	Pb (II)		-	97.1			
	As (III)		-	80.1			
HS-UVM7	Pb	Air	177.6	95	5	-	[188]
NH_2-UVM7			265.6	60			

3.4.2.2. Organic Pollutants

Besides the ability of these NPs to sequester metal ions, they are also able to remove organic pollutants from water samples, as reported in many studies (Table 10). In addition to the already mentioned work on the adsorption of Pb, Chatterjee *et al*. (2020), also described, in the same study, the efficiency of adsorption of MG by the mesoporous alumina–silica nanosorbent. The authors found that the MG adsorption shows maximum adsorption capacities of 478.9, 584.3 and 1655.2 mg g^{-1}at 283, 303 and 313 K, respectively, being that, however, when the MG is found in a mixture with Pb, the maximum adsorption capacities for MG become only as high as 103.7, 391 and 445 mg g^{-1} at 283, 303 and 313 K, respectively [180]. Mesoporous SiO_2 NPs functionalized with β-cyclodextrin (βCD-SNHS) to apply in MB removal, achieved at pH values of 10.5 a maximum removal efficiency of 95.5% [189]. Czepa *et al*. (2020), also achieved promising results at pH values around 10 when applying mesoporous SiO_2- graphene oxide hybrid material (SiO_2NH_2-GO) as an adsorbent for removal of cationic organic dyes from water, namely MB, rhodamine B (RhB) and methyl violet (MV). In this study, at pH 10, ~99.7% of MB, RhB and MV were removed from water samples in mere 3 minutes [190]. Lignosulfonate/amino-functionalized SBA-15 nanocomposite was tested for the adsorption of MB. The presence of the calcium lignosulate (LS) was described as crucial to achieve good dispersibility and stability of the sorbent in water, high surface area, and large pore volume, which is highly required for a rapid and efficient adsorption of MB. Addition of LS to N-SBA-15 could enhance the adsorption capacity of MB by the nanocomposite reaching almost 100% at the optimal pH (9 to 11) and temperature conditions [191]. Cobalt–carbon/silica nanocomposites (CoC@SiO_2-850) were tested for adsorption of the cationic crystal violet (CV) dye with results showing that the adsorption capacity towards the cationic dye was 214 mg g^{-1} at 25ºC and pH 7, being the adsorption process endothermic and entropically favourable and, thus, spontaneous and more favourable at higher temperature. [192].

Three-dimensional (3D) cubic mesoporous silicas SB-16 functionalized with -COOH groups were synthesized to be employed in adsorption of MB and phenosafranine (PF) and anionic dye acid blue 25 (AB25). With the aim to test the adsorption capacity and to understand the adsorption mechanism played by the functional groups, the authors of the study found that the adsorption is dependent of favourable electrostatic interactions between the COO− anion, resulting from the deprotonation of the COOH groups at high pH. While for the cationic dyes, PF and MB, there was a remarkable adsorption capacity, for the anionic dye AB25, however, the adsorption was not efficient in the same conditions of pH. Nonetheless, the authors stated that a combination of high density of functional groups and the high surface area are the key for the adsorption capacity demonstrated by -COOH functionalized SBA-16 [193].

Table 11. Efficacy of SiO_2 NPs based adsorbents towards organic pollutants, in aqueous media based on their adsorption capacity, % of metal ions removal, sample pH and reusability.

Adsorbent	**Pollutant**	**Sample**	**Adsorption Capacity (mg g $^{-1}$)**	**Removal (%)**	**pH**	**Reusability (Cycle nº)**	**Reference**
SiA-2	MG	Aqueous solution	478.9 (283 K) 584.3 (303 K) 1655.2 (313 K)	-	5	5-6	[180]
βCD-SNHS	MB	Aqueous solution	99.22	95.5	10.5	-	[189]
SiO_2NH2-GO	MB RhB MV	Aqueous solution	300 358 178	~99.7	10	10	[190]
LS@N-SBA-15	MB	Aqueous solution	62.89	~100	9 -11	4	[191]
CoC@SiO_2-850	CV	Aqueous solution	214.2	98.3	7	3	[192]
-COOH@SBA-16	MB PF AB25	Aqueous solution	561 519 43	~100	9	5	[193]

Table 1. Compilation of the adsorption mechanisms of some SiO_2 NPs based adsorbents towards heavy metal ions and organic pollutants according to their functional groups.

Adsorbent	**Functionalization**	**Pollutant**	**Adsorption mechanism**	**Reference**
K40-SH G60-SH MCM41-SH MPS-10% MPS-20% MPS-40%	Thiol groups	Hg (II)	Complexation	[170]

Thiol-SNHS	Thiol groups	Hg (II) Pb (II) Cd (II)	Chemisorption	[172]
APTS-SBA15 APTS-SBA-15-AB	Amine groups Hydroxyl groups	Cu (II)	Complexation Ion exchange	[174]
NH2-MCM-41 NH2-MCM-41 NPs	Amino groups	Ni (II) Cd (II) Pb (II)	Complexation	[175]
aMSP/SA	Carboxyl groups Hydroxyl groups Amino groups	U(VI)	Ion exchange (Carboxyl) Coordination (hydroxyl and amino groups)	[176]
EDTA-SBA-15	Amino groups Carboxylic acid groups	Pb (II)	Ion exchange Complexation	[177]
EDTA-SiO_2	Hydroxyl groups	Pb (II)	Ion exchange	[178]
GO-SiO_2	Carboxylic acid groups Carbonyl groups Hydroxyl groups	Pb (II) As (III)	Chemisorption	[179]
SiA-2	-	Pb (II) MG	Chemisorption	[180]
Faujasite Si-based nanomaterial	-	Pb (II) Co (II) Cr (III)	Chemisorption	[181]
SiO_2	Silanol groups	Cd (II)	Ion Exchange	
βCD-SNHS	Hydroxyl groups	MB	Complexation	[189]
SiO_2NH_2-GO	Amine groups Silanol groups Carbonyl groups	MB RhB MV	Electrostatic interactions π-π Interactions	[190]
LS@N-SBA-15	Hydroxyl groups Carboxylic groups sulfonate groups	MB	Hydrogen bonds Electrostatic attraction	[191]
CoC@SiO_2-850	Carboxylic acid group Amine groups	CV	Hydrogen bonds π-π interactions	[192]
-COOH@SBA-16	Carboxylic acid groups Silanol groups Sulfonate groups	MB PF AB25	Electrostatic interactions	[193]

4. Challenges and Overall Considerations

Magnetic nanoparticles and SiO_2 NPs are in good position to be considered as suitable sorbents, however, along with their advantageous features come some limitations and concerns regarding their use (Table 12).

The main advantages of these NPs are associated with their good dispersion in solution, their very high specific surface area, their ability to be functionalized and become adsorbents of specific to the target pollutants, their biocompatibility, in the case of the SiO_2 NPs, and their ability to be controlled and separated with an external magnetic field, in the case of the MNPs. Compared to other conventional extraction methods, which often use large volumes of solution, this adsorption method using NPs is also advantageous for having high efficiency and recovery, ease of handling, and for being of rapid speed and low cost [70].

There are some limitations for the practical application of NPs as adsorbents, especially when applied in large-volume water samples. These limitations, are related to the possible residue of the NPs in the adsorption process, making it difficult to analyse the contaminants accurately, and to the fact that, in large-volume water samples, the aggregation and dispersibility phenomena of NPs could limit its applications [76]. The particles small size increases the risk that reacted pollutants will be transported to different locations rather than being safely controlled [194].

To overcome these potential limitations, Sorwat *et al*. (2020), proposed to remediate Cr(VI) from a solution by immobilizing magnetite onto sand, stating that with this method magnetite can be fixed in place and maintain the advantages of using “free” magnetite NPs towards Cr(VI) removal performance. The authors observed that abiogenic magnetite (formed by natural weathering or chemical precipitation) coated sand is the better choice in comparison to the biogenically (formed by microbiological processes such as microbial reduction of Fe(III) (oxyhydr)oxide minerals) coated one [194]. In addition, Sundman *et al*. (2020), raises a pertinent concern as it has been shown that organic substances and Fe-metabolizing bacteria, which can use magnetite as either an electron donor, or an electron acceptor depending upon the geochemical conditions, can alter their reactivity and limit their efficiency. In fact, they realized that microbial reduction and oxidation of magnetite can improve the removal rate of Cr(VI) from solution but not of As(V), and that the presence of humic substances lead to a decreased reactivity towards both metal ions [195]. Kumar *et al*. (2019), stated that in adsorption system, the powder form of adsorbents creates a pressure drop during filtration that limits their field applications, suggesting a solution consisting of a hybrid bead form of magnetic biopolymeric clay composites, namely, magnetic-chitosan-assisted hydrotalcite (MCSHT) and magnetic-alginate-assisted hydrotalcite (MAlgHT) composite beads. To test the adsorbent, the authors utilized it for phosphate removal from water and found that the adsorbent was efficient and able to be reutilized in up to 4 cycles [146].

As for SiO_2 NPs, while they do not establish good interactions with nonpolar organic compounds unless when functionalized, they may also originate an irreversible adsorption because of their silanol groups. Thus, in addition to lacking the magnetic properties of the MNPs, SiO_2 NPs are also extremely dependent of a good functionalization to be effective in remediation, being that the surface modification of colloidal SiO_2 NPs can also disrupt the electric double layer of the nanoparticles [70], [168], [169].

The main concern regarding using these or any kind of NPs based adsorbents to remove contaminants from the environment lies in the possibility of secondary pollution. By introducing these NPs in the environment there is always the possibility of presence of residues or leaching of internal components, which may lead to adverse effects to the fauna and flora of the sites where they are employed. Thus, even though these NPs possess tremendous potential, they must also be biocompatible, which raises the fundamental need to study their toxicity for the overall fauna and flora in depth. A detailed review on the issue will be presented next.

Table 13. Main limitations and advantages of MNPs based adsorbents in environmental remediation.

Nanoparticle	Advantageous Features	Limitations	Concerns
Magnetic Nanoparticles	▪ Low cost; ▪ Ease of handling; ▪ Separation through magnetic field; ▪ Overall good separability; ▪ Overall good Reusability; ▪ Specificity towards pollutants; ▪ High surface area.	▪ Aggregation; ▪ Possible transportation to other sites; ▪ Presence of organic substances; ▪ Presence of fe-metabolizing bacteria; ▪ Antagonistic effect from ions present in solution.	▪ Secondary pollution through possible residues; ▪ Leaching of internal components; ▪ Toxicity to living beings.
Silica Nanoparticles	▪ Low cost; ▪ Ease of handling; ▪ Overall good separability; ▪ Overall good Reusability; ▪ Specificity towards pollutants; ▪ High surface area; ▪ Biocompatibility.	▪ Aggregation; ▪ Possible transportation to other sites; ▪ Lack magnetic properties; ▪ Poor interactions with nonpolar compounds; ▪ Possible irreversible binding; ▪ Possible disruption of electric double layer upon surface modification.	

5. References

[1] E. R. Christensen, “Aquatic ecotoxicology,” *Schweizerische Zeitschrift für Hydrol.*, vol. 46, no. 1, pp. 100–108, 1984.

[2] C. Filipe, C. Jo, and J. C. Silva, *Chitin-Based Nanocomposites : Biomedical Applications Chitin-Based Nanocomposites : Biomedical Applications*, no. July 2015. 2016.

[3] V. H. Freed, C. T. Chiou, and R. Haque, “Chemodynamics: Transport and behavior of chemicals in the environment. A problem in environmental health,” *Environ. Health Perspect.*, vol. VOL.20, no. October, pp. 55–70, 1977.

[4] D. S. Moura, R. O. D. da Mota, J. F. Gonçalves Júnior, N. F. de Vasconcelos, M. A. Reis, and C. K. Grisolia, “Evaluation of the embryotoxicity in zebrafish (Danio rerio) of the flocculant and coagulant compounds used for water remediation,” *Acta Limnol. Bras.*, vol. 31, no. Wf 424, 2019.

[5] M. M. Khin, A. S. Nair, V. J. Babu, R. Murugan, and S. Ramakrishna, “A review on nanomaterials for environmental remediation,” *Energy Environ. Sci.*, vol. 5, no. 8, pp. 8075–8109, 2012.

[6] M. L. Campbell, F. D. Guerra, J. Dhulekar, F. Alexis, and D. C. Whitehead, “Target-Specific Capture of Environmentally Relevant Gaseous Aldehydes and Carboxylic Acids with Functional Nanoparticles,” *Chem. - A Eur. J.*, vol. 21, no. 42, pp. 14834–14842, 2015.

[7] O. Pourret and A. Hursthouse, “It’s time to replace the term ‘heavy metals’ with ‘potentially toxic elements’ when reporting environmental research,” *Int. J. Environ. Res. Public Health*, vol. 16, no. 22, 2019.

[8] P. B. Tchounwou, C. G. Yedjou, A. K. Patlolla, and D. J. Sutton, “Molecular, clinical and environmental toxicicology Volume 3: Environmental Toxicology,” *Mol. Clin. Environ. Toxicol.*, vol. 101, pp. 133–164, 2012.

[9] A. Aprile and L. De Bellis, “Editorial for special issue ‘heavy metals accumulation, toxicity, and detoxification in plants,’” *Int. J. Mol. Sci.*, vol. 21, no. 11, pp. 1–5, 2020.

[10] L. Huang *et al.*, “Risk Assessment in Huixian Wetland , South China,” *Water*, vol. 12, no. 431, pp. 1–14, 2020.

[11] I. Beniah Obinna and *Enyoh Christian Ebere, “A review: Water pollution by heavy metal and organic pollutants: Brief review of sources, effects and progress on remediation with aquatic plants,” *Anal. Methods Environ. Chem. J.*, no. November, pp. 5–38, 2019.

[12] E. Rolka, A. C. Żołnowski, and M. M. Sadowska, “Assessment of heavy metal content in soils adjacent to the dk16-route in olsztyn (North-Eastern Poland),” *Polish J. Environ. Stud.*, vol. 29, no. 6, pp. 4303–4311, 2020.

[13] U. Imran, A. Ullah, and K. Shaikh, “Pollution loads and ecological risk assessment of metals and a metalloid in the surface sediment of keenjhar lake, pakistan,” *Polish J. Environ. Stud.*, vol. 29, no. 5, pp. 3629–3641, 2020.

[14] J. Yabe, M. Ishizuka, and T. Umemura, “Current levels of heavy metal pollution in Africa,” *J. Vet. Med. Sci.*, vol. 72, no. 10, pp. 1257–1263, 2010.

[15] WHO Europe, “Exposure of children to chemical hazards in food,” *Eur. Environ. Heal. Inf. Syst.*, no. Fact Sheet 4.4, 2009.

[16] G. K. Kinuthia, V. Ngure, D. Beti, R. Lugalia, A. Wangila, and L. Kamau,

“Levels of heavy metals in wastewater and soil samples from open drainage channels in Nairobi, Kenya: community health implication,” *Sci. Rep.*, vol. 10, no. 1, pp. 1–13, 2020.

[17] U. C. Nkwunonwo, P. O. Odika, and N. I. Onyia, “A Review of the Health Implications of Heavy Metals in Food Chain in Nigeria,” *Sci. World J.*, vol. 2020, 2020.

[18] S. Ekino, M. Susa, T. Ninomiya, K. Imamura, and T. Kitamura, “Minamata disease revisited: An update on the acute and chronic manifestations of methyl mercury poisoning,” *J. Neurol. Sci.*, vol. 262, no. 1–2, pp. 131–144, 2007.

[19] M. A. Bradley, B. D. Barst, and N. Basu, “A review of mercury bioavailability in humans and fish,” *Int. J. Environ. Res. Public Health*, vol. 14, no. 2, p. 20, 2017.

[20] M. Nishijo, H. Nakagawa, Y. Suwazono, K. Nogawa, and T. Kido, “Causes of death in patients with Itai-itai disease suffering from severe chronic cadmium poisoning: A nested case-control analysis of a follow-up study in Japan,” *BMJ Open*, vol. 7, no. 7, pp. 1–8, 2017.

[21] M. Kaji, “Role of experts and public participation in pollution control: The case of Itai-itai disease in Japan,” *Ethics Sci. Environ. Polit.*, vol. 12, no. 2, pp. 99–111, 2012.

[22] H. Galal-Gorchev, “WHO guidelines for drinking-water quality,” *Water Supply*, vol. 11, no. 3–4, pp. 1–16, 1993.

[23] CCME, “Canadian Council of Ministers of the Environment. Canadian Water Quality Guidelines for the Protection of Aquatic Life: Organotins - tributyltin, triphenyltin, and tricyclohexyltin. In: Canadian Environmental Quality Guidelines, 1999, Canadian Council of,” 2007.

[24] U. S. E. P. Agency and O. Water, “2018 Edition of the Drinking Water Standards and Health Advisories Tables,” no. March, 2018.

[25] M. Hassan, R. Naidu, J. Du, Y. Liu, and F. Qi, “Critical review of magnetic biosorbents: Their preparation, application, and regeneration for wastewater treatment,” *Sci. Total Environ.*, vol. 702, p. 134893, 2020.

[26] S. A. Shetaia, A. M. A. Khatita, N. A. Abdelhafez, I. M. Shaker, and S. B. El Kafrawy, “Evaluation of potential health risk, heavy metal pollution indices and water quality of edku lagoon- egypt,” *Egypt. J. Aquat. Biol. Fish.*, vol. 24, no. 2, pp. 265–290, 2020.

[27] R. Abdeldayem, “A preliminary study of heavy metals pollution risk in water,” *Appl. Water Sci.*, vol. 10, no. 1, pp. 1–4, 2020.

[28] A. Ahmad *et al.*, “Comparative studies of lead and heavy metals concentrations in pakistan soil and its toxic effects,” *Polish J. Environ. Stud.*, vol. 29, no. 4, pp. 2533–2542, 2020.

[29] F. Zhang, Y. He, C. Zhao, Y. Kou, and K. Huang, “Heavy metals pollution characteristics and health risk assessment of farmland soils and agricultural products in a mining area of henan province, china,” *Polish J. Environ. Stud.*, vol. 29, no. 5, pp. 3929–3941, 2020.

[30] M. A. T. M. T. Rahman, M. Paul, N. Bhoumik, M. Hassan, M. K. Alam, and Z. Aktar, “Heavy metal pollution assessment in the groundwater of the Meghna Ghat industrial area, Bangladesh, by using water pollution indices approach,” *Appl. Water Sci.*, vol. 10, no. 8, pp. 1–15, 2020.

[31] C.-B. Angela, *The impact of persistent organic pollutants on freshwater ecosystems and human health*, no. November. 2016.

[32] L. Y. Liu, W. L. Ma, H. L. Jia, Z. F. Zhang, W. W. Song, and Y. F. Li, “Research on persistent organic pollutants in China on a national scale: 10 years after the enforcement of the Stockholm Convention,” *Environ. Pollut.*, vol. 217, pp. 70–81, 2016.

[33] L. Camenzuli, M. Scheringer, and K. Hungerbühler, “Local organochlorine pesticide concentrations in soil put into a global perspective,” *Environ. Pollut.*, vol. 217, pp. 11–18, 2016.

[34] Convenção de Estocolmo, “Stockholm convention,” *IUPAC Compend. Chem. Terminol.*, 2008.

[35] H. Hung, A. A. Katsoyiannis, and R. Guardans, “Ten years of global monitoring under the Stockholm Convention on Persistent Organic Pollutants (POPs): Trends, sources and transport modelling,” *Environ. Pollut.*, vol. 217, pp. 1–3, 2016.

[36] J. J. Alava *et al.*, “Persistent Organic Pollutants and Mercury in Genetically Identified Inner Estuary Bottlenose Dolphin (Tursiops truncatus) Residents of the Guayaquil Gulf, Ecuador: Ecotoxicological Science in Support of Pollutant Management and Cetacean Conservation,” *Front. Mar. Sci.*, vol. 7, no. March, 2020.

[37] European Commission, *Persistent organic pollutants: towards a POPs-free future*, no. 19. 2017.

[38] C. Betianu and M. Gavrilescu, “Persistent organic pollutants in environment: Inventory procedures and management in the context of the stockholm convention,” *Environ. Eng. Manag. J.*, vol. 5, no. 5, pp. 1011–1028, 2006.

[39] D. Lakhmanov *et al.*, “Persistent organic pollutants (POPs) in fish consumed by the indigenous peoples from nenets autonomous okrug,” *Environ. - MDPI*, vol. 7, no. 1, 2020.

[40] H. Singh, N. Bhardwaj, S. K. Arya, and M. Khatri, “Environmental impacts of oil spills and their remediation by magnetic nanomaterials,” *Environ. Nanotechnology, Monit. Manag.*, vol. 14, no. November 2019, p. 100305, 2020.

[41] G. Mceneff, W. Schmidt, and B. Quinn, *Pharmaceuticals in the Aquatic Environment: A Short Summary of Current Knowledge and the Potential Impacts on Aquatic Biota and Humans Synthesis report (EPA Research Report 143) available for download at Prepared for the Environmental Protection Agency*. 2015.

[42] L. Gunnarsson *et al.*, “Pharmacology beyond the patient – The environmental risks of human drugs,” *Environ. Int.*, vol. 129, no. April, pp. 320–332, 2019.

[43] L. F. Angeles *et al.*, “Assessing pharmaceutical removal and reduction in toxicity provided by advanced wastewater treatment systems,” *Environ. Sci. Water Res. Technol.*, vol. 6, no. 1, pp. 62–77, 2020.

[44] S. Kar, H. Sanderson, K. Roy, E. Benfenati, and J. Leszczynski, “Ecotoxicological assessment of pharmaceuticals and personal care products using predictive toxicology approaches,” *Green Chem.*, vol. 22, no. 5, pp. 1458–1516, 2020.

[45] T. aus der Beek *et al.*, “Pharmaceuticals in the environment-Global occurrences and perspectives,” *Environ. Toxicol. Chem.*, vol. 35, no. 4, pp. 823–835, 2016.

[46] Nordea, “Impacts of Pharmaceutical Pollution on Communities and

Environment in India: Researched and Prepared for Nordea Asset Management by Changing Markets and Ecostorm," 2016.
[47] A. Pereira, L. Silva, C. Laranjeiro, C. Lino, and A. Pena, "Selected pharmaceuticals in different aquatic compartments: Part II-Toxicity and environmental risk assessment," *Molecules*, vol. 25, no. 8, 2020.
[48] Markandeya, S. P. Shukla, and D. Mohan, "Toxicity of Disperse Dyes and its Removal from Wastewater Using Various Adsorbents: A Review," *Res. J. Environ. Toxicol.*, vol. 11, no. 2, pp. 72–89, 2017.
[49] A. Tkaczyk, K. Mitrowska, and A. Posyniak, "Synthetic organic dyes as contaminants of the aquatic environment and their implications for ecosystems: A review," *Sci. Total Environ.*, vol. 717, p. 137222, 2020.
[50] B. D. C. Ventura-camargo and M. A. Marin-morales, "Azo Dyes: Characterization and Toxicity– A Review," *Text. Light Ind. Sci. Technol.*, no. October, 2013.
[51] B. Lellis, C. Z. Fávaro-Polonio, J. A. Pamphile, and J. C. Polonio, "Effects of textile dyes on health and the environment and bioremediation potential of living organisms," *Biotechnol. Res. Innov.*, vol. 3, no. 2, pp. 275–290, 2019.
[52] M. Ismail *et al.*, "Pollution, Toxicity and Carcinogenicity of Organic Dyes and their Catalytic Bio-Remediation," *Curr. Pharm. Des.*, vol. 25, no. 34, pp. 3645–3663, 2019.
[53] M. Berradi *et al.*, "Textile finishing dyes and their impact on aquatic environs," *Heliyon*, vol. 5, no. 11, 2019.
[54] S. Benkhaya, S. M. Rabet, and A. El Harf, "A review on classifications, recent synthesis and applications of textile dyes," *Inorg. Chem. Commun.*, no. 115, 2020.
[55] C. W. Cho, T. P. T. Pham, S. Kim, Y. R. Kim, Y. C. Jeon, and Y. S. Yun, "Toxicity assessment of common organic solvents using a biosensor based on algal photosynthetic activity measurement," *J. Appl. Phycol.*, vol. 21, no. 6, pp. 683–689, 2009.
[56] C. Brauner *et al.*, "Exposure to organic solvents and hepatotoxicity," *J. Environ. Sci. Heal. - Part A Toxic/Hazardous Subst. Environ. Eng.*, vol. 55, no. 10, pp. 1173–1178, 2020.
[57] D. R. Joshi and N. Adhikari, "An Overview on Common Organic Solvents and Their Toxicity," *J. Pharm. Res. Int.*, no. June, pp. 1–18, 2019.
[58] M. Matsumoto, K. Mochiduki, and K. Kondo, "Toxicity of ionic liquids and organic solvents to lactic acid-producing bacteria," *J. Biosci. Bioeng.*, vol. 98, no. 5, pp. 344–347, 2004.
[59] N. Uzma, B. M. K. M. Salar, B. Santhosh Kumar, N. Aziz, M. A. David, and V. D. Reddy, "Impact of organic solvents and environmental pollutants on the physiological function in petrol filling workers," *Int. J. Environ. Res. Public Health*, vol. 5, no. 3, pp. 139–146, 2008.
[60] M. I. Lone, Z. L. He, P. J. Stoffella, and X. E. Yang, "Phytoremediation of heavy metal polluted soils and water: Progresses and perspectives," *J. Zhejiang Univ. Sci. B*, vol. 9, no. 3, pp. 210–220, 2008.
[61] M. I. A. Abdel Maksoud, A. M. Elgarahy, C. Farrell, A. H. Al-Muhtaseb, D. W. Rooney, and A. I. Osman, "Insight on water remediation application using magnetic nanomaterials and biosorbents," *Coord. Chem. Rev.*, vol. 403, p. 213096, 2020.
[62] F. D. Guerra, M. F. Attia, D. C. Whitehead, and F. Alexis, "Nanotechnology

for environmental remediation: Materials and applications," *Molecules*, vol. 23, no. 7, pp. 1–23, 2018.

[63] M. Alaraby, B. Annangi, R. Marcos, and A. Hernández, "Drosophila melanogaster as a suitable in vivo model to determine potential side effects of nanomaterials: A review," *J. Toxicol. Environ. Heal. - Part B Crit. Rev.*, vol. 19, no. 2, pp. 65–104, 2016.

[64] E. Chang, N. Thekkek, W. W. Yu, V. L. Colvin, and R. Drezek, "Evaluation of quantum dot cytotoxicity based on intracellular uptake," *Small*, vol. 2, no. 12, pp. 1412–1417, 2006.

[65] N. Sanvicens and M. P. Marco, "Multifunctional nanoparticles - properties and prospects for their use in human medicine," *Trends Biotechnol.*, vol. 26, no. 8, pp. 425–433, 2008.

[66] S. J. Klaine *et al.*, "Nanomaterials in the environment: Behavior, fate, bioavailability, and effects," *Environ. Toxicol. Chem.*, vol. 27, no. 9, pp. 1825–1851, 2008.

[67] N. Kumar and S. Kumbhat, *Essentials in Nanoscience and Nanotechnology*, First. John Wiley & Sons, Inc., 2016.

[68] J. I. Park and J. Cheon, "Synthesis of 'solid solution' and 'core-shell' type cobalt-platinum magnetic nanoparticles via transmetalation reactions," *J. Am. Chem. Soc.*, vol. 123, no. 24, pp. 5743–5746, 2001.

[69] D. L. Leslie-Pelecky and R. D. Rieke, "Magnetic properties of nanostructured materials," *Chem. Mater.*, vol. 8, no. 8, pp. 1770–1783, 1996.

[70] M. Khajeh, S. Laurent, and K. Dastafkan, "Nanoadsorbents: Classification, preparation, and applications (with emphasis on aqueous media)," *Chem. Rev.*, vol. 113, no. 10, pp. 7728–7768, 2013.

[71] S. S. Syamchand and G. Sony, "Multifunctional hydroxyapatite nanoparticles for drug delivery and multimodal molecular imaging," *Microchim. Acta*, vol. 182, no. 9–10, pp. 1567–1589, 2015.

[72] P. V. Kamat and D. Meisel, "Nanoscience opportunities in environmental remediation," *Comptes Rendus Chim.*, vol. 6, no. 8–10, pp. 999–1007, 2003.

[73] P. G. Tratnyek and R. L. Johnson, "Nanotechnologies for environmental cleanup," *Nano Today*, vol. 1, no. 2, pp. 44–48, 2006.

[74] B. Pandey and M. H. Fulekar, "Nanotechnology: Remediation Technologies to Clean Up the Environmental Pollutants," *Res. J. Chem. Sci.*, vol. 2, no. 2, pp. 90–96, 2012.

[75] C. Plank *et al.*, "The magnetofection method: Using magnetic force to enhance gene delivery," *Biol. Chem.*, vol. 384, no. 5, pp. 737–747, 2003.

[76] D. Yang, S. K. Tammina, X. Li, and Y. Yang, "Enhanced removal and detection of benzo[a]pyrene in environmental water samples using carbon dots-modified magnetic nanocomposites," *Ecotoxicol. Environ. Saf.*, vol. 170, no. September 2018, pp. 383–390, 2019.

[77] J. Kudr *et al.*, "Magnetic nanoparticles: From design and synthesis to real world applications," *Nanomaterials*, vol. 7, no. 9, pp. 1–29, 2017.

[78] Y. Li, Z. W. Chen, and N. Gu, "In vitro biological effects of magnetic nanoparticles," *Chinese Sci. Bull.*, vol. 57, no. 31, pp. 3972–3978, 2012.

[79] O. Veiseh, J. W. Gunn, and M. Zhang, "Design and fabrication of magnetic nanoparticles for targeted drug delivery and imaging," *Adv. Drug Deliv. Rev.*, vol. 62, no. 3, pp. 284–304, 2010.

[80] A. H. Lu, E. L. Salabas, and F. Schüth, “Magnetic nanoparticles: Synthesis, protection, functionalization, and application,” *Angew. Chemie - Int. Ed.*, vol. 46, no. 8, pp. 1222–1244, 2007.

[81] R. A. Revia, Z. R. Stephen, and M. Zhang, “Theranostic Nanoparticles for RNA-Based Cancer Treatment,” *Acc. Chem. Res.*, vol. 52, no. 6, pp. 1496–1506, 2019.

[82] C. C. Berry, S. Wells, S. Charles, and A. S. G. Curtis, “Dextran and albumin derivatised iron oxide nanoparticles: Influence on fibroblasts in vitro,” *Biomaterials*, vol. 24, no. 25, pp. 4551–4557, 2003.

[83] S. E. A. Gratton, P. D. Pohlhaus, J. Lee, J. Guo, M. J. Cho, and J. M. DeSimone, “Nanofabricated particles for engineered drug therapies: A preliminary biodistribution study of PRINT^{TM} nanoparticles,” *J. Control. Release*, vol. 121, no. 1–2, pp. 10–18, 2007.

[84] N. Torres-Gómez, O. Nava, L. Argueta-Figueroa, R. García-Contreras, A. Baeza-Barrera, and A. R. Vilchis-Nestor, “Shape tuning of magnetite nanoparticles obtained by hydrothermal synthesis: Effect of temperature,” *J. Nanomater.*, vol. 2019, p. 15, 2019.

[85] P. J. Vikesland, A. M. Heathcock, R. L. Rebodos, and K. E. Makus, “Particle size and aggregation effects on magnetite reactivity toward carbon tetrachloride,” *Environ. Sci. Technol.*, vol. 41, no. 15, pp. 5277–5283, 2007.

[86] D. E. Discher, “Shape effects of filaments versus spherical particles in flow and drug delivery,” *Proc. ASME Summer Bioeng. Conf. SBC2008*, vol. 2, no. PART B, p. 739, 2009.

[87] S. J. Park, S. Kim, S. Lee, Z. G. Khim, K. Char, and T. Hyeon, “Synthesis and magnetic studies of uniform iron nanorods and nanospheres [12],” *J. Am. Chem. Soc.*, vol. 122, no. 35, pp. 8581–8582, 2000.

[88] J. H. Park *et al.*, “Magnetic iron oxide nanoworms for tumor targeting and imaging,” *Adv. Mater.*, vol. 20, no. 9, pp. 1630–1635, 2008.

[89] S. J. Son, X. Bai, A. Nan, H. Ghandehari, and S. B. Lee, “Template synthesis of multifunctional nanotubes for controlled release,” *J. Control. Release*, vol. 114, no. 2, pp. 143–152, 2006.

[90] Z. Liu, S. Tabakman, K. Welsher, and H. Dai, “Carbon nanotubes in biology and medicine: In vitro and in vivo detection, imaging and drug delivery,” *Nano Res.*, vol. 2, no. 2, pp. 85–120, 2009.

[91] R. Singh *et al.*, “Tissue biodistribution and blood clearance rates of intravenously administered carbon nanotube radiotracers,” *Proc. Natl. Acad. Sci. U. S. A.*, vol. 103, no. 9, pp. 3357–3362, 2006.

[92] E. Umut, “Surface Modification of Nanoparticles Used in Biomedical Applications,” in *Modern Surface Engineering Treatments*, 2013, pp. 185–208.

[93] N. Tran and T. J. Webster, “Magnetic nanoparticles: Biomedical applications and challenges,” *J. Mater. Chem.*, vol. 20, no. 40, pp. 8760–8767, 2010.

[94] S. C. McBain, H. H. P. Yiu, and J. Dobson, “Magnetic nanoparticles for gene and drug delivery,” *Int. J. Nanomedicine*, vol. 3, no. 2, pp. 169–180, 2008.

[95] S. Doswald, W. J. Stark, and B. Beck-Schimmer, “Biochemical functionality of magnetic particles as nanosensors: How far away are we to implement them into clinical practice?,” *J. Nanobiotechnology*, vol. 17, no. 1, pp. 1–11, 2019.

[96] A. K. Gupta and M. Gupta, “Synthesis and surface engineering of iron oxide nanoparticles for biomedical applications,” *Biomaterials*, vol. 26, no. 18, pp. 3995–4021, 2005.

[97] A. Seyfoori, S. A. S. Ebrahimi, S. Omidian, and S. M. Naghib, “Multifunctional magnetic ZnFe 2 O 4 -hydroxyapatite nanocomposite particles for local anti-cancer drug delivery and bacterial infection inhibition: An in vitro study,” *J. Taiwan Inst. Chem. Eng.*, vol. 96, pp. 503–508, 2019.

[98] W. Ling *et al.*, “Synthesis, surface modification, and applications of magnetic iron oxide nanoparticles,” *J. Mater. Res.*, vol. 34, no. 11, pp. 1828–1844, 2019.

[99] N. Zhu *et al.*, “Surface modification of magnetic iron oxide nanoparticles,” *Nanomaterials*, vol. 8, no. 10, pp. 1–27, 2018.

[100] F. J. Lázaro, A. R. Abadía, M. S. Romero, L. Gutiérrez, J. Lázaro, and M. P. Morales, “Magnetic characterisation of rat muscle tissues after subcutaneous iron dextran injection,” *Biochim. Biophys. Acta - Mol. Basis Dis.*, vol. 1740, no. 3, pp. 434–445, 2005.

[101] A. A. Belanova, N. Gavalas, Y. M. Makarenko, M. M. Belousova, A. V. Soldatov, and P. V. Zolotukhin, “Physicochemical Properties of Magnetic Nanoparticles: Implications for Biomedical Applications in Vitro and in Vivo,” *Oncol. Res. Treat.*, vol. 41, no. 3, pp. 139–143, 2018.

[102] A. Ito, K. Ino, T. Kobayashi, and H. Honda, “The effect of RGD peptide-conjugated magnetite cationic liposomes on cell growth and cell sheet harvesting,” *Biomaterials*, vol. 26, no. 31, pp. 6185–6193, 2005.

[103] Z. Chunfu, C. Jinquan, Y. Duanzhi, W. Yongxian, F. Yanlin, and T. Jiajü, “Preparation and radiolabeling of human serum albumin (HSA)-coated magnetite nanoparticles for magnetically targeted therapy,” *Appl. Radiat. Isot.*, vol. 61, no. 6, pp. 1255–1259, 2004.

[104] N. Nitin, L. E. W. LaConte, O. Zurkiya, X. Hu, and G. Bao, “Functionalization and peptide-based delivery of magnetic nanoparticles as an intracellular MRI contrast agent,” *J. Biol. Inorg. Chem.*, vol. 9, no. 6, pp. 706–712, 2004.

[105] L. Chu *et al.*, “Synthesis and application of a series of amphipathic chitosan derivatives and the corresponding magnetic nanoparticle-embedded polymeric micelles,” *Carbohydr. Polym.*, vol. 223, no. June, p. 114966, 2019.

[106] Y. Wang *et al.*, “Recyclable Multifunctional Magnetic Mesoporous Silica Nanocomposite for Ratiometric Detection, Rapid Adsorption, and Efficient Removal of Hg(II),” *ACS Sustain. Chem. Eng.*, vol. 6, no. 2, pp. 1744–1752, 2018.

[107] R. Hardman, “A toxicologic review of quantum dots: Toxicity depends on physicochemical and environmental factors,” *Environmental Health Perspectives*, vol. 114, no. 2. pp. 165–172, 2006.

[108] Y. Xiao, K. T. Ho, R. M. Burgess, and M. Cashman, “Aggregation, Sedimentation, Dissolution, and Bioavailability of Quantum Dots in Estuarine Systems,” *Environ. Sci. Technol.*, vol. 51, no. 3, pp. 1357–1363, 2017.

[109] M. Aye *et al.*, “Genotoxic and mutagenic effects of lipid-coated CdSe/ZnS quantum dots,” *Mutat. Res. - Genet. Toxicol. Environ. Mutagen.*, vol. 750, no. 1–2, pp. 129–138, 2013.

[110] C. Ladhar *et al.*, “Impact of dietary cadmium sulphide nanoparticles on

Danio rerio zebrafish at very low contamination pressure," *Nanotoxicology*, vol. 8, no. 6, pp. 676–685, 2014.

[111] G. Libralato, E. Galdiero, A. Falanga, R. Carotenuto, E. De Alteriis, and M. Guida, "Toxicity Effects of Functionalized Quantum Dots, Gold and Polystyrene Nanoparticles on Target Aquatic Biological Models: A Review," *Molecules*, vol. 22, no. 9, 2017.

[112] D. Kwon, M. J. Kim, C. Park, J. Park, K. Choi, and T. H. Yoon, "In vivo biodegradation of colloidal quantum dots by a freshwater invertebrate, Daphnia magna," *Aquat. Toxicol.*, vol. 114–115, pp. 217–222, 2012.

[113] H. Zhu *et al.*, "Magnetic Porous Polymers Prepared via High Internal Phase Emulsions for Efficient Removal of Pb2+ and Cd2+," *ACS Sustain. Chem. Eng.*, vol. 6, no. 4, pp. 5206–5213, 2018.

[114] R. Nicola *et al.*, "Silica-coated magnetic nanocomposites for Pb2+ removal from aqueous solution," *Appl. Sci.*, vol. 10, no. 8, 2020.

[115] O. Plohl, M. Finšgar, S. Gyergyek, U. Ajdnik, I. Ban, and L. F. Zemljič, "Efficient copper removal from an aqueous anvironment using a novel and hybrid nanoadsorbent based on derived-polyethyleneimine linked to silica magnetic nanocomposites," *Nanomaterials*, vol. 9, no. 2, 2019.

[116] S. Bao, K. Li, P. Ning, J. Peng, X. Jin, and L. Tang, "Highly effective removal of mercury and lead ions from wastewater by mercaptoamine-functionalised silica-coated magnetic nano-adsorbents: Behaviours and mechanisms," *Appl. Surf. Sci.*, vol. 393, pp. 457–466, 2017.

[117] S. Villa, P. Riani, F. Soggia, E. Magi, and F. Canepa, "Thiol-functionalized magnetic nanoparticles for static and dynamic removal of Pb(II) ions from waters," *J. Nanoparticle Res.*, vol. 21, no. 3, 2019.

[118] Ş. Yılmaz, A. Zengin, Y. Akbulut, and T. Şahan, "Magnetic nanoparticles coated with aminated polymer brush as a novel material for effective removal of Pb(II) ions from aqueous environments," *Environ. Sci. Pollut. Res.*, vol. 26, no. 20, pp. 20454–20468, 2019.

[119] Y. Y. Yu, Q. W. Cheng, C. Sha, Y. X. Chen, S. Naraginti, and Y. C. Yong, "Size-controlled biosynthesis of FeS nanoparticles for efficient removal of aqueous Cr(VI)," *Chem. Eng. J.*, vol. 379, no. July 2019, p. 122404, 2020.

[120] B. Verma and C. Balomajumder, "Synthesis of magnetic nickel ferrites nanocomposites: An advanced remediation of electroplating wastewater," *J. Taiwan Inst. Chem. Eng.*, vol. 112, pp. 106–115, 2020.

[121] A. Gallo-Cordova, M. del P. Morales, and E. Mazarío, "Effect of the surface charge on the adsorption capacity of chromium(VI) of iron oxide magnetic nanoparticles prepared by microwave-assisted synthesis," *Water (Switzerland)*, vol. 11, no. 11, pp. 1–12, 2019.

[122] J. Alchouron *et al.*, "Assessing South American Guadua chacoensis bamboo biochar and Fe3O4 nanoparticle dispersed analogues for aqueous arsenic(V) remediation," *Sci. Total Environ.*, vol. 706, p. 135943, 2020.

[123] A. Ayub, Z. A. Raza, M. I. Majeed, M. R. Tariq, and A. Irfan, "Development of sustainable magnetic chitosan biosorbent beads for kinetic remediation of arsenic contaminated water," *Int. J. Biol. Macromol.*, vol. 163, pp. 603–617, 2020.

[124] H. Zeng, L. Zhai, T. Qiao, Y. Yu, J. Zhang, and D. Li, "Efficient removal of As(V) from aqueous media by magnetic nanoparticles prepared with Iron-containing water treatment residuals," *Sci. Rep.*, vol. 10, no. 1, pp. 1–12, 2020.

[125] X. Liu *et al.*, “Stimuli-responsive adsorption behavior toward heavy metal ions based on comb polymer functionalized magnetic nanoparticles,” *J. Clean. Prod.*, vol. 253, p. 119915, 2020.

[126] T. Chen, X. Quan, Z. Ji, X. Li, and Y. Pei, “Synthesis and characterization of a novel magnetic calcium-rich nanocomposite and its remediation behaviour for As(III) and Pb(II) co-contamination in aqueous systems,” *Sci. Total Environ.*, vol. 706, p. 135122, 2020.

[127] H. Wang *et al.*, “Functional group-rich hyperbranched magnetic material for simultaneous efficient removal of heavy metal ions from aqueous solution,” *J. Hazard. Mater.*, vol. 384, no. September 2019, p. 121288, 2020.

[128] E. K. Tetteh and S. Rathilal, “Application of magnetized nanomaterial for textile effluent remediation using response surface methodology,” *Mater. Today Proc.*, no. xxxx, 2020.

[129] Z. Wang *et al.*, “Highly effective remediation of Pb(II) and Hg(II) contaminated wastewater and soil by flower-like magnetic MoS2 nanohybrid,” *Sci. Total Environ.*, vol. 699, p. 134341, 2020.

[130] J. Lin, M. Sun, B. Su, G. Owens, and Z. Chen, “Immobilization of cadmium in polluted soils by phytogenic iron oxide nanoparticles,” *Sci. Total Environ.*, vol. 659, pp. 491–498, 2019.

[131] B. Eyvazi, A. Jamshidi-Zanjani, and A. Khodadadi Darban, “Immobilization of hexavalent chromium in contaminated soil using nano-magnetic MnFe2O4,” *J. Hazard. Mater.*, vol. 365, no. August 2018, pp. 813–819, 2019.

[132] J. H. Kim, S. M. Kim, I. H. Yoon, S. J. Choi, and I. Kim, “Selective separation of Cs-contaminated clay from soil using polyethylenimine-coated magnetic nanoparticles,” *Sci. Total Environ.*, vol. 706, p. 136020, 2020.

[133] D. Baragaño, J. Alonso, J. R. Gallego, M. C. Lobo, and M. Gil-Díaz, “Magnetite nanoparticles for the remediation of soils co-contaminated with As and PAHs,” *Chem. Eng. J.*, vol. 399, no. June, p. 125809, 2020.

[134] C. C. Fu, H. N. Tran, X. H. Chen, and R. S. Juang, “Preparation of polyaminated Fe3O4@chitosan core-shell magnetic nanoparticles for efficient adsorption of phosphate in aqueous solutions,” *J. Ind. Eng. Chem.*, vol. 83, pp. 235–246, 2020.

[135] P. Karthikeyan and S. Meenakshi, “In situ fabrication of magnetic particles decorated biopolymeric composite beads for the selective remediation of phosphate and nitrate from aqueous medium,” *J. Environ. Chem. Eng.*, vol. 8, no. 2, p. 103530, 2020.

[136] W. Gan, L. Gao, W. Zhang, J. Li, L. Cai, and X. Zhan, “Removal of oils from water surface via useful recyclable CoFe2O4/sawdust composites under magnetic field,” *Mater. Des.*, vol. 98, pp. 194–200, 2016.

[137] A. Kamgar and S. Hassanajili, “Super-hydrophobic Fe3O4@SiO2@MPS nanoparticles for oil remediation: The influence of pH and concentration on clustering phenomenon and oil sorption,” *J. Mol. Liq.*, vol. 315, 2020.

[138] T. Lü, Y. Chen, D. Qi, Z. Cao, D. Zhang, and H. Zhao, “Treatment of emulsified oil wastewaters by using chitosan grafted magnetic nanoparticles,” *J. Alloys Compd.*, vol. 696, pp. 1205–1212, 2017.

[139] S. F. Soares, M. I. Rodrigues, T. Trindade, and A. L. Daniel-da-Silva, “Chitosan-silica hybrid nanosorbents for oil removal from water,” *Colloids Surfaces A Physicochem. Eng. Asp.*, vol. 532, no. May, pp. 305–313, 2017.

[140] S. Mirshahghassemi, A. D. Ebner, B. Cai, and J. R. Lead, “Application of

high gradient magnetic separation for oil remediation using polymer-coated magnetic nanoparticles," *Sep. Purif. Technol.*, vol. 179, pp. 328–334, 2017.

[141] A. M. Atta *et al.*, "Green technology for remediation of water polluted with petroleum crude oil: Using of Eichhornia crassipes (Mart.) solms combined with magnetic nanoparticles capped with myrrh resources of Saudi Arabia," *Nanomaterials*, vol. 10, no. 2, 2020.

[142] W. Liao, Y. Ma, A. Chen, and Y. Yang, "Preparation of fatty acids coated Fe3O4 nanoparticles for adsorption and determination of benzo(a)pyrene in environmental water samples," *Chem. Eng. J.*, vol. 271, pp. 232–239, 2015.

[143] L. Hu *et al.*, "Adsorption behavior of dyes from an aqueous solution onto composite magnetic lignin adsorbent," *Chemosphere*, vol. 246, p. 125757, 2020.

[144] M. K. Seliem, M. Barczak, I. Anastopoulos, and D. A. Giannakoudakis, "A novel nanocomposite of activated serpentine mineral decorated with magnetic nanoparticles for rapid and effective adsorption of hazardous cationic dyes: Kinetics and equilibrium studies," *Nanomaterials*, vol. 10, no. 4, pp. 1–12, 2020.

[145] A. S. Liyanage, S. Canaday, C. U. Pittman, and T. Mlsna, "Rapid remediation of pharmaceuticals from wastewater using magnetic Fe3O4/Douglas fir biochar adsorbents," *Chemosphere*, vol. 258, p. 127336, 2020.

[146] I. A. Kumar and N. Viswanathan, "Development of Magnetic Particles Encrusted LDH-Admixed Biopolymeric Complex Beads for Selective Phosphate Remediation," *J. Chem. Eng. Data*, vol. 64, no. 12, pp. 5725–5736, 2019.

[147] S. Barua, S. Gogoi, R. Khan, and N. Karak, *Silicon-Based Nanomaterials and Their Polymer Nanocomposites*. Elsevier Inc., 2018.

[148] L. Chen *et al.*, "The toxicity of silica nanoparticles to the immune system," *Nanomedicine*, vol. 13, no. 15. pp. 1939–1962, 2018.

[149] M. Kim *et al.*, "An Evaluation of the in vivo Safety of Nonporous Silica Nanoparticles: Ocular Topical Administration versus Oral Administration," *Sci. Rep.*, vol. 7, no. 1, pp. 1–8, 2017.

[150] C. L. LIANG *et al.*, "Subchronic Oral Toxicity of Silica Nanoparticles and Silica Microparticles in Rats," *Biomed. Environ. Sci.*, vol. 31, no. 3, pp. 197–207, 2018.

[151] S. Murugadoss *et al.*, "Toxicology of silica nanoparticles: an update," *Archives of Toxicology*, vol. 91, no. 9. Springer Berlin Heidelberg, pp. 2967–3010, 2017.

[152] J. H. E. Arts, H. Muijser, E. Duistermaat, K. Junker, and C. F. Kuper, "Five-day inhalation toxicity study of three types of synthetic amorphous silicas in Wistar rats and post-exposure evaluations for up to 3 months," *Food Chem. Toxicol.*, vol. 45, no. 10, pp. 1856–1867, 2007.

[153] R. Merget *et al.*, "Health hazards due to the inhalation of amorphous silica," *Arch. Toxicol.*, vol. 75, no. 11, pp. 625–634, 2002.

[154] I. I. Slowing, J. L. Vivero-Escoto, C. W. Wu, and V. S. Y. Lin, "Mesoporous silica nanoparticles as controlled release drug delivery and gene transfection carriers," *Adv. Drug Deliv. Rev.*, vol. 60, no. 11, pp. 1278–1288, 2008.

[155] C. M. Li *et al.*, "Functionalized porous silica-based nano/micro particles for

environmental remediation of hazard ions," *Nanomaterials*, vol. 9, no. 2, 2019.

[156] F. P. Chang *et al.*, "A simple plant gene delivery system using mesoporous silica nanoparticles as carriers," *J. Mater. Chem. B*, vol. 1, no. 39, pp. 5279–5287, 2013.

[157] X. Wu, J. Hu, J. Qi, Y. Hou, and X. Wei, "Graphene-supported ordered mesoporous composites used for environmental remediation: A review," *Sep. Purif. Technol.*, vol. 239, no. January, p. 116511, 2020.

[158] L. Li *et al.*, "Unexpected Size Effect: The Interplay between Different-Sized Nanoparticles in Their Cellular Uptake," *Small*, vol. 15, no. 38, pp. 1–8, 2019.

[159] M. Yu *et al.*, "Size-dependent gene delivery of amine-modified silica nanoparticles," *Nano Res.*, vol. 9, no. 2, pp. 291–305, 2016.

[160] H. Sierra, M. Cordova, C. S. J. Chen, and M. Rajadhyaksha, "Confocal imaging-guided laser ablation of basal cell carcinomas: An ex vivo study," *J. Invest. Dermatol.*, vol. 135, no. 2, pp. 612–615, 2015.

[161] X. Huang, X. Teng, D. Chen, F. Tang, and J. He, "The effect of the shape of mesoporous silica nanoparticles on cellular uptake and cell function," *Biomaterials*, vol. 31, no. 3, pp. 438–448, 2010.

[162] N. Hao *et al.*, "The shape effect of PEGylated mesoporous silica nanoparticles on cellular uptake pathway in Hela cells," *Microporous Mesoporous Mater.*, vol. 162, pp. 14–23, 2012.

[163] X. Huang *et al.*, "The shape effect of mesoporous silica nanoparticles on biodistribution, clearance, and biocompatibility in vivo," *ACS Nano*, vol. 5, no. 7, pp. 5390–5399, 2011.

[164] P. G. Jeelani, P. Mulay, R. Venkat, and C. Ramalingam, "Multifaceted Application of Silica Nanoparticles. A Review," *Silicon*, vol. 12, no. 6, pp. 1337–1354, 2020.

[165] R. P. Bagwe, L. R. Hilliard, and W. Tan, "Bagwe 2006.pdf," *Langmuir*, vol. 22, no. 9, pp. 4357–4362, 2006.

[166] S. Wadhawan, A. Jain, J. Nayyar, and S. K. Mehta, "Role of nanomaterials as adsorbents in heavy metal ion removal from waste water: A review," *J. Water Process Eng.*, vol. 33, no. June 2019, p. 101038, 2020.

[167] R. P. Bagwe, L. R. Hilliard, and W. Tan, "Surface modification of silica nanoparticles to reduce aggregation and nonspecific binding," *Langmuir*, vol. 22, no. 9, pp. 4357–4362, 2006.

[168] W. He *et al.*, "Surface modification of colloidal silica nanoparticles: Controlling the size and grafting process," *Bull. Korean Chem. Soc.*, vol. 34, no. 9, pp. 2747–2752, 2013.

[169] S. Zeb *et al.*, "Silica-based nanomaterials as designer adsorbents to mitigate emerging organic contaminants from water matrices," *J. Water Process Eng.*, vol. 38, no. May, p. 101675, 2020.

[170] A. Walcarius and C. Delacôte, "Mercury(II) binding to thiol-functionalized mesoporous silicas: Critical effect of pH and sorbent properties on capacity and selectivity," *Anal. Chim. Acta*, vol. 547, no. 1, pp. 3–13, 2005.

[171] A. Arencibia, J. Aguado, and J. M. Arsuaga, "Regeneration of thiol-functionalized mesostructured silica adsorbents of mercury," *Appl. Surf. Sci.*, vol. 256, no. 17, pp. 5453–5457, 2010.

[172] R. Rostamian, M. Najafi, and A. A. Rafati, "Synthesis and characterization of thiol-functionalized silica nano hollow sphere as a novel adsorbent for

removal of poisonous heavy metal ions from water: Kinetics, isotherms and error analysis," *Chem. Eng. J.*, vol. 171, no. 3, pp. 1004–1011, 2011.

[173] J. Aguado, J. M. Arsuaga, A. Arencibia, M. Lindo, and V. Gascón, "Aqueous heavy metals removal by adsorption on amine-functionalized mesoporous silica," *J. Hazard. Mater.*, vol. 163, no. 1, pp. 213–221, 2009.

[174] E. Da'na and A. Sayari, "Adsorption of copper on amine-functionalized SBA-15 prepared by co-condensation: Equilibrium properties," *Chem. Eng. J.*, vol. 166, no. 1, pp. 445–453, 2011.

[175] A. Heidari, H. Younesi, and Z. Mehraban, "Removal of Ni(II), Cd(II), and Pb(II) from a ternary aqueous solution by amino functionalized mesoporous and nano mesoporous silica," *Chem. Eng. J.*, vol. 153, no. 1–3, pp. 70–79, 2009.

[176] X. Jiang, H. Wang, Q. Wang, E. Hu, and Y. Duan, "Immobilizing amino-functionalized mesoporous silica into sodium alginate for efficiently removing low concentrations of uranium," *J. Clean. Prod.*, vol. 247, p. 119162, 2020.

[177] J. Huang *et al.*, "Pb (II) removal from aqueous media by EDTA-modified mesoporous silica SBA-15," *J. Colloid Interface Sci.*, vol. 385, no. 1, pp. 137–146, 2012.

[178] P. Shao *et al.*, "Evaluating the adsorptivity of organo-functionalized silica nanoparticles towards heavy metals: Quantitative comparison and mechanistic insight," *J. Hazard. Mater.*, vol. 387, no. August 2019, p. 121676, 2020.

[179] B. Barik, A. Kumar, P. S. Nayak, L. S. K. Achary, L. Rout, and P. Dash, "Ionic liquid assisted mesoporous silica-graphene oxide nanocomposite synthesis and its application for removal of heavy metal ions from water," *Mater. Chem. Phys.*, vol. 239, no. August 2019, p. 122028, 2020.

[180] A. Chatterjee, S. Shamim, A. K. Jana, and J. K. Basu, "Insights into the competitive adsorption of pollutants on a mesoporous alumina-silica nano-sorbent synthesized from coal fly ash and a waste aluminium foil," *RSC Adv.*, vol. 10, no. 26, pp. 15514–15522, 2020.

[181] M. Maiti, M. Sarkar, S. Xu, S. Das, D. Adak, and S. Maiti, "Application of silica nanoparticles to develop faujasite nanocomposite for heavy metal and carcinogenic dye degradation," *Environ. Prog. Sustain. Energy*, vol. 38, no. s1, pp. S15–S23, 2019.

[182] M. E. Khalifa, E. A. Abdelrahman, M. M. Hassanien, and W. A. Ibrahim, "Application of Mesoporous Silica Nanoparticles Modified with Dibenzoylmethane as a Novel Composite for Efficient Removal of Cd(II), Hg(II), and Cu(II) Ions from Aqueous Media," *J. Inorg. Organomet. Polym. Mater.*, vol. 30, no. 6, pp. 2182–2196, 2020.

[183] R. Foroutan, R. Mohammadi, S. J. Peighambardoust, S. Jalali, and B. Ramavandi, "Application of nano-silica particles generated from offshore white sandstone for cadmium ions elimination from aqueous media," *Environ. Technol. Innov.*, vol. 19, p. 101031, 2020.

[184] Y. Wang *et al.*, "Long-term stabilization of Cd in agricultural soil using mercapto-functionalized nano-silica (MPTS/nano-silica): A three-year field study," *Ecotoxicol. Environ. Saf.*, vol. 197, no. January, p. 110600, 2020.

[185] Z. S. Khan *et al.*, "Effects of silicon nanoparticles on growth and physiology of wheat in cadmium contaminated soil under different soil moisture levels," *Environ. Sci. Pollut. Res.*, vol. 27, no. 5, pp. 4958–4968, 2020.

[186] Y. Wang *et al.*, “A field experiment on stabilization of Cd in contaminated soils by surface-modified nano-silica (SMNS) and its phyto-availability to corn and wheat,” *J. Soils Sediments*, vol. 20, no. 1, pp. 91–98, 2020.

[187] P. Cao *et al.*, “Mercapto propyltrimethoxysilane- and ferrous sulfate-modified nano-silica for immobilization of lead and cadmium as well as arsenic in heavy metal-contaminated soil,” *Environ. Pollut.*, vol. 266, p. 115152, 2020.

[188] A. F. Zarandi, H. Shirkhanloo, and P. Paydar, “A novel method based on functionalized bimodal mesoporous silica nanoparticles for efficient removal of lead aerosols pollution from air by solid-liquid gas-phase extraction 03 Chemical Sciences 0306 Physical Chemistry (incl. Structural),” *J. Environ. Heal. Sci. Eng.*, vol. 18, no. 1, pp. 177–188, 2020.

[189] A. Ebadi and A. A. Rafati, “Preparation of silica mesoporous nanoparticles functionalized with β-cyclodextrin and its application for methylene blue removal,” *J. Mol. Liq.*, vol. 209, no. 1, pp. 239–245, 2015.

[190] W. Czepa, D. Pakulski, S. Witomska, V. Patroniak, A. Ciesielski, and P. Samorì, “Graphene oxide-mesoporous SiO2 hybrid composite for fast and efficient removal of organic cationic contaminants,” *Carbon N. Y.*, vol. 158, pp. 193–201, 2020.

[191] M. Abboud *et al.*, “Synthesis and characterization of lignosulfonate/amino-functionalized SBA-15 nanocomposites for the adsorption of methylene blue from wastewater,” *New J. Chem.*, vol. 44, no. 6, pp. 2291–2302, 2020.

[192] N. Alotaibi, H. H. Hammud, R. K. Karnati, S. G. Hussain, J. Mazher, and T. Prakasam, “Cobalt-carbon/silica nanocomposites prepared by pyrolysis of a cobalt 2,2′-bipyridine terephthalate complex for remediation of cationic dyes,” *RSC Adv.*, vol. 10, no. 30, pp. 17660–17672, 2020.

[193] C. H. Tsai, W. C. Chang, D. Saikia, C. E. Wu, and H. M. Kao, “Functionalization of cubic mesoporous silica SBA-16 with carboxylic acid via one-pot synthesis route for effective removal of cationic dyes,” *J. Hazard. Mater.*, vol. 309, pp. 236–248, 2016.

[194] J. Sorwat, A. Mellage, A. Kappler, and J. M. Byrne, “Immobilizing magnetite onto quartz sand for chromium remediation,” *J. Hazard. Mater.*, vol. 400, no. February, p. 123139, 2020.

[195] A. Sundman *et al.*, “Effect of Fe-metabolizing bacteria and humic substances on magnetite nanoparticle reactivity towards arsenic and chromium,” *J. Hazard. Mater.*, vol. 384, no. July 2019, p. 121450, 2020.

Chapter 2 – Toxicity of Silica and Magnetic Nanoparticles

1. Nanotoxicology

For the NPs to be used in environmental applications, toxicity is, without doubt, one of the key aspects to be clarified. Thus, studies on the toxicity of NPs *in vitro* and *in vivo* are of great importance to understand nanoparticle–cell interactions and possible toxic effects to living organisms.

In the literature, nanoparticle-associated toxicity is linked to the accumulation of the NPs in specific organs, increasing the probability to provoke intracellular changes that, in its turn, might affect cellular and, consequently, organ functions [1]. It is already reported that NMs often have effects regarding the metabolic activity of cells, their membrane integrity and induction of cell apoptosis and proliferation, which has been linked to the formation of ROS [2–10]. Cells respond to increased levels of ROS by activating “detoxification” mechanisms that involve non enzymatic defences (e.g. non protein thiols like glutathione) and antioxidant enzymes (e.g. superoxide dismutase (SOD), catalase (CAT) and glutathione peroxidase (GPX)). These responses may provide information on the ability of NPs to produce sublethal effects. Among the reported toxic effects are lipid peroxidation, DNA strand breaks, alteration in gene transcription, and generation of protein radicals [4]. It is then safe to say that if the NPs induce the formation of ROS, they might as well increase the risk for these oxidative related effects to happen. But, as widely recognized, NPs toxicity depends on numerous factors including, dose, chemical composition, method of administration, size, biodegradability, solubility, biodistribution, surface chemistry, shape and structure. Therefore, to fully understand and assess the toxicity of NPs, these aspects must be taken into consideration. The modification of the surface properties can also be a main tool to modulate their toxicity, and one to evaluate as well [1], [4], [11].

2. Magnetic Nanoparticles

2.1. *in vitro* Studies

MNPs are a great resource and useful in numerous applications. However, their toxicologic profile is yet to be fully understood, there are numerous aspects needing to be addressed. Iron oxide MNPs in the blood stream face the initial uptake via endocytosis in Kupffer cells of the liver and macrophages of spleen (REF). They are then degraded in the lysosomes by macrophages releasing free iron. These released iron ions can participate in the Fenton reaction to produce hydroxyl radicals and can also be stored in the form of proteins, such as ferritin. When the iron storage capacity of these proteins is exceeded, the iron overload can trigger the production of ROS [4]. Thus, to better comprehend their potential toxic effect at a cellular level, some studies *in vitro* have already been performed.

For instance, Pöttler *et al*. (2015), examined the role of different coatings in the biocompatibility of the MNPs, studying the genotoxic effects of lauric acid- (SEON^{LA}), bovine serum albumin- (SEON$^{LA\text{-}BSA}$) and dextran-coated SPIONs (SEON^{DEX}) on human granulosa cells (HLG-5), very important for female fertility. These different coatings of SPIONs improve biocompatibility as neither of them presented relevant genotoxicity towards the cells at 50, 100 and 150 µg.mL^{-1}[12]. Berry *et al*. (2003), studying the effects of dextran derivatized, albumin derivatized and underivatized magnetite NPs in human fibroblasts, found that there is a rapid uptake and internalisation through endocytosis by human fibroblasts, and that derivatization of the NPs with either dextran or albumin altered the pattern of this uptake. The dextran NPs and underivatized MNPs caused cell death, formation of vacuoles and inhibition of cell proliferation whereas the albumin derivatised NPs, induced cell proliferation [13]. This study not only highlighted the importance of the surface modifications of MNPs but also the ability of these particles to induce toxic effects, even though it is suggested that MNPs present low cytotoxic action in concentrations relevant for biomedical and environmental use [14]. Dextran- and citric acid-coated MNPs at a concentration of 0.08 to 20 mM drastically affected human umbilical vein endothelial cells (HUVECs) growth and proliferation, a phenomenon attributed to the ROS generation through iron-catalysed Haber- Weiss reactions and auto phagocytosis that caused cell morphology changes and, consequently, cell death. Changes in cytoskeleton organization and cell morphology, like cell retraction, rounding, disruption of F-actin and microtubules, were also observed [15]. Iron oxide NPs uptake by Porcine aortic endothelial cells (PAEC) has been shown to increase the intracellular levels of ROS in a dose- and time-dependent manner, as the cells elongated and formed actin stress fibres in response. Interestingly, when ROS formation was blocked using scavengers, the actin cytoskeleton remained intact and cell viability was increased, which implies that the formation of ROS might be the main mechanism of toxicity behind the observed effects [16].

When Arbab *et al*. (2003), evaluated the effect of the ferumoxides–poly-L-lysine (PLL) complex in human mesenchymal stem cells and human cervical carcinoma cells, namely HeLa cells, they found that the ferumoxides-PLL complex at a concentration of 25 µg.mL^{-1} had no short or long-term effects on cell viability, proliferation, rates of apoptosis or ROS formation of human mesenchymal stem cells or human cervical carcinoma cells [17]. Khalid *et al*. (2018), in their turn, studied the effects of dextran 70,000-coated SPIONs in C6 glioma cells and primary neural cells. The results indicated that these MNPs were non-toxic but only at low concentrations, below 250 µg.mL^{-1} and at short incubation times. The same was noted on primal neural cells, as no detectable toxic effects were found when the NP concentrations were 62 µg.mL^{-1} or lower [3]. In another study on neural cells, Berman *et al*. (2013), labelled C17.2 murine neural stem cells with rhodamine-SPIONs and found that SPIO-labelling can reduce the overall motility of transplanted cells, with exocytosis of SPIONs mitigating this effect [18]. Cengelli *et al*. (2006), evaluated the brain biocompatibility and the potential for drug delivery to the brain of dextran- and PVA-coated iron oxide MNPs, observing that none of the NPs was cytotoxic or induced the production of inflammatory mediators [19].

Zhang *et al*. (2010), investigated the effects of *in vitro* exposure of Caco-2 human intestinal cells to hematite MNPs according to the concentration (100, 200 and 300 mg.L^{-1}) and particle size (26, 53, 76 and 98 nm) on the adsorption behaviours and on cellular impairment, observing adverse cellular effects, such as dynamic reorganization and detachment of microvilli structures on Caco-2 cell surfaces, mainly caused by the smallest MNPs with 26 nm [20]. These findings were in line with the ones obtained by Kalive *et al*. (2012), that also evaluated the effect of 10 mg.L^{-1} of different-sized hematite MNPs (17, 53, and, 100 nm) on their potential cytotoxicity in Caco-2 human intestinal cells [21]. The 17 nm NPs were reported as the most toxic to the epithelial integrity causing disruption of epithelial structures such as apical microvilli and disruption of the cell–cell junctions [21]. Thus, both studies demonstrated a tendency for the smallest size NPs to generate more toxic effects compared to bigger ones. However, information on the size effects on MNP behaviour and toxic effects in living beings and cellular lines is still poorly studied, which, given its importance, should be addressed in more depth by future works.

Table 1. Toxicity of various MNPs in vitro according to their concentration.

MNP	Sample	Concentration	Toxicity	Reference
$Fe_3O_4^{DEX}$ $Fe_3O_4^{BSA}$ Fe_3O_4	Infinity Telomerase Immortalised primary human fibroblasts (hTERT-BJ1)	-	$Fe_3O_4^{DEX}$ and Fe_3O_4: formation of vacuoles; inhibition of cell proliferation; cell death	[13]
$IONP^{DEX}$ $IONP^{CA}$	Human umbilical vein endothelial cells (HUVECs)	0.08–20 mM	Inhibition of cells growth and proliferation; free radical generation; cell morphology changes; cell death.	[15]
Fe_3O_4	Porcine aortic endothelial cells (PAEC)	0–1.0 mg. mL^{-1}	Free radical generation; actin stress fibre formation; increased cell stiffness; cell death	[16]
Ferumoxides-PLL complex	HeLa Cells	25 µg.mL^{-1}	-	[17]

Rhodamine-SPIO	C17.2 murine NSCs	25 mg. mL^{-1}	Reduced cell motility	[18]
α-Fe_2O_3	Caco-2 human intestinal cells	100 mg.L^{-1} 200 mg.L^{-1} 300 mg.L^{-1}	Dynamic reorganization; detachment of microvilli structures; junctional disruption	[20]
α-Fe_2O_3	Caco-2 human intestinal cells	10 mg.L^{-1}	Detachment of microvilli structures; junctional disruption	[21]

2.2. *in vivo* Studies

Although some studies addressed the *in vitro* toxicity of these MNPs, there is still a lack of crucial information about their *in vivo* behaviour such as their pharmacokinetics, bioavailability, and, above all, toxicity. Thus, to adequately evaluate the MNPs potential toxicity, especially in environmental applications, *in vitro* studies should be complemented with *in vivo* studies. To study the effects of 40 mg/kg of fluorescein-loaded magnetic nanoparticles (FMNPs) and fluorescein-loaded magnetic nanoparticles functionalized with polyamide-amine (PAMAM) dendrimer (PFMNPs) in ICR mice (6 weeks old with body weight of 20–25 g), their biodistribution and free iron liberation by the MNPs were evaluated by Zhao *et al*. (2014), that found that FMNPs modified with PAMAM had a low uptake in the lungs and liver and high distribution in brain and testicles of the mice, with no detectable physiological changes that could relate to organ toxicity [22]. Similar results were found by Kim *et al*. (2006) also in mice, using silica-overcoated MNPs containing rhodamine B isothiocyanate (RITC) within a silica shell [MNPs@SiO_2(RITC)] [23]. The toxic effects of PEG functionalized iron oxide and ferrite manganese NPs in cell cultures, *Danio rerio* embryos and in mice [24] were assessed by Caro *et al*. (2019), observing that at concentrations of 50 μg.mL^{-1}, iron oxide NPs induced no mortality and did not interfere with the normal hatching rate of zebrafish embryos. However, in contrast to *in vitro* results, significant toxicity, represented by the low survival rate, after 6 days, were found for *D. rerio* embryos exposed to 100 μg.mL^{-1} manganese ferrite MNPs [24]. In their turn, Madhubala *et al*. (2019), exposed *D. rerio* embryos to different shapes and concentrations of α-Fe_2O_3 NPs (0.39, 0.78, 1.56, 3.13, 6.25, 12.5, 25 and 50 μg.mL^{-1}) and monitored their potential physical anomalies. Highly crystalline rhombohedral and hexagonal shaped α-Fe_2O_3 NPs with particles size around 200 nm expressed less toxicity on early life stages of zebrafish compared to nanorods, cubic and needle-shaped NPs. At low concentrations, up to 12.5 μg.mL^{-1}, the α-Fe_2O_3 NPs were non-toxic, however, at higher concentrations some malformations were reported [25]. Similar results were obtained by Jurewicz *et al*. (2020), as minimal toxic effects were observed in *D. rerio* embryos, this time at a high concentration (800 µg.mL^{-1}) of Fe_3O_4 conjugated with CR dye, causing, however mortality and delay in hatching cycles. Furthermore, a life stage dependent toxicity was found, increasing when the exposures start at the larval life stage (at 2 weeks) [26]. *In vivo* evaluation of the acute toxicity of cobalt ferrite ($CoFe_2O_4$) NPs (40nm; 10–500µM) in larval-embryo *D. rerio,* performed by Ahmad *et al*., (2015), revealed acute developmental toxicity including apoptosis, decreased metabolism, hatching delay, instable heartbeat, cardiac/yolk sac edema, tail and spinal cord flexture, and loss of membrane integrity in the head, heart and tail region, probably due to the generation of ROS. In addition, behavioural changes were also observed, being this, one of the few studies to date to consider the behaviour as an integral part of *in vivo* evaluation of MNPs toxicity [27]. Another one was carried by Malhotra *et al*. (2019), in which behavioural changes in *D. rerio* at low (1 ppm) or high (10 ppm) concentration levels of Fe_3O_4 MNPs were assessed, with modest reduction in fish exploratory behaviour and a significant reduction in conspecific social interaction behaviour reported in the higher concentration. In addition, the fish also had elevated cortisol, acetylcholine and CAT levels and a reduction in serotonin, acetylcholine esterase, and dopamine levels in the brain [28].

According to Ahmad *et al.* (2015)*,* the endocrine disruption potential of these MNPs is also a concern, although poorly studied. Thus, the authors proposed to evaluate the thyroid endocrine disrupting ability of $CoFe_2O_4$ NPs (0, 10, 62.5,125, 250, and 500 µM) in zebrafish larvae for 168-h post fertilization (hpf), observing elevated amounts of thyroxine (T4) and triiodothyronine (T3) hormones due to malformation of the hypothalamus pituitary axis in zebrafish larvae. These amounts of T4 and T3 hormones, in turn, lead to delayed hatching, head and eye malformation, arrested development, and alterations in metabolism and DNA [29]. Villacis *et al*. (2017), assessed the toxicity of maghemite NPs, at concentrations ranging from 4.7 to 74.4 mg.L^{-1}, using adult *D. rerio* and a combination of classical (genotoxicity, oxidative stress) and molecular (transcriptomic) methodologies. A significant number of DNA lesions were found at all concentrations tested, the mRNA expression of genes related to cation/metal ion binding, membrane formation, and morphogenesis were among the transcripts overrepresented and mRNAs encompassing genes associated with RNA biogenesis, translation, ribosomes, and several metabolic processes underrepresented, which could be translated to genotoxic effects affecting cell growth and their ability to produce new proteins [30].

Zheng *et al*. (2018), tried to understand the impact of coatings on the toxicity of NPs, characterizing gill and liver transcriptomes from adult *D. rerio* exposed to 100 mg.L^{-1} of bare and starch stabilized Fe_3O_4 NPs. As a result they found that the MNPs could induce oxidative stress, DNA damage, and apoptosis in liver, with coating mitigating the toxic effects of Fe_3O_4 NPs on gill, but intensifying the hepatic toxicity [31]. Also, regarding the role of the coatings in the toxicity of

MNPs, Oliveira *et al*. (2020), studied the effect of dextran, chitosan, polyethylene glycol, carboxy-silane, and silica coatings in the potential toxicity of SPIONs in *D. rerio* embryos. Using concentrations of MNPs ranging from 0.125 to 8.0 mM, the authors observed that the coating really plays an important role in the toxicity of these NPs, with dextran coated MNPs exhibiting no toxic effects, and chitosan-coated NPs presenting the highest toxicity in terms of survival and behavioural parameters, with mortality levels reaching 100% in concentration is higher than 2 mM [32]. In a similar study de Oliveira *et al.* (2017), also observed that exposure to dextran coated MNPs did not cause significant mortality nor changes in hatching rate of zebrafish larvae, noticing, however, that at lower concentrations (1 µg.mL^{-1}) the MNPs tended to be better absorbed by zebrafish larvae and damage the locomotor behaviour. In fact, at that concentration there seems to be effects at the transcriptional level, impairing the locomotor behaviour, possibly involving inflammation- and apoptosis-related processes [33].

In another approach, Gebara *et al*. (2019), evaluated the acute and chronic effects of various concentrations (0.00; 0.01; 0.10; 1.00; 10.00 and 100.00 mg.L^{-1}) of iron oxide NPs (Fe_3O_4-NPs) to *Ceriodaphnia silvestrii*, considering endpoints such as immobility, lethality and physiological responses. Regarding acute toxicity, even though no immobility was found, the respiration rates at the highest concentration were much higher than those in the control, indicating that this endpoint was more sensitive during acute toxicity. In chronic assays, Fe_3O_4-NPs provoked growth inhibition and inhibited reproduction, being that the toxicity may be due to disturbed food absorption, being found agglomerates in the digestive tract of the individuals [34]. Marimon-Bolívar *et al*. (2019), studied the potential effects of Glutathione@MNPs to the nematode *Caenorhabditis elegans*, after its application in the remediation of pollutants in water, evaluating mortality, fertility, growth, mobility and gene expression upon exposure to different concentrations of MNPs (10–200 mg.L^{-1}). Even though the MNPs did not produce a significant effect in terms of mortality, growth and gene expression, the fertility of the nematode was reduced up to 52% and locomotion 25% in organisms exposed the concentration of 200 mg.L^{-1} of MNPs [35]. The toxicity and potential alterations of relevant physiological parameters caused to the microalga *Chlamydomonas reinhardtii* upon exposure to synthetic γ-Fe_2O_3 or Fe_3O_4 NMs with DMSA coating with different concentrations (0-100 mg.L^{-1}) was studied by Hurtado-Gallego *et al*. (2020), that found that these MNPs could inhibit algal growth and induce the production of ROS, as well as alter photosynthesis of *C. reinhardtii* by diminishing the access of light [36]. Piccinetti *et al*. (2014), in order to study the behaviour and effects of MNPs through the food web, investigated the effects of silica-coated MNP (Si@Fe_3O_4) when administered through food (zooplankton) in *D. rerio* individuals. The NPs did not induce toxicity in the *D. rerio*, a fact that the authors associated to the silica shell coating that prevented interactions with biological systems. There was also no evidence of NP build-up in organs, tissues (including liver), or cells, and no signs of activation of stress pathways or detoxification processes, which suggests that these MNPs found in contaminated food are not processed as toxic matter, but as indigestible compounds, being excreted through faeces [37].

However, the actual MNPs concentrations in environment are not known. The MNPs concentrations used in some remediation processes are much higher than the concentrations that were toxic in many of the above mentioned studies [36]. Therefore, the use of SPIONs for site remediation may cause increased concentrations in aquatic environment. To address this issue, Coppola *et al*. (2019), evaluated the ecotoxicological risk of seawater previously contaminated with arsenic (As) and remediated by using manganese-ferrite NPs ($MnFe_2O_4$-NPs), exposing the mussel species *Mytilus galloprovincialis* to As (1000 $\mu g.L^{-1}$) contaminated and remediated (As 70 $\mu g.L^{-1}$) seawater and water containing $MnFe_2O_4$- NPs (50 $mg.L^{-1}$) with and without the presence of As. The organisms exposed to seawater previously contaminated with As and remediated by $MnFe_2O_4$- NPs presented significantly less effects (oxidative related parameters and metabolism) than those exposed to As contaminated water [38].

Table 2. Toxicity of various MNPs in vivo according to their concentration.

NP	Sample	Concentration	Toxicity	Reference
$MnFe_2O_4$	*Danio rerio* embryos	100 $mg.L^{-1}$	Low percentage of survival 6 days post fertilization	[24]
α-Fe_2O_3	*Danio rerio* embryos	12.5 $\mu g.ml^{-1}$	Malformations	[25]
CR@Fe_3O_4	*Danio rerio* embryos	800 $\mu g.mL^{-1}$	Mortality and delay in hatching cycles	[26]
$CoFe_2O_4$	*Danio rerio* embryos	10–500 µM	Apoptosis; decreased metabolism; hatching delay; instable heartbeat; cardiac/yolk sac edema; tail and spinal cord flexture; loss of membrane integrity	[27]
Fe_3O_4	*Danio rerio* embryos	1 ppm 10 ppm	Reduction in fish exploratory behaviour; reduction in conspecific social interaction; elevated cortisol, acetylcholine, catalase; reduced serotonin, acetylcholine esterase, dopamine levels	[28]

$CoFe_2O_4$	*Danio rerio* embryos	10-500 µM	Malformation of the hypothalamus pituitary axis; elevation of T4 and T3 hormone level; delayed hatching; head and eye malformation; arrested development; alterations in metabolism and DNA	[29]
γ-Fe_2O_3	*Danio rerio*	4.7-74.4 mg.L^{-1}	DNA lesions; genotoxic effects related to cell growth and protein production	[30]
Fe3O4 Starch- Fe3O4	*Danio rerio*	100 mg.L^{-1}	Oxidative stress; DNA damage; apoptosis in liver	[31]
SPION-CS	*Danio rerio* embryos	0.125 - 8.0 mM	Behavioural changes; 100% of mortality when concentration was 2 mM or higher	[32]
CLIO-NH2	*Danio rerio* larvae	1 µg.mL^{-1}	Effects at the transcriptional level; locomotor behaviour impairment	[33]
Fe_3O_4	*Ceriodaphnia silvestrii*	0.01-100 mg.L^{-1}	Growth inhibition; inhibited reproduction; agglomerates in the digestive tract	[34]
Glutathione@MNPs	*Caenorhabditis elegans*	10–200 mg.L^{-1}	Reduction in fertility Reduction in locomotion	[35]
DMSA@γ-Fe2O3 DMSA@Fe3O4	*Chlamydomonas reinhardtii*	0-100 mg.L^{-1}	Inhibition of algal growth; free radical generation; alteration of photosynthesis	[36]

3. Silica Nanoparticles

One of the main reasons for silica NPs varied applications is their supposed superior biocompatible properties. However, some studies have already indicated correlations between these NPs and ROS generation and increased oxidative stress [39], with NP surface area, dependent on particle size, recognized as one of the most critical factors contributing to toxicity in both *in vitro* and *in vivo* experiments.. Furthermore, it has already been reported that, while amorphous silica is considered safe, crystalline silica is capable to induce chronic obstructive pulmonary disease, silicosis, and lung cancer [40]. Thus, as the use of SiO_2 NPs may lead to increased bioavailability to organisms, in the case of environmental applications, or because it requires administration to target sites within the body via ingestion, inhalation, intravenous injection, or transdermal penetration, in the case of biomedical applications, investigation and understanding of their uptake, retention, cytotoxic potential, and cellular interactions in different tissues, organs and organisms are of critical importance [40].

3.1. *in vitro* Studies

Some studies *in vitro* have been performed, and even though SiO_2 NPs are considered safe, some toxic effects have been reported. For instance, Park *et al*. (2019), used well characterized SiO_2 NPs of various sizes in a concentration range of 1-100 $\mu g.mL^{-1}$ to investigate whether these NPs are able to inhibit the differentiation of mouse embryonic stem cells. The authors found that NPs provoke inhibition of the differentiation of D3 cells, which indicates that the widespread application of amorphous SiO_2 NPs may not be without health hazards [41]. Kim *et al*. (2015), found that monodisperse spherical SiO_2 NPs with diameters of 20–200 nm, at concentrations ranging from 10 to 500 $\mu g.mL^{-1}$ produce effects in A549 and HepG2 epithelial cells and NIH/3T3 fibroblasts. For the A549 and NIH/3T3 cells, SiO_2 NPs of all sizes caused a reduction in viability at doses ≥50 $\mu g.mL^{-1}$, while HepG2 cells did not show size dependent changes in viability in response to SiO_2 NPs doses greater than 50 $\mu g.mL^{-1}$, except for the highest dose of 60 nm SiO_2 NPs. Furthermore, the authors observed that 60 nm NPs at 500 $\mu g.mL^{-1}$ induce a high reduction in GSH levels and an increase in ROS production in all three cell types [40]. In fact, in another similar study in which Ahmad *et al.* (2012), tested the toxicity of 14 nm SiO_2 NPs (25–200 $\mu g.mL^{-1}$) in human liver cell line HepG2. The SiO_2 NPs induced oxidative stress by induction of ROS resulting in lipid peroxidation and depletion of glutathione (GSH). Also, the authors not only found that both the mRNA and protein expressions of cell cycle checkpoint gene p53 and apoptotic genes (bax and caspase-3) were up-regulated while the anti-apoptotic gene bcl-2 was down-regulated in exposed cells, but also that co-treatment of ROS scavenger vitamin C significantly attenuated the modulation of apoptotic markers [42]. Similar results in the same parameters were found by Sun *et al.* (2013)*,* this time following a 43 nm non-modified amorphous SiO_2 NPs exposure (25–200 $\mu g.mL^{-1}$) [43].

Feng *et al.* (2020)*,* in their turn, explored the adverse effects and underlying mechanisms of subacute exposure to 25 $\mu g.mL^{-1}$ of SiO_2 NPs on Human cardiomyocytes cell line AC16 and in mice, reporting that the NPs promoted a cardiac inflammatory response, oxidative damage and myocardial contractile dysfunction, accompanied with increased levels of ROS, Ca^{2+} overload and apoptosis of cardiomyocytes, being the JNK/TF/PAR1 signalling pathway critical for the myocardial contractile dysfunction [44]. In mouse keratinocytes (HEL-30), Yu *et al.* (2009)*,* examined the uptake, localization, and the cytotoxic effects of different concentrations of well-dispersed amorphous silica nanoparticles with 30, 48, 118, and 535 nm (10, 50, 100, and 200 µg.mL^{-1}). Even though all sizes of silica were taken up into the cells and localized into the cytoplasm, the ones exhibiting significant toxicity, including depletion of GSH levels and mitochondria unviability, were the NPs with 30 and 48 nm at 100 µg.mL^{-1}, reinforcing the idea that the size of the particles is critical to produce biological effects [45]. Vo *et al.* (2014)*,* in another approach, studied the effect of SiO_2 NPs with different sizes (16, 24 and 44 nm) and concentrations (1.8–1,800 µg.mL^{-1}) in the cell viability of twelve adherent fish cell lines derived from six species, namely *Oncorhynchus mykiss* (RTgill-W1, RTgut-GC, RTL-W1, RTBrain), *Pimephales promelas* (FHML2-6, FHMT-W1), *D. rerio* (GloFish, ZEB2J), *Carassius auratus* (GFB3C, GFSk-S1), *Melanogrammus aeglefinius* (HEW), and *Anguilla rostrata* (EelBrain), observing morphological alterations such as cell shivering, cell detachment from the tissue culture surfaces, nuclear condensation, disruption of cell monolayers, and accumulation of cell fragmented debris, being that the cells were altered more severely and the cell monolayers were damaged more quickly upon exposure to 16 nm NPs [46]. In their turn, Huang *et al*. (2010), found that particles with larger aspect ratios, in a concentration of 50 mg.mL^{-1}, can be more readily internalized in A375 human melanoma cells by nonspecific cellular uptake, also having a greater impact on different aspects of cellular function including cell proliferation, apoptosis, cytoskeleton formation, adhesion and migration [47]. Moreover, Passagne *et al.* (2012)*,* studied the cytotoxicity of SiO_2 NPs with 20 and 100 nm with concentrations of 10 µg.mL^{-1} and 25 µg.mL^{-1}, respectively, on two renal proximal tubular cell lines (human HK-2 and porcine LLC-PK1). They found that the internalization process of NPs in the cells was by macropinocytosis and clathrin-mediated endocytosis, with NPs with 100 nm found in vesicles. Toxicity increased with NPs size decrease, being oxidative stress pointed as the major mechanism through the formation of ROS and lipid peroxidation [48]. With another approach, Lin *et al*. (2006), investigated the cytotoxicity of 15 nm and 46 nm SiO_2 NPs in cultured human bronchoalveolar carcinoma-derived cells, using concentrations between 10 and 100 µg.mL^{-1}. A decrease in cell viability, with both NPs promoting the formation of ROS, reduction of glutathione levels, increased production of malondialdehyde and release of lactate dehydrogenase by the cells, indicating lipid peroxidation and membrane damage were among the toxic effects reported [49].

Liang *et al.,* explored the role of the surface coating in the toxicity of SiO_2 NPs, studying the biocompatibility of PEG-modified and PEG-unmodified of RhB-encapsulating SiO_2 NPs (35 nm) in endothelial cells and zebrafish. The SiO_2 NPs modified with PEG were found to effectively alleviate the cytotoxicity, inflammation and vascular endothelial damage *in vitro* and *in vivo*, since there was a reduction of inflammatory response and vascular damage, with a significant decline in the levels of ROS, inflammatory cytokines and mitochondrial-mediated apoptosis in vascular endothelial cells compared to SiNPs [50]. In another study addressing the effect of coating in the toxicity of these NPs, Christen *et al.* (2012), compared the effects of SiO_2 NPs and SiO_2 NPs doped with silver (SiO_2–Ag-NPs) on survival and cellular function of human liver cells (Huh7) and *Pimephales promelas* (fathead minnow) fibroblast cells (FMH). They found aggregates in cell culture media and in vesicular-like structures of the cells, with cytotoxicity more pronounced in Huh7 than in FMH cells, increasing with silver content in silver-doped NPs. In fact, according to the authors, the silver ions released from the NPs were the most significant factor for cytotoxicity, inducing perturbations in the function of ER, as there was an induction of the expression of Binding immunoglobulin protein (BiP) and splicing of XBP1 mRNA, two selective markers of ER stress. Additionally, both NPs were found to promote the formation of ROS and a significant reduction in the levels of CYP1A activity [51].

Table 3. Toxicity of SiO_2 NPs in vitro according to their concentration.

MNP	Sample	Concentration	Toxicity	Reference
SiO_2 NPs	D3 embryonic stem cells	1-100 $\mu g.ml^{-1}$	Inhibition of the cell differentiation	[41]
SiO_2 NPs	A549 cell line HepG2 cell line NIH/3T3 fibroblasts	10-500 $\mu g.ml^{-1}$	Reduction in viability; loss of membrane integrity; reduction in GSH levels; increase in ROS production	[40]
SiO_2 NPs	HepG2 cell line	25–200 $\mu g.ml^{-1}$	Induction of ROS; lipid peroxidation; depletion of GSH; up-regulation of gene p53 and apoptotic genes (bax and caspase-3); down-regulation of apoptotic gene bcl-2	[42]
SiO_2 NPs	HepG2 cell line	25-200 $\mu g.ml^{-1}$	ROS production; mitochondrial damage; cell apoptosis	[43]
SiO_2 NPs	Human cardiomyocytes cell line AC16	25 $\mu g.ml^{-1}$	Cardiac inflammatory response; myocardial contractile dysfunction, increased levels of ROS; Ca^{2+} overload; apoptosis of cardiomyocytes	[44]

SiO_2 NPs	Mouse keratinocytes (HEL-30)	10-200 μg.ml^{-1}	Depletion of GSH levels; Compromised mitochondrial function	[45]
SiO_2 NPs	RTgill-W1 RTgut-GC RTL-W1 RTBrain FHML2-6 FHMT-W1 GloFish ZEB2J GFB3C GFSk-S1 HEW EelBrain	1.8–1,800 μg.ml^{-1}	Cell shivering; cell detachment; nuclear condensation; disruption of cell monolayers; accumulation of cell fragmented debris	[46]
NS100 NSR240 NLR450	A375 human melanoma cells	50 mg.ml^{-1}	Impact on cell proliferation, apoptosis, cytoskeleton formation, adhesion and migration	[47]
SiO_2 NPs	Human renal proximal tubular cell lines HK-2 Porcine renal proximal tubular cell lines LLC-PK1	10 μg.ml^{-1} (20 nm) 25 μg.ml^{-1} (100 nm)	Increased cytotoxicity with smaller size; formation of ROS; lipid peroxidation	[48]
SiO_2 NPs	Human bronchoalveolar carcinoma-derived cells	10 μg.ml^{-1} 100 μg.ml^{-1}	Decrease in cell viability; formation of ROS; reduction in glutathione levels; increased production of malondialdehyde; release of lactate dehydrogenase; lipid peroxidation	[49]
SiO_2 NPs	Tg (fli-1: EGFP) Tg (mpo: GFP)	12.5, 25, 50, 100 μg.ml^{-1}	increased levels of ROS; increased inflammatory cytokines; mitochondrial-mediated apoptosis	[50]
PEG@SiO_2 NPs			-	
SiO_2 NPs SiO_2–Ag NPs	Human liver cells (Huh7) *Pimephales promelas*	1-0.0075 mg.mL^{-1}	Increasing cytotoxicity with silver content; perturbations in the function of ER; formation of ROS;	[51]

	fibroblast cells (FMH)	reduction of CYP1A activity

3.2. *in vivo* Studies

In addition to *in vitro* studies*, in vivo* studies are of particular importance, especially if the end goal is to use these NPs in environmental media. Duan *et al.* (2018)*,* assessed the effects of SiO_2 NPs on the serum and hepatic lipid levels of ICR mice and *D. rerio* embryos. Inflammatory cell infiltration and mild steatosis was induced by SiO_2 NPs in the liver of mice, and cholesterol, triglyceride, and low-density lipoprotein cholesterol levels significantly increased in both blood serum and liver tissue, whereas the ratio of high-density: low-density lipoprotein cholesterol was decreased. In addition, protein markers of lipogenesis (ACC1 and FAS) were significantly higher in liver tissue, while the key enzyme of fatty acid β-oxidation, CPT1A, was decreased significantly. In zebrafish, SiO_2 NPs caused hepatic damage and steatosis and enhanced hyperlipemia in high-cholesterol diet zebrafish [52]. Furthermore, Hu *et al*. (2016), studied the toxic effects and molecular mechanisms of SiO_2 NPs in zebrafish embryos based on microarray analysis and bioinformatics analysis, reporting that the expression of 2515 genes related to many important functions, including response to stimuli, immune response, cellular processes, and embryonic development was affected. In addition, the authors found that gap junction, vascular smooth muscle contraction, and metabolic pathways, apoptosis, the MAPK signalling pathway, the calcium signalling pathway and the JAK-STAT signalling pathway were the most prominent significant pathways in SiO_2 NPs induced toxicity in *D. rerio* embryos, with the IL-6 dependent JAK1/STAT3 signalling pathway also being activated [53]. In another study, Wei *et al.* (2020)*,* studied the neurotoxicity of SiO_2 NPs at various concentrations (3, 6, 12 $ng.nL^{-1}$) on zebrafish embryos, reporting disruption of the axonal integrity, decreased length of axons, and a tendency to increase the number of apoptotic cells in the brain and central nervous system, in the presence of 12 $ng.nL^{-1}$ of SiO_2 NPs. The particles were also found to downregulate genes associated with neural function. This altogether suggests that SiO_2 NPs can induce developmental neurotoxicity by affecting the neuroactive ligand–receptor interaction signalling pathway [54].

Some effects at the cardiovascular levels have already been reported by a series of studies. For instance, Duan *et al*. (2013), reported that SiO_2 NPs (25, 50, 75, 100 $mg.mL^{-1}$) are able to induce pericardia toxicity and bradycardia in *D. rerio*, inhibiting angiogenesis and disturbing the heart formation and development in embryos ROS and apoptosis were found as a major factor to endothelial cells dysfunction being involved in several molecular mechanisms of cardiovascular diseases [55]. In further studies, in albino strain zebrafish and Tg(mpo:GFP) strain zebrafish, the authors also found that these NPs (1, 3, 6, 12 $mg.mL^{-1}$)

induce whole-embryo oxidative stress and neutrophil-mediated cardiac inflammation, inhibit calcium signalling pathway and cardiac muscle contraction, reduce the area of sub intestinal vessels with weakened expression of vascular endothelial cells in embryos and inhibit macrophage activity [56],[57]. In addition, in an albino strain zebrafish Tg(fli-1:EGFP), and Tg(mpo:GFP) strain, co-exposure study with SiO_2 NPs and MeHg (0.5 µg.mL^{-1}), tachycardia, enhanced vascular endothelial damage in Tg(fli-1:EGFP) and activated the oxidative stress and inflammatory response in neutrophils-specific Tg(mpo:GFP) was observed, with overall effects more severe than in individual exposures [58]. In another co-exposure study, this time with 0.5 mg.mL^{-1} (BaP), a pronounced cardiovascular toxicity (pericardial edema and bradycardia), with significant neutrophil-mediated inflammation and erythrocyte aggregation in caudal vein of embryos was observed. Furthermore, the co-exposure of SiO_2 NPs and B[a]P, also significantly enhanced the expression of proinflammatory and procoagulant genes [59]. Also in a co-exposure study with BaP, Asweto *et al.* (2018)*,* found that the MAPK, calcium signalling, p53, PI3k/Akt and several pathways associated with immune response were induced by the co-exposure of SiO_2 NPs and BaP in zebrafish embryos [60].

Toxic effects of silica coated NPs have also been addressed. Liang *et al*. (2020), compared the biocompatibility of 3 ng.nL^{-1} fluorescent PEG-modified SiO_2 NPs and unmodified SiO_2 NPs in zebrafish, reporting that PEG-modified SiO_2 NPs significantly declined the levels of ROS, inflammatory cytokines and mitochondrial-mediated apoptosis in vascular endothelial cells compared to SiO_2 NPs, proving the benefits in biocompatibility of these coatings [50]. However, coating SiO_2 NPs may not always improves the biocompatibility of the NPs, demonstrated by the study of Dumitrescu *et al*. (2017), that assessed the effects of glycine-silica NPs to zebrafish embryos at concentrations up to 3 mg.mL^{-1}. While glycine is a simple amino acid, excess concentrations can be toxic to vertebrates at later stages of development. The authors found that glycine increased mortality and induced developmental defects in embryos, with these defects being associated to damage localized in the brain, heart, and liver of the embryos, suggesting a complex mechanism of toxicity. Glycine maintained its toxic activity even when covalently bound on silica surface [61]. Moreover, Paatero *et al*. (2017), found that, in zebrafish embryos, different coatings of SiO_2 NPs modulate their toxicity especially due to differences in the cellular uptake. Thus, 50µg/ml PEI-coated mesoporous SiO_2 NPs were found to induce 100% lethality 48 hpf, while NH_2-MSNs and PEG-MSNs were well tolerated. Dechorionated embryos were found more sensitive to PEI- and PEG- but not NH_2-SiO_2 NPs. Notwithstanding, PEI-SiO_2 NPs were more toxic than other particles *in vivo* when embryos were incubated with the NPs, with positive surface charge promoting cellular uptake and, consequently, decreasing cell viability [62].

Gambardella *et al*. (2015), investigated the potential toxicity of SiO_2 NPs in seawater organisms, by using the sea urchin *Paracentrotus lividus* as the biological model. Using SiO_2 NPs suspensions ranging from 0.0001 mg.L^{-1} to 50 mg.L^{-1} the authors found that, even though the NPs did not interfere with the fertilization ability, they did induce anomalies in the offspring at the gastrula stage, including undeveloped and anomalous embryos, and at pluteus stage, including skeletal anomalies and delayed larvae. According to the authors, these effects are probably associated with rising of ROS and inflammation, with neurotoxic effects involving a decrease of AChE expression being also reported [63].

Table 4. Toxicity of SiO_2 NPs in vivo according to their concentration.

MNP	Sample	Concentration	Toxicity	Reference
SiO_2 NPs	ICR Mice *Danio rerio*	0, 12.5, 25, 50 µg.mL^{-1}	ICR Mice: inflammatory cell infiltration; mild steatosis; higher cholesterol, triglyceride, and low-density lipoprotein cholesterol levels; decreased ratio of high-density: low-density lipoprotein cholesterol; increase in protein markers of lipogenesis; decrease in key enzyme of fatty acid β-oxidation *Danio rerio:* Hepatic damage and steatosis enhanced hyperlipemia	[52]
SiO_2 NPs	*Danio rerio* embryos	-	Differential expression of genes related to response to stimuli, immune response, cellular processes, and embryonic development	[53]
SiO_2 NPs	*Danio rerio* embryos	3, 6, 12 ng.nL^{-1}	Disruption of the axonal integrity; decrease in the length of axons; downregulation of genes associated with neural function; Effects on the neuroactive ligand–receptor interaction signalling pathway	[54]

SiO_2 NPs	*Danio rerio* *Danio rerio* embryos	25, 50, 75, 100 $mg.mL^{-1}$	Formation of ROS; endothelial cells dysfunction; bradycardia; inhibition of angiogenesis; disturbances in heart formation and development	[55]
SiO_2 NPs	*Danio rerio* transgenic lines, Tg(fli- 1:EGFP) and Albino	1, 3, 6, 12 $mg.mL^{-1}$	Whole-embryo oxidative stress; neutrophil-mediated cardiac inflammation; inhibition of the calcium signalling pathway and cardiac muscle contraction	[56]
SiO_2 NPs	*Danio rerio* transgenic lines, Tg(fli- 1:EGFP) and Albino	1, 3, 6, 12 $ng.nL^{-1}$	Reduction in SIVs; weakened expression of vascular endothelial cells; decline in the number of macrophages and macrophage activity; inhibition of angiogenesis	[57]
SiO_2 NPs (+ MeHg)	*Danio rerio* transgenic lines, Tg(fli- 1:EGFP), Tg(mpo:GFP) and Albino	0.5 $\mu g.mL^{-1}$	Inhibition effect on tachycardia; enhanced vascular endothelial damage; oxidative stress; inflammatory response in neutrophils	[58]
SiO_2 NPs (+ B[a]P)	Albino strain zebrafish and Tg(mpo:GFP) strain zebrafish	0.5 $mg.mL^{-1}$	Pericardial edema; bradycardia; neutrophil-mediated inflammation; erythrocyte aggregation in caudal vein of embryos; enhanced expression of proinflammatory and procoagulant genes	[59]
SiO_2 NPs (+ B[a]P)	*Danio rerio* embryos	3 $mg.mL^{-1}$	Induction of MAPK signaling pathway, calcium signaling pathway, p53 signaling pathway, PI3k/Akt signaling pathway, and several pathways associated with immune response	[60]

PEG@SiNPs	*Danio rerio*	3 ng.nL^{-1}	Declined levels of ROS, inflammatory cytokines and mitochondrial-mediated apoptosis in vascular endothelial cells	[50]
Gly-Si NPs	*Danio rerio* embryos	3 mg.mL^{-1}	mortality percentage; induced developmental defects; damage localized in the brain, heart and liver	[61]
PEI-MSNs	*Danio rerio* embryos	10, 50, 100 µg.mL^{-1}	100% lethality at 48hours post fertilization (hpf); decrease in cell viability; cardiovascular toxicity prior to death	[62]
SiO_2 NPs	*Paracentrotus lividus*	0.0001-50 mg.L^{-1}	Undeveloped and anomalous embryos; skeletal anomalies; delayed larvae; formation of ROS; inflammation; decrease of AChE expression	[63]

4. Conclusions

MNPs and SiO_2 NPs are undoubtely materials with great potential that are already being integrated in novel and innovative applications. However, before they can be applied it is important to understand their toxicity profile and develop strategies to minimize the existing drawbacks in this matter.

This review made it clear that MNPs cannot be used in environmental and biomedical applications without proper treatment, as many *in vitro* and *in vivo* toxic effects have been reported. Among those, *in vitro*, the inhibition of cell proliferation, reduction in cell viability, loss of membrane integrity, cell apoptosis, increased cell stiffness and the reduction in motility stand out as the main effects related to MNPs toxicity. *in vivo* effects such as malformations, delay in hatching cycles, alteration in behaviour, DNA lesions and death in *D. rerio* embryos, inhibition in growth and reproduction in *C. silvestrii*, reduction in fertility and locomotion in *C. elegans*, and inhibition of growth and photosynthesis in *C. reinhardtii*, were reported. Furthermore, both *in vitro* and *in vivo*, the formation of ROS leading to oxidative stress is thought to be the main mechanism of toxicity of these MNPs.

Regarding SiO_2 NPs, their advantage to their counterparts in this study is their supposedly better biocompatibility, but this review points out that it might not be that simple. In fact, *in vitro*, SiO_2 NPs can produce effects like inhibition of cell differentiation, reduction in viability, loss of membrane integrity, induced cell apoptosis, cardiac dysfunction and compromised mitochondrial function, which may be due to the capacity of the NPs to induce the formation of ROS. *in vivo*, effects related to hepatic damage, disruption of axonal integrity, dysfunction of endothelial cells, tachycardia, inhibition of angiogenesis, developmental defects, delayed larvae and mortality were reported for *D. rerio*, while undeveloped and anomalous embryos, skeletal anomalies, delayed larvae and decrease of AChE expression was already found for *P. lividus*. Once again, the ROS formation is the key to their toxicity.

Thus, it is important to develop strategies to minimize their toxicity, which can be achieved by surface modification. By functionalizing a certain coating onto the surface of the NPs, a desirable level of biocompatibility can be obtained, as some studies explain that dextran or starch coatings significantly reduce the toxicity of MNPs, and that PEG and NH_2 can help SiO_2 NPs achieve the same biocompatibility. However, a poorly chosen coating can result in higher toxicity, which is why it is such a delicate step in NP design.

Also of note is the need to direct the toxicity assessment of MNPs and SiO_2 NPs towards the behaviour alterations of individuals. This is a promising and very sensitive approach, making possible to assess the neurotoxicity of these NPs and to reveal the effects at the whole organism level.

5. References

[1] N. Sanvicens and M. P. Marco, “Multifunctional nanoparticles - properties and prospects for their use in human medicine,” *Trends Biotechnol.*, vol. 26, no. 8, pp. 425–433, 2008.

[2] M. Mahmoudi, H. Hofmann, B. Rothen-Rutishauser, and A. Petri-Fink, “Assessing the in vitro and in vivo toxicity of superparamagnetic iron oxide nanoparticles,” *Chem. Rev.*, vol. 112, no. 4, pp. 2323–2338, 2012.

[3] M. K. Khalid *et al.*, “Evaluation of toxicity and neural uptake in vitro and in vivo of superparamagnetic iron oxide nanoparticles,” *Int. J. Mol. Sci.*, vol. 19, no. 9, pp. 1–14, 2018.

[4] U. S. Patil, S. Adireddy, A. Jaiswal, S. Mandava, B. R. Lee, and D. B. Chrisey, *In vitro/in vivo toxicity evaluation and quantification of iron oxide nanoparticles*, vol. 16, no. 10. 2015.

[5] A. M. Derfus, W. C. W. Chan, and S. N. Bhatia, “Probing the Cytotoxicity of Semiconductor Quantum Dots,” *Nano Lett.*, vol. 4, no. 1, pp. 11–18, 2004.

[6] E. Morelli, P. Cioni, M. Posarelli, and E. Gabellieri, “Chemical stability of CdSe quantum dots in seawater and their effects on a marine microalga,” *Aquat. Toxicol.*, vol. 122–123, pp. 153–162, 2012.

[7] M. Aye *et al.*, “Genotoxic and mutagenic effects of lipid-coated CdSe/ZnS quantum dots,” *Mutat. Res. - Genet. Toxicol. Environ. Mutagen.*, vol. 750, no. 1–2, pp. 129–138, 2013.

[8] R. Hardman, “A toxicologic review of quantum dots: Toxicity depends on physicochemical and environmental factors,” *Environmental Health Perspectives*, vol. 114, no. 2. pp. 165–172, 2006.

[9] M. Saleem Khan, F. Jabeen, N. Aziz Qureshi, M. Saleem Asghar, M. Shakeel, and A. Noureen, “Toxicity of silver nanoparticles in fish: a critical review,” *J. Biodivers. Environ. Sci.*, vol. 6, no. 5, pp. 211–227, 2015.

[10] A. Picado *et al.*, “A multi-integrated approach on toxicity effects of engineered TiO2 nanoparticles,” *Front. Environ. Sci. Eng.*, vol. 9, no. 5, pp. 793–803, 2015.

[11] N. Tran and T. J. Webster, “Magnetic nanoparticles: Biomedical applications and challenges,” *J. Mater. Chem.*, vol. 20, no. 40, pp. 8760–8767, 2010.

[12] M. Pöttler *et al.*, “Genotoxicity of superparamagnetic iron oxide nanoparticles in granulosa cells,” *Int. J. Mol. Sci.*, vol. 16, no. 11, pp. 26280–26290, 2015.

[13] C. C. Berry, S. Wells, S. Charles, and A. S. G. Curtis, “Dextran and albumin derivatised iron oxide nanoparticles: Influence on fibroblasts in vitro,” *Biomaterials*, vol. 24, no. 25, pp. 4551–4557, 2003.

[14] K. Astanina, Y. Simon, C. Cavelius, S. Petry, A. Kraegeloh, and A. K. Kiemer, “Superparamagnetic iron oxide nanoparticles impair endothelial integrity and inhibit nitric oxide production,” *Acta Biomater.*, vol. 10, no. 11, pp. 4896–4911, 2014.

[15] X. Wu, Y. Tan, H. Mao, and M. Zhang, “Toxic effects of iron oxide nanoparticles on human umbilical vein endothelial cells,” *Int. J. Nanomedicine*, vol. 5, no. 1, pp. 385–399, 2010.

[16] K. Buyukhatipoglu and A. M. Clyne, “Superparamagnetic iron oxide nanoparticles change endothelial cell morphology and mechanics via reactive oxygen species formation,” *J. Biomed. Mater. Res. - Part A*, vol.

96 A, no. 1, pp. 186–195, 2011.
[17] A. S. Arbab *et al.*, “Characterization of Biophysical and Metabolic Properties of Cells Labeled with Superparamagnetic Iron Oxide Nanoparticles and Transfection Agent for Cellular MR Imaging,” *Radiology*, vol. 229, no. 3, pp. 838–846, 2003.
[18] S. M. Cromer Berman *et al.*, “Cell motility of neural stem cells is reduced after SPIO-labeling, which is mitigated after exocytosis,” *Magn. Reson. Med.*, vol. 69, no. 1, pp. 255–262, 2013.
[19] F. Cengelli *et al.*, “Interaction of functionalized superparamagnetic iron oxide nanoparticles with brain structures.[erratum appears in J Pharmacol Exp Ther. 2006 Sep;318(3):1388],” *J. Pharmacol. Exp. Ther.*, vol. 318, no. United States PT-Comparative Study PT-Journal Article PT-Research Support, Non-U.S. Gov’t LG-English, pp. 108–116, 2006.
[20] W. Zhang, M. Kalive, D. G. Capco, and Y. Chen, “Adsorption of hematite nanoparticles onto Caco-2 cells and the cellular impairments: Effect of particle size,” *Nanotechnology*, vol. 21, no. 35, pp. 1–9, 2010.
[21] M. Kalive, W. Zhang, Y. Chen, and D. G. Capco, “Human intestinal epithelial cells exhibit a cellular response indicating a potential toxicity upon exposure to hematite nanoparticles,” *Cell Biol. Toxicol.*, vol. 28, no. 5, pp. 343–368, 2012.
[22] H. Zhao, W. Gu, L. Ye, and H. Yang, “Biodistribution of PAMAM dendrimer conjugated magnetic nanoparticles in mice,” *J. Mater. Sci. Mater. Med.*, vol. 25, no. 3, pp. 769–776, 2014.
[23] J. S. Kim *et al.*, “Toxicity and tissue distribution of magnetic nanoparticles in mice,” *Toxicol. Sci.*, vol. 89, no. 1, pp. 338–347, 2006.
[24] C. Caro, D. Egea-Benavente, R. Polvillo, J. L. Royo, M. Pernia Leal, and M. L. García-Martín, “Comprehensive Toxicity Assessment of PEGylated Magnetic Nanoparticles for in vivo applications,” *Colloids Surfaces B Biointerfaces*, vol. 177, pp. 253–259, 2019.
[25] V. Madhubala, T. Kalaivani, A. Kirubha, J. S. Prakash, V. Manigandan, and H. K. Dara, “Study of structural and magnetic properties of hydro/solvothermally synthesized α-Fe2O3 nanoparticles and its toxicity assessment in zebrafish embryos,” *Appl. Surf. Sci.*, vol. 494, no. June, pp. 391–400, 2019.
[26] A. Jurewicz, S. Ilyas, J. K. Uppal, I. Ivandic, S. Korsching, and S. Mathur, “Evaluation of Magnetite Nanoparticle-Based Toxicity on Embryo-Larvae Stages of Zebrafish (Danio rerio),” *ACS Appl. Nano Mater.*, vol. 3, no. 2, pp. 1621–1629, 2020.
[27] F. Ahmad, X. Liu, Y. Zhou, and H. Yao, “An in vivo evaluation of acute toxicity of cobalt ferrite (CoFe2O4) nanoparticles in larval-embryo Zebrafish (Danio rerio),” *Aquat. Toxicol.*, vol. 166, pp. 21–28, 2015.
[28] N. Malhotra *et al.*, “Ecotoxicity assessment of Fe3O4 magnetic nanoparticle exposure in adult zebrafish at an environmental pertinent concentration by behavioral and biochemical testing,” *Nanomaterials*, vol. 9, no. 6, 2019.
[29] F. Ahmad *et al.*, “Assessment of Thyroid Endocrine System Impairment and Oxidative Stress Mediated by Cobalt Ferrite (CoFe2O4) Nanoparticles in Zebrafish Larvae,” *Environ. Toxicol.*, 2015.
[30] R. A. R. Villacis *et al.*, “Integrated assessment of toxic effects of maghemite (Γ-Fe2O3) nanoparticles in zebrafish,” *Aquat. Toxicol.*, vol. 191, no.

December 2016, pp. 219–225, 2017.

[31] M. Zheng, J. Lu, and D. Zhao, “Effects of starch-coating of magnetite nanoparticles on cellular uptake, toxicity and gene expression profiles in adult zebrafish,” *Sci. Total Environ.*, vol. 622–623, pp. 930–941, 2018.

[32] E. M. N. Oliveira *et al.*, “Developmental toxicity of iron oxide nanoparticles with different coatings in zebrafish larvae,” *J. Nanoparticle Res.*, vol. 22, no. 4, 2020.

[33] G. M. T. de Oliveira, E. M. N. de Oliveira, T. C. B. Pereira, R. M. Papaléo, and M. R. Bogo, “Implications of exposure to dextran-coated and uncoated iron oxide nanoparticles to developmental toxicity in zebrafish,” *J. Nanoparticle Res.*, vol. 19, no. 12, 2017.

[34] R. C. Gebara, J. P. Souza, A. da S. Mansano, H. Sarmento, and M. da G. G. Melão, “Effects of iron oxide nanoparticles (Fe3O4) on life history and metabolism of the Neotropical cladoceran Ceriodaphnia silvestrii,” *Ecotoxicol. Environ. Saf.*, vol. 186, no. October, p. 109743, 2019.

[35] W. Marimon-Bolívar, L. P. Tejeda-Benítez, C. A. Núñez-Avilés, and D. De De Léon-Pérez, “Evaluation of the in vivo toxicity of green magnetic nanoparticles using Caenorhabditis elegans as a biological model,” *Environ. Nanotechnology, Monit. Manag.*, vol. 12, no. February, p. 100253, 2019.

[36] J. Hurtado-Gallego *et al.*, “Toxicity of superparamagnetic iron oxide nanoparticles to the microalga Chlamydomonas reinhardtii,” *Chemosphere*, vol. 238, 2020.

[37] C. C. Piccinetti *et al.*, “Transfer of silica-coated magnetic (Fe3O4) nanoparticles through food: A molecular and morphological study in zebrafish,” *Zebrafish*, vol. 11, no. 6, pp. 567–579, 2014.

[38] F. Coppola *et al.*, “Remediation of arsenic from contaminated seawater using manganese spinel ferrite nanoparticles: Ecotoxicological evaluation in Mytilus galloprovincialis,” *Environ. Res.*, vol. 175, no. January, pp. 200–212, 2019.

[39] A. G. Ciucă *et al.*, “Nanostructures for drug delivery: pharmacokinetic and toxicological aspects,” in *Nanostructures for Drug Delivery*, 2017, pp. 941–957.

[40] I. Y. Kim, E. Joachim, H. Choi, and K. Kim, “Toxicity of silica nanoparticles depends on size, dose, and cell type,” *Nanomedicine Nanotechnology, Biol. Med.*, vol. 11, no. 6, pp. 1407–1416, 2015.

[41] M. V. D. Z. Park *et al.*, “In vitro developmental toxicity test detects inhibition of stem cell differentiation by silica nanoparticles,” *Toxicol. Appl. Pharmacol.*, vol. 240, no. 1, pp. 108–116, 2009.

[42] J. Ahmad *et al.*, “Apoptosis induction by silica nanoparticles mediated through reactive oxygen species in human liver cell line HepG2,” *Toxicol. Appl. Pharmacol.*, vol. 259, no. 2, pp. 160–168, 2012.

[43] L. Sun *et al.*, “Cytotoxicity and mitochondrial damage caused by silica nanoparticles,” *Toxicol. Vitr.*, vol. 25, no. 8, pp. 1619–1629, 2011.

[44] L. Feng *et al.*, “Silica nanoparticles induce JNK-mediated inflammation and myocardial contractile dysfunction,” *J. Hazard. Mater.*, vol. 391, no. January, p. 122206, 2020.

[45] K. O. Yu *et al.*, “Toxicity of amorphous silica nanoparticles in mouse keratinocytes,” *J. Nanoparticle Res.*, vol. 11, no. 1, pp. 15–24, 2009.

[46] N. T. K. Vo, M. R. Bufalino, K. D. Hartlen, V. Kitaev, and L. E. J. Lee,

"Cytotoxicity evaluation of silica nanoparticles using fish cell lines," *Vitr. Cell. Dev. Biol. - Anim.*, vol. 50, no. 5, pp. 427–438, 2014.

[47] X. Huang, X. Teng, D. Chen, F. Tang, and J. He, "The effect of the shape of mesoporous silica nanoparticles on cellular uptake and cell function," *Biomaterials*, vol. 31, no. 3, pp. 438–448, 2010.

[48] I. Passagne, M. Morille, M. Rousset, I. Pujalté, and B. L'Azou, "Implication of oxidative stress in size-dependent toxicity of silica nanoparticles in kidney cells," *Toxicology*, vol. 299, no. 2–3, pp. 112–124, 2012.

[49] W. Lin, Y. wern Huang, X. D. Zhou, and Y. Ma, "In vitro toxicity of silica nanoparticles in human lung cancer cells," *Toxicol. Appl. Pharmacol.*, vol. 217, no. 3, pp. 252–259, 2006.

[50] S. Liang *et al.*, "RhB-encapsulating silica nanoparticles modified with PEG impact the vascular endothelial function in endothelial cells and zebrafish model," *Sci. Total Environ.*, vol. 711, p. 134493, 2020.

[51] V. Christen and K. Fent, "Silica nanoparticles and silver-doped silica nanoparticles induce endoplasmatic reticulum stress response and alter cytochrome P4501A activity," *Chemosphere*, vol. 87, no. 4, pp. 423–434, 2012.

[52] J. Duan, S. Liang, L. Feng, Y. Yu, and Z. Sun, "Silica nanoparticles trigger hepatic lipid-metabolism disorder in vivo and in vitro," *Int. J. Nanomedicine*, vol. 13, pp. 7303–7318, 2018.

[53] H. Hu, Q. Li, L. Jiang, Y. Zou, J. Duan, and Z. Sun, "Genome-wide transcriptional analysis of silica nanoparticle-induced toxicity in zebrafish embryos," *Toxicol. Res. (Camb).*, vol. 5, no. 2, pp. 609–620, 2016.

[54] J. Wei, J. Liu, S. Liang, M. Sun, and J. Duan, "Low-dose exposure of silica nanoparticles induces neurotoxicity via neuroactive ligand–receptor interaction signaling pathway in zebrafish embryos," *Int. J. Nanomedicine*, vol. 15, pp. 4407–4415, 2020.

[55] J. Duan, Y. Yu, Y. Li, Y. Yu, and Z. Sun, "Cardiovascular toxicity evaluation of silica nanoparticles in endothelial cells and zebrafish model," *Biomaterials*, vol. 34, no. 23, pp. 5853–5862, 2013.

[56] J. Duan *et al.*, "Low-dose exposure of silica nanoparticles induces cardiac dysfunction via neutrophil-mediated inflammation and cardiac contraction in zebrafish embryos," *Nanotoxicology*, vol. 10, no. 5, pp. 575–585, 2016.

[57] J. Duan, H. Hu, L. Feng, X. Yang, and Z. Sun, "Silica nanoparticles inhibit macrophage activity and angiogenesis via VEGFR2-mediated MAPK signaling pathway in zebrafish embryos," *Chemosphere*, vol. 183, pp. 483–490, 2017.

[58] J. Duan *et al.*, "Combined toxicity of silica nanoparticles and methylmercury on cardiovascular system in zebrafish (Danio rerio) embryos," *Environ. Toxicol. Pharmacol.*, vol. 44, pp. 120–127, 2016.

[59] J. Duan, Y. Yu, Y. Li, Y. Wang, and Z. Sun, "Inflammatory response and blood hypercoagulable state induced by low level co-exposure with silica nanoparticles and benzo[a]pyrene in zebrafish (Danio rerio) embryos," *Chemosphere*, vol. 151, pp. 152–162, 2016.

[60] C. O. Asweto *et al.*, "Gene profiles to characterize the combined toxicity induced by low level co-exposure of silica nanoparticles and benzo[a]pyrene using whole genome microarrays in zebrafish embryos," *Ecotoxicol. Environ. Saf.*, vol. 163, no. February, pp. 47–55, 2018.

[61] E. Dumitrescu, D. P. Karunaratne, M. K. Prochaska, X. Liu, K. N. Wallace,

and S. Andreescu, “Developmental toxicity of glycine-coated silica nanoparticles in embryonic zebrafish,” *Environ. Pollut.*, vol. 229, pp. 439–447, 2017.

[62] I. Paatero, E. Casals, R. Niemi, E. Özliseli, J. M. Rosenholm, and C. Sahlgren, “Analyses in zebrafish embryos reveal that nanotoxicity profiles are dependent on surface-functionalization controlled penetrance of biological membranes,” *Sci. Rep.*, vol. 7, no. 1, pp. 1–13, 2017.

[63] C. Gambardella *et al.*, “Multidisciplinary screening of toxicity induced by silica nanoparticles during sea urchin development,” *Chemosphere*, vol. 139, pp. 486–495, 2015.

Chapter 3 - Behavioural effects of SiO_2 NPs in *Danio rerio* embryos

1. Introduction

1.1. *Danio rerio* as an Indicator Species

Fish can serve as valuable sentinels to identify environmental contaminations, and as an efficient, low-cost, and excellent model system for environmental risk assessments [1]. The *Danio (Brachydanio) rerio*, known as zebrafish, is one of the most widely used model systems in the developmental biology of lower vertebrates being original from the Asiatic continent. The zebrafish belongs to the family *Cyprinidae* in the order *Cypriniformes*, and *Rasborinae* sub-family and usually inhabits in locations with temperature range from 18ºC to 24ºC and pH between 6 and 8 [2], [3].

This species has a substantial historical database regarding developmental biology, toxicology and risk assessment and shares lots of cellular, anatomical, and physiological characteristics with other vertebrates and mammals. In addition, the small size (the length of the *D. rerio* individuals is about 3 to 5 cm in adult), transparent embryo, rapid development and short life cycle make zebrafish attractive to study and elucidate mechanisms of toxicity [1]. This model organism has shown a great sensitivity to chemicals as it may quickly absorb the compounds present in the water, accumulating them in several tissues [4], even though the embryos prior to the hatching possess an impermeable membrane, the chorion, that acts like a barrier to the entry of compounds. The fact that the zebrafish breed in large numbers and are easy to manipulate, along with the previous features, make this species recommended by the USA EPA for acute toxicity tests with embryos and adult fish [2].

This species has been used in many fields of research, with special emphasis to the field of toxicology. Furthermore, this species, in particular *D. rerio embryos*, is emerging as a good model organism for neurobehavioral studies, these including the study of normal and pathological conditions [5]. The zebrafish embryos hatch between 48-72 hpf, becoming larvae with a complex behavioural repertoire [6]. The external fertilisation and development of the eggs (which reduces maternal behavioural influences) along with their transparency [6] support their use in toxicological studies.

1.2. Behaviour as a Sensitive Indicator of Toxicity

Behaviour of fish species has been studied in the past years as a way to predict toxic effects in living beings. Behaviour is the primary means by which an organism interacts with its environment allowing it to survive. Thus, organisms must be sensitive to events occurring in their environments and respond appropriately [7]. Any behavioural study includes characteristics associated with the whole animal such development and longevity of the animal and the functional integrity and quality of performance that animal is capable of engaging in, as is the emotional reactivity of the animal. As our ultimate goal is to study the effects on individuals, studying alterations in behaviour is of interest, as it reflects the summed and integrated capacity of an organism to handle the surrounding environment [7].

Zebrafish is a very suitable biological model to assess toxicity of many compounds, as it can be later extrapolated to other species, including humans. Many genes implicated in behaviour, are highly conserved between the zebrafish and humans, and the neurochemistry of the zebrafish is also very similar to humans and rodents [6], [8]. The zebrafish brain contains all the major components required for neurotransmission, such as neurotransmitter receptors, transporters, and enzymes of synthesis and metabolism, having the same neurotransmitter system as that of higher vertebrates such as GABA, glutamate, dopamine, noradrenaline, serotonin, histamine, and acetylcholine [8]. Furthermore, many compounds have been found to induce behavioural changes in zebrafish, being easily detected and analysed by video tracking equipment and software [6]. To understand the effects these compounds might provoke in the behaviour and development of the zebrafish, it is important to know about the normal development and behaviour of the species.

The zebrafish embryo development takes place very rapidly, with the first detectable behaviour observed at 17 hpf, classified as spontaneous movement, during which embryos repeatedly perform slow, alternating tail coils [6]. This spontaneous movement is independent of sensory stimulation and is driven by activity in the spinal cord [6], presenting a decreased frequency of coiling after 21 hpf [6]. At 21 hpf, the embryos begin to show a new motor behaviour in response to mechanical stimuli, reacting with rapid tail coils with two or three rapid trunk contractions [6]. After 24 h, the organisation of the embryo is already discernible, and anatomical structures such as somites, notochord, otoliths, and eye anlage as well as the heart anlage can be localised [9]. After 48 hpf, dechorionation can easily be performed, craniofacial features have further developed, blood flow and an unlooped heart region can be discerned, major sensory organs such as eye and ear are fully developed, and various components of the brain and the spine above the notochord can be distinguished. Furthermore, embryos show an increasing number of epidermal pigment cells and the caudal fin as well as the

Table 1. Acquired behavioural and developmental characteristics of zebrafish individuals according to its time post fertilization and developmental stage

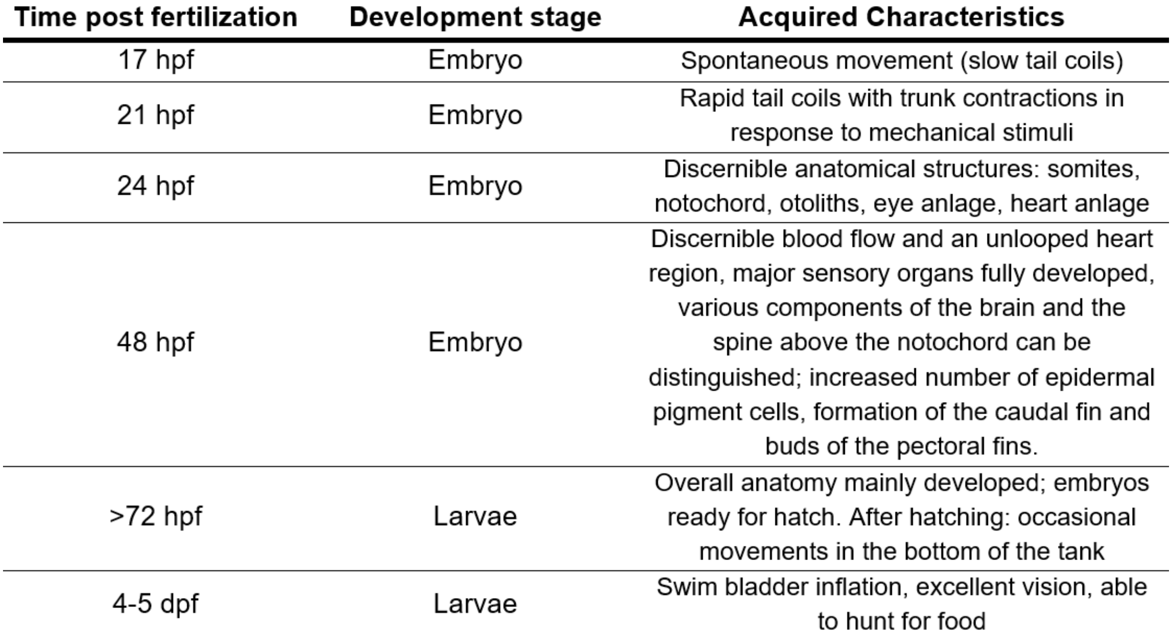

Time post fertilization	Development stage	Acquired Characteristics
17 hpf	Embryo	Spontaneous movement (slow tail coils)
21 hpf	Embryo	Rapid tail coils with trunk contractions in response to mechanical stimuli
24 hpf	Embryo	Discernible anatomical structures: somites, notochord, otoliths, eye anlage, heart anlage
48 hpf	Embryo	Discernible blood flow and an unlooped heart region, major sensory organs fully developed, various components of the brain and the spine above the notochord can be distinguished; increased number of epidermal pigment cells, formation of the caudal fin and buds of the pectoral fins.
>72 hpf	Larvae	Overall anatomy mainly developed; embryos ready for hatch. After hatching: occasional movements in the bottom of the tank
4-5 dpf	Larvae	Swim bladder inflation, excellent vision, able to hunt for food

Source: [6], [9]

buds of the pectoral fins have formed [9]. When close to hatching, embryos show rhythmic movement of the pectoral fins, together with sudden changes of position of the embryo, every 20 s or so [6]. After 72 hpf, the overall anatomy is mainly developed and the embryos are ready for hatch. After hatching, zebrafish larvae occasionally move and remain on the bottom of the tank. At 4–5 dpf not only the swim bladder gradually inflates, and they acquire excellent vision, becoming able to hunt for food [6]. The larval stage of zebrafish, that starts from 72 hpf (from protruding mouth stage), lasts until they undergo metamorphosis to become juvenile (1-month post fertilization). During the larvae period, the zebrafish possess a plethora of behaviours which could be analysed automatically or manually in quantitative or qualitative terms.

To measure the effects of a given compound in the behaviour and development of zebrafish embryos, some endpoints are frequently considered. Thigmotaxis is one of the most commonly measured behavioural endpoints. Individuals displaying thigmotactic behaviour strongly avoid the centre of an arena and stay close to the boundaries of a novel environment [6]. Another endpoint frequently assessed involves the quantification of erratic movements, defined as sudden sharp changes in direction of movement and/or velocity, indicating rapid anxiety-like darting behaviours. These movements usually occur at high speed, being these high-speed movements capable to indirectly measure erratic movements in stressed zebrafish [6]. As part of locomotion-based behaviour endpoints that can be measured in larvae, the response to a startle stimulus is another frequently assessed, as is considered an animal protection against a harmful stimuli and can be reliably measured as the distance larvae swim following stimulation [10]. Freezing is another classic index of anxiety and very used in behaviour studies, being defined as the partial or total absence of movement except for the gills and eyes [6]. The analysis of locomotion and responses to dark and light stimuli is also frequently studied. The locomotion in zebrafish is a complex behaviour produced by the activity of various neurons and can reveal much in terms of neurotic effects of a given compound. In a light-dark locomotion test, the locomotor activity and movement pattern of zebrafish larvae are often analysed via high-throughput automatic tracking by placing them in multi-well plates inside a closed chamber and exposing them to alternating light and dark conditions. The distance travelled and the pattern of movement of zebrafish larvae in each of the conditions is evaluated for understanding the neurobehavioral effects [8].

Thus, studying the effects on behaviour as proven to be advantageous due to many reasons. For instance, the clear chorion and embryo during the development of the zebrafish allow for continuous visualization of the anatomical changes associated with development. However, the species short maturation times and the capability for complex behaviour beginning at just 3 dpf are no less important factors [7]. In addition, there is the desire to reduce the numbers of rodents used in investigation, and fact is that the aquatic paradigms adhere to the 3Rs principle, as fish are less sentient than rodents, and typically use less invasive administration of drugs (i.e., immersion/inhalation vs. injections) [5]. Thus, automated systems aided by video tracking technology and analytical software to study effects in *D. rerio* behaviour might be a good alternative to the similar systems used with rodents [6].

1.3. Aim of This Work

The nanomaterial-based adsorbents are efficient in environmental remediation, but it is still crucial to assess the toxicity of their components. Therefore, as silica based adsorbents are being considered to that use, a complete risk assessment must be carried on. Even though some studies exist on this matter for silica NPs, very few have been done on their effect on behaviour of aquatic organisms, which is a crucial and very sensitive endpoint that should not be overlooked [7].

Thus, the aims of this work were to: assess the behavioural effects of two sized (80 and 150 nm) silica nanoparticles using an *in vivo* model, the established model organism *D. rerio*; study and understand the effects at the behaviour level, promoting a very sensitive and integrated approach to adress toxicology studies; and based on the results, to understand the viability of adsorbents based on silica nanomaterials to be used in environmental remediation, taking into account their impact on biota.

2. Experimental Procedure

2.1. Preparation and Characterization of NPs Suspensions

SiO_2 NPs were prepared according to Pinto et. al [11]. Briefly, for the synthesis of the 150 nm silica NPs, 2.25 mL of tetraethoxysilane (TEOS, 0.2 mol.dm^{-3}) were added to an Erlenmeyer flask followed by the addition of 41.51 mL of ethanol, 4.50 mL of ultrapure water (5 mol.dm^{-3}) and 1.74 mL of ammonium hydroxide 25% (0.21 mol.dm^{-3}), under constant stirring. The reaction proceeded overnight, at room temperature, under moderate stirring. For the synthesis of the 80 nm SiO_2 NPs, 2.25 mL of TEOS were added to an Erlenmeyer flask followed by the addition of 42.45 mL of ethanol, 4.50 mL of deionised water and 0.8 mL of ammonium hydroxide 25% (0.14 mol.dm^{-3}), also under constant stirring. The reaction was allowed to proceed for 24 h, at room temperature, under moderate stirring. The SiO_2 NPs were then collected by centrifugation, washed once with ethanol and washed twice with deionised water and, finally, were placed in an oven to dry at 50 C, over 24 h. SiO_2 NPs were characterized using scanning electron microscopy (SEM - Hitachi SU70 microscope) The average particle size (D) and the standard deviation (r) were determined by measuring the size of more than 100 particles. The hydrodynamic size was determined by dynamic light scattering (DLS - Zeta Sizer Nano Series,Malvern).

2.2. Test Organism

The zebrafish (*D. rerio*) eggs were provided by the facility established at the Biology Department from University of Aveiro (Portugal), collected within 30 min after natural mating of adult fish, rinsed in fish system water and screened using a stereomicroscope (Stereoscopic Zoom Microscope-SMZ 1500, Nikon Corporation) to exclude unfertilized eggs, injured embryos or embryos with irregularities during cleavage. Adult fish are maintained in carbon-filtered water at 26.0±1ºC under a 16:8 h light/ dark photoperiod cycle. Conductivity is kept at 750±50 µS, pH at 7.5±0.5 and dissolved oxygen at 95% saturation. Adult fish are fed twice a day with commercially available artificial diet (ZM 400 Granular) and brine shrimp.

2.3. Zebrafish Embryotoxicity Test (ZET)

Zebrafish embryo toxicity test (ZET) for SiO_2 NPs was performed according to the Organisation for Economic Co-operation and Development (OECD) guideline [12]. Briefly, embryos were transferred to 24-well plates (1 embryo per well) within 3 hpf following the distribution scheme (Figure 1). There were a total of six plates, five containing test suspensions (0.1 µg.L^{-1}, 1 µg.L^{-1}, 10 µg.L^{-1}, 100 µg.L^{-1} and 1000 µg.L^{-1}) in 20 wells and dilution water as internal plate control in four wells (1a) and one plate with all 24 wells filled with dilution water as a negative control (1b). The 24-well plates were covered with the lids provided with the plates and incubated at 26.0 ± 1.0 °C for 96 h and a light phase of 16–8 h. At 24, 48, 72 and 96 hpf, the survival rate as assessed. Other endpoints included hatching time, and gross morphological changes were recorded using a stereomicroscope (Stereoscopic Zoom Microscope-SMZ 1500, Nikon Corporation).

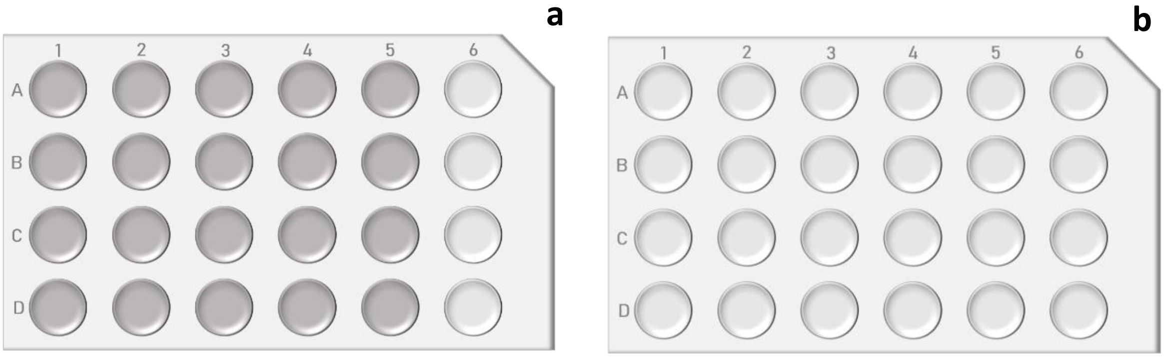

Figure 1. Representations of the 24-well plates: **a** - Image representation of the five plates with the respective test solutions (0.1 µg.L^{-1}, 1 µg.L^{-1}, 10 µg.L^{-1}, 100 µg.L^{-1} and 1000 µg.L^{-1}) in 20 wells (in grey) and dilution water as internal plate control in four wells (light grey); **b** –negative control with dilution water in all 24 wells (light grey).

2.4. Behavioural Assessment

Locomotor activity was measured by placing the plates individually into a ZebraBox (Viewpoint Life sciences, Lyon, France) using the tracking setting during periods of 3 min light/ 3 min dark. Briefly, this system that monitors movement by automated video recording is equipped with internal LED lights that were used for stimulation/inhibition of the larvae, which tend to remain still during a light period and move actively during dark periods. Recordings were made directly on the 24-well plates used for chemical exposure in order to reduce possible acclimation bias. Assessment of sub-lethal behavioural effects was performed by tracking the movement of each larvae during alternating periods of light, used as a stimulus (LED illumination) and dark (infrared illumination) and recording distances and time moving for each 60 s integration during both the dark and light periods. Data was compiled and mean distance or proportion of time spent moving in each treatment group during the light and dark periods calculated.

Three types of movements were considered for analysis: low velocity (hypoactivity and inactivity) < 8 mm/s; medium velocity for movements between 8 and 40 mm/s (normal activity) and high velocity (hyperactivity) > 40 mm/s.

Percentage of time or distance moved in each type of movement was calculated dividing the respective time or distance by the total swimming time or distance and multiplying by 100. In the protocol built on the ZebraLab® v3 Automated Behavioural Analysis program, two monitoring zones were defined in the recording arena: an inner and an outer zone, allowing the analysis of the tendency to swim near the edges of the container (as a measure of thigmotactic behaviour). Given that distance swum in the outer zone also reflects the total distance swum, to analyse tendency to swim near the edges the percentage of distance swum in this zone was calculated (dividing the distance moved in the outer area by the overall swimming distance and multiplying by 100). Fish path angle was also recorded and 8 classes of angles were defined as described by Almeida *et al.* (2019) [13]. Angles were calculated through the vector of fish swimming direction and the turn path performed by the animal. Angles of low amplitude (classes 4 and 5) indicate straightforward movements while high amplitude angles (1, 2, 7 and 8) indicate movements with significant changes of direction and suggest erratic swimming behaviour, a measure of stress. Angles of medium amplitude (class 3 and 6) indicate average turns.

2.5. Statistical Analysis

The normality of the ZET results was tested using the Shapiro-Wilk test and the comparison between different concentrations groups and the control was made using the Kruskal-Wallis non-parametric test, with value defined to reject the null hypothesis established at $p<0.05$ (significantly different data).

A linear mixed effects analysis using maximum likelihood estimation was performed to investigate the effect of light/dark stimulus and time (cycle) on the behavioural endpoints (swimming activity parameters). Normality was tested using the Shapiro–Wilk normality test. When presumptions were met, a One-way ANOVA was used to infer statistically significant differences. When significant, Dunnett’s method was used to verify differences between tested concentrations and control.

3. Results

3.1. Characterization of the Nanoparticles

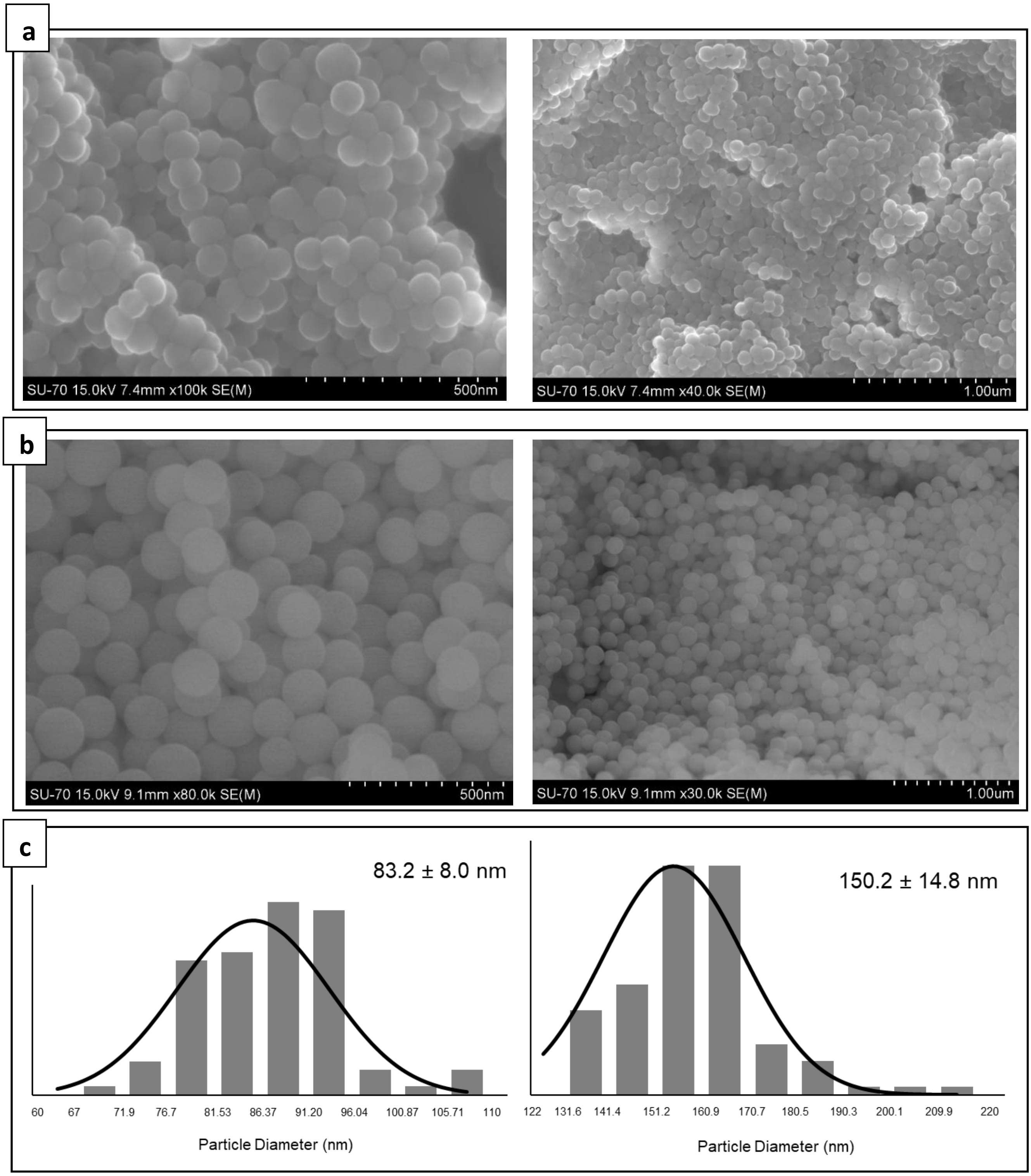

Figure 2. a - Scanning electron microscopy (SEM) images of SiO_2 NPs with diameters of 83.3 ± 8.0 (80). **b** - Scanning electron microscopy (SEM) images of SiO_2 NPs with diameters of 150.2 ± 14.8 (150). **c** – Size distribution of 80 nm and 150 nm SiO_2 NPs.

Figure 2 shows scanning electron microscopy (SEM) images of SiO_2 NPs with diameters of 80.16 ± 6.58 (80), 155.55 ± 16.32 (150), indicating that the particles are spherical and well-defined in size. The 80 nm and 150 nm SiO_2 NPs subjected to dynamic light scattering (DLS) to measure hydrodynamic sizes in DI water, had sizes of 96.52 ± 31.62 and 170.5 ± 42.04, respectively.

Table 2. DLS measures of size for the 80 and 150 nm SiO_2 NPs

Nanoparticle	**Size**
80 nm SiO_2 NPs	96.52 ± 31.62
150 nm SiO_2 NPs	170.5 ± 42.04

3.2. Effects of SiO_2 NPs on the Development of Zebrafish Embryos

3.2.1. SiO_2 NPs with 80 nm

The results indicate that, in term of fish development, there were no significant effects of the different tested concentrations.

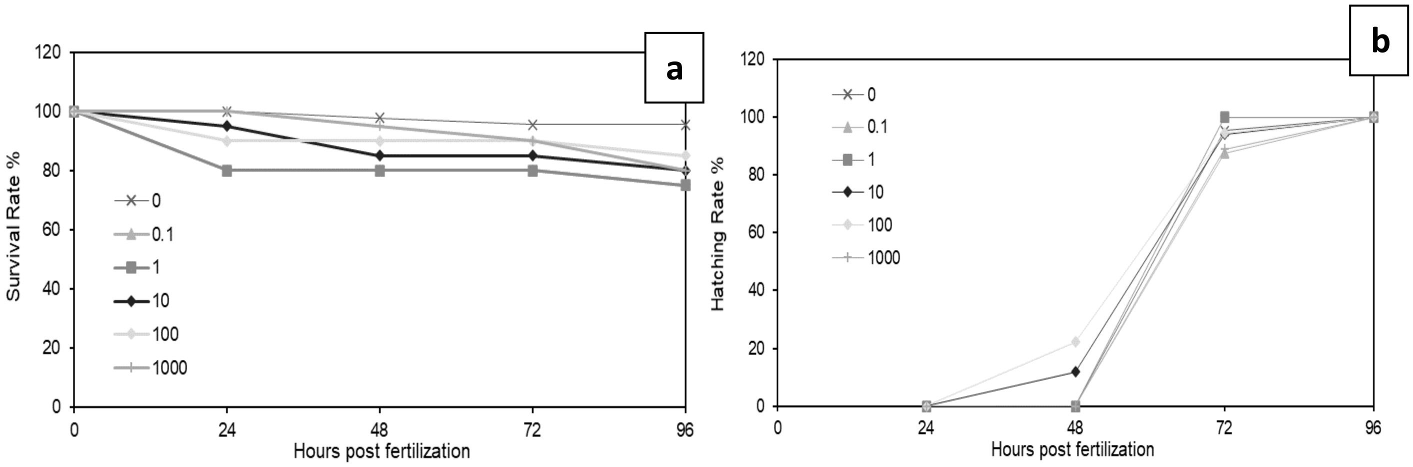

Figure 3. Survival and hatching rate: **a** – Graphic representation of the survival rate of *D. rerio* embryos/larvae exposed to 80 nm SiO_2 NPs in each concentration 24-well plate (0, 0.1, 1, 10, 100, 1000 $\mu g.L^{-1}$) and time (24, 48, 72, 96 hpf); **b** –Graphic representation of the hatching rates of zebrafish embryos exposed to 80 nm SiO_2 NPs per each concentration 24-well plate (0, 0.1, 1, 10, 100, 1000 $\mu g.L^{-1}$) and time (24, 48, 72, 96 hpf);

Survival was also not significantly affected by the tested SiO_2 NPs tested concentrations. As shown in Figure 3a, a non-significant tendency decreased was observed at 24 and 48 hpf in the animals exposed to 1 and 10 $\mu g.L^{-1}$, respectively. Regarding the hatching rate, even though there were no statistical differences between the NPs treatments and the control group, a non-significant tendency for the embryos exposed to 10 and 100 $\mu g.L^{-1}$ SiO_2 NPs to hatch earlier (at 48 hpf) was observed. In the higher concentrations, a non-significant tendency for larvae to lose equilibrium was observed.

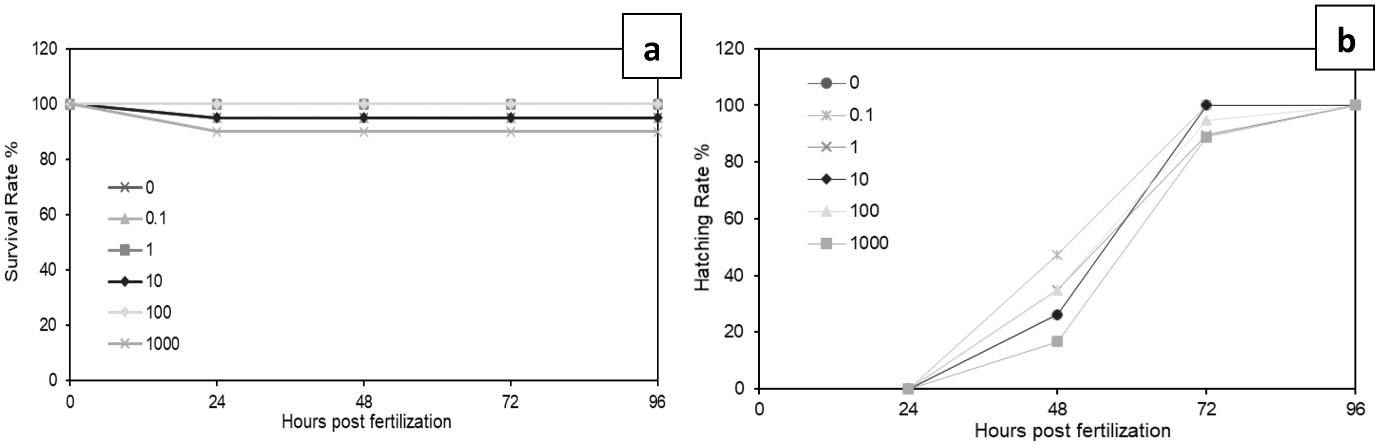

Figure 4. Survival and hatching rate: **a** – Graphic representation of the survival rate of *D. rerio* embryos/larvae exposed to 150 nm SiO_2 NPs in each concentration 24-well plate (0, 0.1, 1, 10, 100, 1000 $\mu g.L^{-1}$) and time (24, 48, 72, 96 hpf); **b** –Graphic representation of the hatching rates of zebrafish embryos exposed to 150 nm SiO_2 NPs per each concentration 24-well plate (0, 0.1, 1, 10, 100, 1000 $\mu g.L^{-1}$) and time (24, 48, 72, 96 hpf)

3.2.2. SiO_2 NPs with 150 nm

The results showed no significant effects of the tested concentrations of 150 nm SiO2 NPs in terms of zebrafish embryos development.

The tested concentrations of 150 nm SiO_2 NPs had no significant effects for on zebrafish embryos development. SiO_2 NPs exposure had no effect in terms of gross morphological changes, survival rate or hatching rate (Figures 4 a,b). Notwithstanding, a slight delay in hatching was observed in animals exposed to 1000 $\mu g.L^{-1}$ whereas the group exposed to 0.1 $\mu g.L^{-1}$ presented an opposite response, presenting earlier hatching

3.3. Effects of SiO_2 NPs on the behaviour of Zebrafish Embryos

3.3.1. SiO_2 NPs with 80 nm

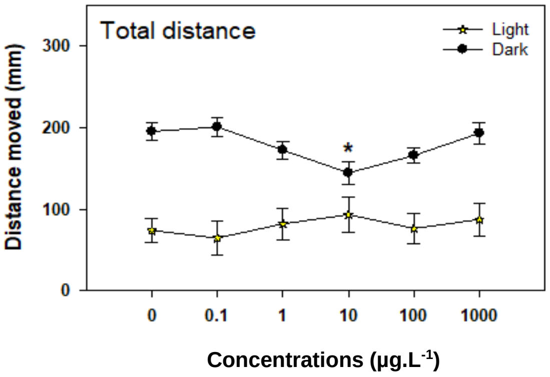

Figure 5. Total distance moved by the *D. rerio* larvae exposed to different concentrations of 80 nm SiO_2 NPs (0, 0.1, 1, 10, 100, 1000 $\mu g.L^{-1}$) (in mm) in light and dark periods. * denotes statistically significant when compared to control ($p<0.05$)

Overall, a non-linear response of locomotor activity was observed in which a reduction of distance travelled (statistically significant at 10 µg.L^{-1}) is observed at lower concentrations but this reduction faded out at higher concentration.

In terms of total distance moved by the zebrafish larvae in the dark, a general trend to move less was observed although this effect was only significant for fish exposed to 10 µg.L^{-1} SiO_2 NPs. In the light period, no significant effects were observed in terms of total distance moved.

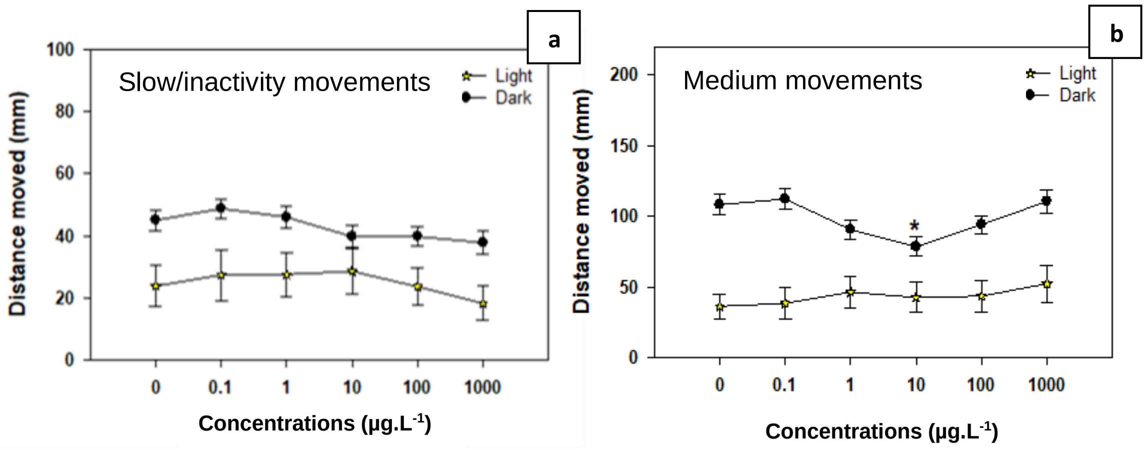

Figure 6. Distance moved in slow/inactivity movements and medium movements by the *D. rerio*: **a** – Distance moved with slow/inactivity movements by the *D. rerio* larvae (in mm) exposed to different concentrations of 80 nm SiO_2 NPs (0, 0.1, 1, 10, 100, 1000 µg.L^{-1}), in light and dark periods; **b -** Distance moved with medium movements by the *D. rerio* larvae (in mm) exposed to different concentrations of 80 nm SiO_2 NPs (0, 0.1, 1, 10, 100, 1000 µg.L^{-1}), in light and dark periods; * denotes statistically significant ($p<0.05$)

Slow movements/Inactivity were not significantly different between NPs exposed and control organisms, in both periods of light and dark, although a tendency for decreased activity with increasing concentrations can be observed in the dark. Regarding medium and rapid movements, the pattern of response was similar to the total distance as the distance moved was significantly lower in

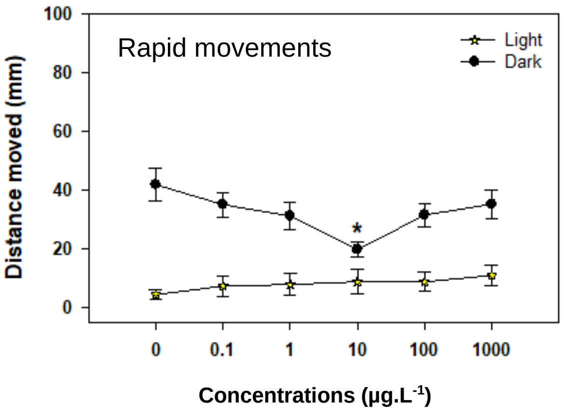

Figure 7. Distance moved with rapid movements by the *D. rerio* larvae (in mm) exposed to different concentrations of 80 nm SiO_2 NPs (0, 0.1, 1, 10, 100, 1000 µg.L^{-1}), in light and dark periods; * denotes statistically significant ($p<0.05$)

organisms exposed to 10 µg.L^{-1} NPs. In the light period, no significant differences were found.

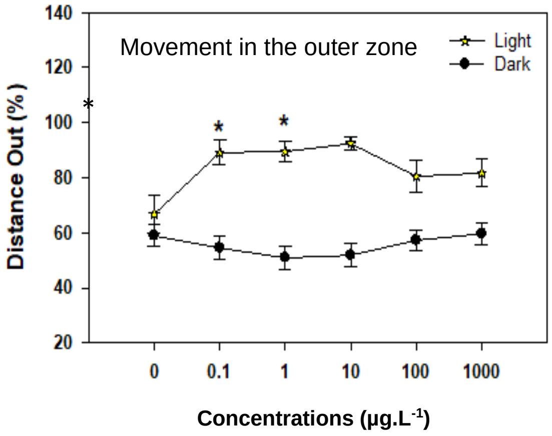

Figure 8. Distance moved by the *D. rerio* larvae exposed to different concentrations of 80 nm SiO_2 NPs (0, 0.1, 1, 10, 100, 1000 µg.L^{-1}) in the outer zone of the wells "Distance Out", expressed as percentage, in light and dark periods; * denotes statistically significant ($p<0.05$)

The percentage of distance moved in the outer zone of the well, distance out, depicted in Figure 8, shows in the light periods, a significant increase in the distance moved in the outer zones by the larvae exposed to 0.1, 1 and 10 µg.L^{-1} SiO_2 NPs. A tendency for its increase was also observed at the higher concentrations tested although not statistically significant.

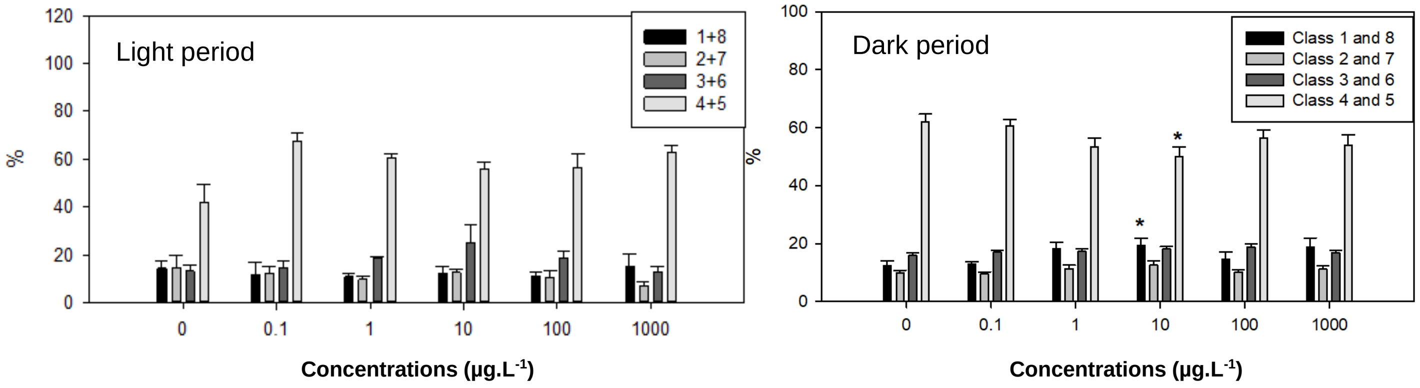

Figure 9. Movement angles made by *D. rerio* larvae after exposure to different SiO_2 NPs with 80 nm concentrations (0.1, 1, 10, 100, 1000 µg.L^{-1}) during light and dark periods. Low amplitude angles (classes 4 and 5) - straightforward movements; high amplitude angles (1, 2, 7 and 8) - movements with significant changes of direction (erratic swimming behaviour); medium amplitude angles (class 3 and 6) - average turns. * meaning statistically significant ($p<0.05$)

The angles fish displayed in their movement were also analysed (Figure 8). Significant differences to control organisms were only found in dark periods, where a significant increase in high amplitude angles and a significant decrease in low amplitude angles was found for the individuals exposed to 10 µg.L^{-1} of SiO_2 NPs ($p<0.05$).

3.3.2. SiO_2 NPs with 150 nm

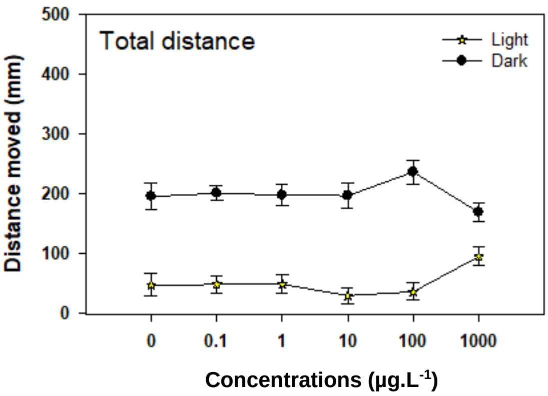

Figure 10. Total distance moved (in mm) by the *D. rerio* larvae exposed to different concentrations of 150 nm SiO_2 NPs (0, 0.1, 1, 10, 100, 1000 µg.L^{-1}) in light and dark periods; * denotes statistically significant ($p<0.05$)

The total distance moved in the dark of zebrafish larvae, exposed to 150 nm NPs was not significantly different than control organisms. A slight non-significant trend for an increase was observed in terms of total distance moved, for organisms exposed to 100 µg.L^{-1} NPs. In the light period, a slight non-significant tendency for increase in distance moved was observed in organisms exposed to SiO_2 NPs statistical effects were also found although fish exposed to 1000 µg.L^{-1}.

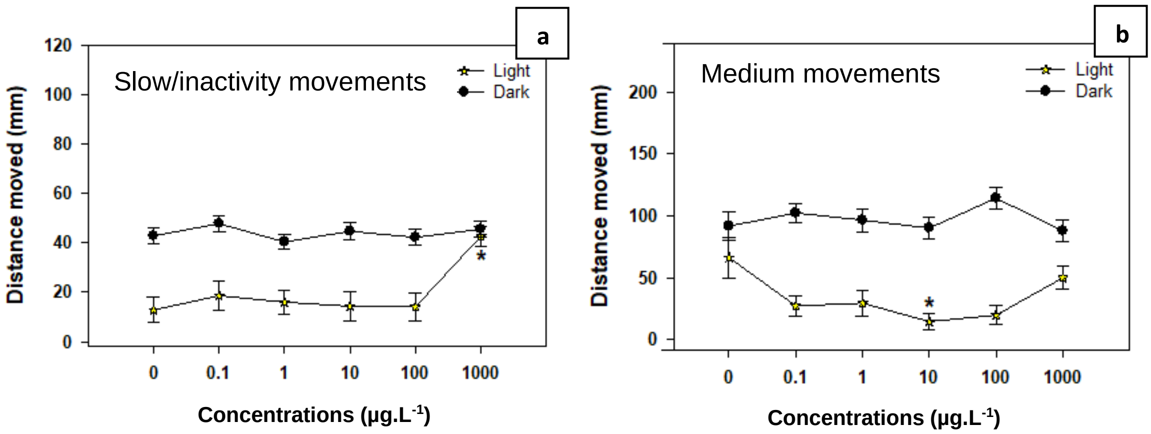

Figure 11. Distance moved in slow/inactivity movements and medium movements by the *D. rerio*: **a** – Distance moved with slow/inactivity movements by the *D. rerio* larvae (in mm) exposed to different concentrations of 150 nm SiO_2 NPs (0, 0.1, 1, 10, 100, 1000 µg.L^{-1}) in light and dark periods; **b**- Distance moved with medium movements by the *D. rerio* larvae (in mm) exposed to different concentrations of 150 nm SiO2 NPs (0, 0.1, 1, 10, 100, 1000 µg.L-1) in light and dark periods; * denotes statistically significant ($p<0.05$)

In terms of type of movements, no significant effects of 150 nm SiO_2 NPs were observed in terms of distance moved in slow movements/inactivity, in dark periods. In light periods, organisms exposed to 1000 µg.L^{-1} SiO_2 NPs significantly increased movement.

Regarding medium movements, there were no significant effects of NPs were observed in terms of distance moved in dark periods. Notwithstanding, in the light periods a significant decrease in the distance moved was observed in the group exposed to 10 µg.L^{-1} of SiO_2 NPs, with a non-significant trend to decrease observed in the other exposed groups.

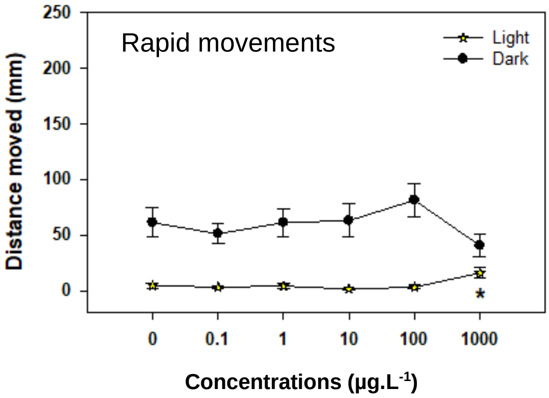

Figure 12. Distance moved with rapid movements by the *D. rerio* larvae (in mm) exposed to different concentrations of 150 nm SiO_2 NPs (0, 0.1, 1, 10, 100, 1000 µg.L^{-1}) in light and dark periods; * meaning statistically significant ($p<0.05$)

Concerning rapid movements made by the embryos, no significant differences in the distance moved in dark periods were found, even though there was a tendency for its increase in the groups exposed to 100 µg.L^{-1} SiO_2 NPs. In the light periods, however, a significant increase in distance moved in rapid movements was found in the group exposed to 1000 µg.L^{-1} SiO_2 NPs.

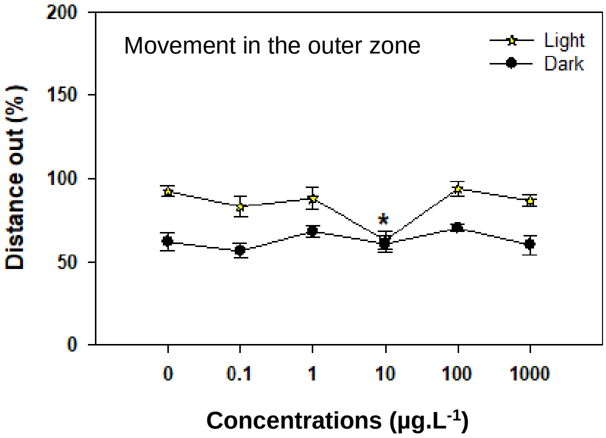

Figure 13. Distance moved by the *D. rerio* larvae exposed to different concentrations of 150 nm SiO_2 NPs (0, 0.1, 1, 10, 100, 1000 µg.L^{-1}) in the outer zone of the wells "Distance Out", expressed as percentage in light and dark periods; * denotes statistically significant ($p<0.05$)

A significant decrease in terms of distance swam in the outer area of the wells was observed in fish exposed to 10 µg.L^{-1} SiO_2 NPs, in the light periods.

However, it is also of note that they had a higher locomotor activity in the light than in the dark, in all other concentrations.

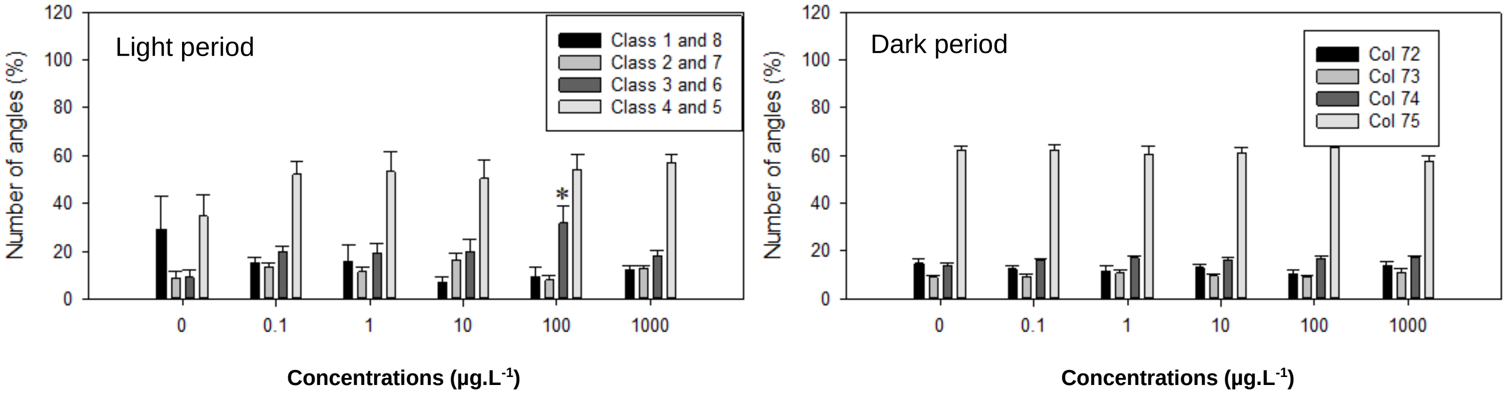

Figure 14. Movement angles made by *D. rerio* larvae after exposure to different SiO_2 NPs with 150 nm concentrations (0.1, 1, 10, 100, 1000 µg.L^{-1}) during light and dark periods. Low amplitude angles (classes 4 and 5) - straightforward movements; high amplitude angles (1, 2, 7 and 8) - movements with significant changes of direction (erratic swimming behaviour); medium amplitude angles (class 3 and 6) - average turns. * denoting statistically significant ($p<0.05$)

The monitored movement angles made by zebrafish larvae revealed, in the dark periods, no statistical effects of SiO_2 NPs. In the light periods there was a significant increase in the medium amplitude angles (class 3 and 6) that refer to average turns.

4. Discussion

Embryos exposed to 80 and 150 nm SiO_2 NPs displayed no relevant alterations in development, even though some non-significant tendencies for the NPs to affect their development could be observed. The 80 nm NPs seemed to promote early hatching and loss of equilibrium at 10 and 100 µg.L^{-1}. A slight delay in hatching was observed in the organisms exposed to 1000 µg.L^{-1} of 150 nm NPs and a nonsignificant trend for early hatch was also found in the ones exposed to 0.1 µg.L^{-1}. Similar results have been reported in the literature. For example, 60 and 200 nm sized fluorescent silica NPs (FSNPs - 0.2, 0.25, 2, 2.56, 25.6 and 200 mg.L^{-1}) induced no effects of the survival of the *D. rerio* embryos and larvae [14]. A slight effect regarding earlier hatching (between 48 hpf and 72 hpf) was reported at 2.56, 25.6 mg.L^{-1} exposed organisms [14]. In another study, SiO_2 NPs induced accelerated hatching when exposed to 80 nm NPs at concentrations ranging from 12.5 to 100 mg.L^{-1} [15]. Usually, zebrafish embryos hatch between 48 and 72 hpf, when they become free swimming larvae with a complex behavioural repertoire [6]. Thus, even though a tendency might be observed for the embryos to hatch earlier compared to the controls, it is still considered, based on the literature, as being in the normal hatching time range for zebrafish embryos. The authors also found no significant effects of NPs on embryos/larvae mortality or malformations. Vranic et al. (2019), studying the effects of 3.125, 6.25, 12.5, 25, 50, and 100 mg.L^{-1} of 25 and 115 nm SiO_2 NPs in the development of zebrafish embryos (considering survival rate, hatching rate, and gross morphological changes) at 12, 24, 36, 48, 60, and 72 hpf after exposure, also reported no significant morphological changes nor changes in survival and hatching rate even at the highest concentration. However, after chemical removal of the chorion at 6 hpf, the embryos exposed to positively surface-charged SiO_2 NPs (25 nm) had a significant reduction in the survival rate at 24 and 48 hpf [16]. This lack of effects of SiO_2 NPs may be explained by a protective effect of the chorion, a semi-transparent and relatively impermeable membrane that acts as a barrier to the entry of some compounds, before hatching [6],[15]. The chorion has pores, important for oxygen/carbon dioxide, nutrients and excretion products transport to and from the embryo, respectively. Chemicals and small NPs may penetrate through these pores or by diffusion. However, as Fent et al. (2010), observed in their work, NPs with sizes similar to those used in this study may not be capable to penetrate this protecting structure [14]. Even if NPs were able to penetrate the chorion individually, there is the possibility that the particles were not totally dispersed and formed agglomerates incapable of penetrating the barrier. Furthermore, Pham et al. (2016), associated the observed early hatching tendency of organisms exposed to NPs to the incapability to penetrate the chorion. NPs may adsorb onto the external surface of the chorion, block its pores, hindering respiration and the excretion of metabolites. Because of this, an increased respiration rate facilitating the release of enzymes related to hatching and rupture of the chorion may have been promoted [15]. The importance of the chorion in the toxicity of the NPs to fish was highlighted by the results of the study of Liu et al. (2015), assessing the effects of 50 and 100 $mg.L^{-1}$ of 45 nm SiO_2 NPs on 20 hpf dechorionated zebrafish embryos, that revealed high embryonic mortality rates, up to 94% at concentrations at 100 $mg.L^{-1}$ [17].

The loss of equilibrium, observed in this study after exposure to the 80 nm NPs, may be a direct consequence of effects on the fin-body coordination. Ehrlich et al. (2019), stated that, in studies where this coordination between the fin and the body is abolished, individuals show an impaired sense of balance and even cerebellar lesions [18]. Nevertheless, the present data showed that in embryos with an intact chorion, SiO_2 NPs with 80 and 150 nm with concentrations ranging from 0.1 to 1000 $\mu g.L^{-1}$ had no significant developmental effects.

Concerning the effects of 80 nm SiO_2 NPs on the behaviour of the zebrafish larvae, the present study revealed higher impact of SiO_2 NPs in organisms exposed to 10 $\mu g.L^{-1}$ of SiO_2 NPs, with data suggesting fish anxiety. In this context, anxiety can be defined as an emotional state in which the animal displays a strong fear response to what would normally be neutral or mild stimuli [6]. For instance, the total distance moved by the zebrafish larvae in the dark decreased significantly in the groups exposed to the 10 $\mu g.L^{-1}$ concentration, with similar trends of response to 1 and 100 $\mu g.L^{-1}$. Furthermore, the total distance of medium movements as well as rapid movements made in the dark by the larvae exposed to 10 $\mu g.L^{-1}$ of 80 nm SiO_2 NPs also decreased. Similar results are found in the literature for SiO_2 NPs [19], which may suggest that the NPs can exert impact on the swimming distance and overall swimming capacity of the larvae. This impact may be associated with partial freezing behaviour, in this context a partial absence of movement compared to the controls, a typical behaviour of zebrafish larvae exposed to anxiogenics [6], [19]. Moreover, a significant reduction of larvae activity in the dark after exposure to 10 $\mu g.L^{-1}$ of 80 nm SiO_2 NPs, suggests a possible neurotic effect of the NPs. Usually, when subjected to short light and dark periods, as tested in the present study, zebrafish display a specific pattern of movement, being that the light-dark transition normally increases locomotor activity whereas the dark-light transition decreases it, with overall activity much higher in dark periods than in light periods [8], [20]. This, according to Kysil et al. (2017), is due to a natural tendency of wild zebrafish to avoid detection by other animals, a response to external stimuli, crucial for survival [21]. However, in this study, the individuals show alterations to this behaviour presenting a decrease in the difference of activity between dark and light periods. This effect may be attributed to a depressive effect of the central nervous system (CNS) of the fish, a profile similar to those displayed by anxiogenic substances or stressors that denunciate an anxiety-type behaviour [8], [21].

In individuals exposed to 10 µg.L^{-1} was also displayed altered movement angles (i.e. turns, straightforward movements and erratic change of directions). A significant increase in high amplitude angles and a decrease in low amplitude angle movements were observed. Usually, low amplitude angles refer to straightforward movements while medium and high amplitude angles are associated with turning behaviour. Zebrafish larvae display two main types of turns. The first type, a routine turn, happens without any apparent stimulus, resulting in a bend of 30° at the completion of first bend, with a slow angular velocity, and lack a counter-bend after the initial turn [6]. These turns are helpful in foraging and predator avoidance, being associated with the above-mentioned medium angle movements. The second type of turns is associated with high amplitude angles and escaping movements, usually characterized by high-velocity turns, making a very fast C-shaped bend with a large counter-bend in a direction opposite to the stimulus [6]. These sudden sharp changes in direction of movement and/or velocity suggest an anxiety-like behaviour being considered erratic movements. Thus, the above-mentioned increase in the high angle movements suggests that 80 nm NPs can alter the normal behaviour and induce a stress response characterized by erratic movements, an indicative of anxiety. These findings are supported by a significant increase in the distance moved in the outer zones of the wells that was found in individuals exposed to 0.1, 1 and 10 µg.L^{-1} SiO_2 NPs with a similar tendency happening in the groups exposed to the higher concentrations. These results suggesting that individuals exposed to those concentrations show a behaviour known as thigmotaxis, an anxiety-like behaviour well conserved in the vertebrates characterized by a preference for a more protected space, such as the rim of the well in opposition to the centre [6], [22].

Other studies have already reported neurologic affecting behaviour effects of these NPs [23], but the intriguing fact is that these effects were obtained mainly at low concentrations. Similar results were obtained by Pham et al. (2016), that found that 80 nm also had a significant increase on locomotor activity in dark conditions at the concentration of 12.5 mg.L^{-1}, although reporting significant differences in higher concentrations as well [15]. In our study, the lack of effects at higher concentrations may however be explained by a possible aggregation phenomenon, limiting the effects produced by higher concentrations. Aggregation of NPs is a common phenomenon, and even though it is affected by the environmental conditions, it is highly modulated by NPs characteristics [24]. It is possible then, that at higher concentrations, there is an increasing tendency for aggregation to occur, as more the probability of NPs collisions at a given temperature will increase by increasing the number of particles per volume (i.e., concentration). This hypothesis was confirmed by Singh et al. (2019), describing the aggregation kinetics as strongly dependent on the concentration of the NPs in the system and that at the initial time for a particular concentration, Columbic forces between NPs is what decides the aggregation rate [25]. The formation of aggregates may contribute to the overall decrease of toxicity of the NPs in aquatic environments [24], [26]. It is possible, then, that the results obtained at 10 µg.L^{-1} may be due to a lower aggregation NPs comparing to the higher concentrations.

The same may not apply for 150 nm SiO_2 NPs. The group exposed to the highest concentration (1000 µg.L^{-1}) was more affected than the groups exposed to lower ones. This might be because the aggregation phenomena, at a particular concentration, may slow down with the increase of the sizes of the NPs. Thus, a significant increase in the distance moved in slow/inactivity movements in the light by the larvae was found. Furthermore, a significant decrease in the swimming behaviour in the outer zones of the well was observed at the concentration of 10 µg.L^{-1} in the light periods. This suggests that at 10 µg.L^{-1} of 150 nm SiO_2 NPs the larvae revealed less thigmotaxis behaviour than the other groups. In fact, none of the results obtained for the 150 nm NPs suggest the existence of effects like those found for 80 nm NPs. This might be due to the size of the NPs, as, according to the literature, the size of the SiO_2 NPs has an important role in their toxicity to zebrafish, being that smaller NPs are able to induce more neurotoxic effects than larger ones [20].

Thus, this data indicates that 80 nm sized SiO_2 NPs are able to induce anxiety behaviour and that their toxicity still needs to be further studied in terms of behaviour endpoints. Also, studies on the protective role of the chorion against these NPs and on the aggregation tendency over time, according to NP size and concentration in solution, are needed to study its relation to developmental toxicity and to characterize the behaviour of SiO_2 NPs in aqueous media, relating it to the toxic effects at various concentrations, respectively. Also, biochemical effects should also be addressed along with the effects of surface charge and surface functionalization, key aspects not only for their successful application but also in their potential toxicity.

5. Conclusion

The aim of this work was to understand the effects at the behaviour level and understand the viability of SiO_2 NPs to be applied as adsorbents in environmental remediation. Using 80 and 150 nm sized NPs with concentrations ranging from 0.1 to 1000 µg.L^{-1}, interesting data was observed, especially regarding 80 nm sized NPs, as a non-significant tendency for early hatching, loss of equilibrium and an anxiety-like behaviour (similar to those induced by anxiogenics) were observed, especially in the group exposed to 10 µg.L^{-1} SiO_2 NPs. This might be due to the aggregation phenomena, as at higher concentrations an increasing tendency for aggregation to occur might exist. Results regarding 150 nm sized NPs show effects very different to those found for 80 nm NPs, which might be due to the size as smaller NPs are able to induce more neurotoxic effects than larger ones. Thus, this data indicates that 80 nm sized SiO_2 NPs are able to induce anxiety behaviour and that their toxicity still needs to be further studied in terms of behaviour endpoints. Also, studies on the protective role of the chorion against these NPs and on the aggregation tendency over time, according to NP size and concentration in solution, are needed to study its relation to developmental toxicity and to characterize the behaviour of SiO_2 NPs in aqueous media, relating it to the toxic effects at various concentrations, respectively. Also, biochemical effects should also be addressed along with the effects of surface charge and surface functionalization, key aspects not only for their successful application but also in their potential toxicity.

6. References

[1] S. Tang, “Toxicity of cadmium quantum dots compared to cadmium and zinc ions in zebrafish (Danio rerio) and water flea (Daphnia pulex),” Texas Tech University, 2013.

[2] R. M. S. L. de Andrade, “Efeitos da exposição de peixe zebra, Danio rerio, a um efluente têxtil,” *Diss. Mestr. em Ecol. Apl. Univ. do Porto*, 2004.

[3] A. Meyer, C. H. Biermann, and G. Orti, “The phylogenetic position of the zebrafish (Danio rerio), a model system in developmental biology: An invitation to the comparative method,” *Proc. R. Soc. B Biol. Sci.*, vol. 252, no. 1335, pp. 231–236, 1993.

[4] S. G. Vascotto, Y. Beckham, and G. M. Kelly, “The zebrafish’s swim to fame as an experimental model in biology,” *Biochem. Cell Biol.*, vol. 75, no. 5, pp. 479–485, 1997.

[5] A. V. Kalueff *et al.*, “Time to recognize zebrafish ‘affective’ behavior,” *Behaviour*, vol. 149, no. 10–12, pp. 1019–1036, 2012.

[6] F. Ahmad, L. P. J. J. Noldus, R. A. J. Tegelenbosch, and M. K. Richardson, “Zebrafish embryos and larvae in behavioural assays,” *Behaviour*, vol. 149, no. 10–12, pp. 1241–1281, 2012.

[7] J. M. Bailey, A. N. Oliveri, and E. D. Levin, “Pharmacological analyses of learning and memory in zebrafish (Danio rerio),” *Pharmacol. Biochem. Behav.*, vol. 139, pp. 103–111, 2015.

[8] R. M. Basnet, D. Zizioli, S. Taweedet, D. Finazzi, and M. Memo, “Zebrafish larvae as a behavioral model in neuropharmacology,” *Biomedicines*, vol. 7, no. 1, 2019.

[9] R. von Hellfeld, K. Brotzmann, L. Baumann, R. Strecker, and T. Braunbeck, “Adverse effects in the fish embryo acute toxicity (FET) test: a catalogue of unspecific morphological changes versus more specific effects in zebrafish (Danio rerio) embryos,” *Environ. Sci. Eur.*, vol. 32, no. 1, 2020.

[10] W. H. J. Norton, “Measuring Larval Zebra fish Behavior: Locomotion, Thigmotaxis, and Startle,” *Chemosphere*, vol. 66, pp. 312–324, 2012.

[11] R. J. B. Pinto, P. A. A. P. Marques, A. M. Barros-Timmons, T. Trindade, and C. P. Neto, “Novel SiO2/cellulose nanocomposites obtained by in situ synthesis and via polyelectrolytes assembly,” *Compos. Sci. Technol.*, vol. 68, no. 3–4, pp. 1088–1093, 2008.

[12] F. Busquet *et al.*, “OECD validation study to assess intra- and inter-laboratory reproducibility of the zebrafish embryo toxicity test for acute aquatic toxicity testing,” *Regul. Toxicol. Pharmacol.*, vol. 69, no. 3, pp. 496–511, 2014.

[13] A. R. Almeida *et al.*, “Long-term effects of oxytetracycline exposure in zebrafish: A multi-level perspective,” *Chemosphere*, vol. 222, pp. 333–344, 2019.

[14] K. Fent, C. J. Weisbrod, A. Wirth-Heller, and U. Pieles, “Assessment of uptake and toxicity of fluorescent silica nanoparticles in zebrafish (Danio rerio) early life stages,” *Aquat. Toxicol.*, vol. 100, no. 2, pp. 218–228, 2010.

[15] D. H. Pham *et al.*, “Use of Zebrafish Larvae as a Multi-Endpoint Platform to Characterize the Toxicity Profile of Silica Nanoparticles,” *Sci. Rep.*, vol. 6, no. May, pp. 1–13, 2016.

[16] S. Vranic *et al.*, “Toxicological evaluation of SiO 2 nanoparticles by zebrafish embryo toxicity test,” *Int. J. Mol. Sci.*, vol. 20, no. 4, 2019.

[17] T. P. Liu, S. H. Wu, Y. P. Chen, C. M. Chou, and C. T. Chen, “Biosafety evaluations of well-dispersed mesoporous silica nanoparticles: Towards in vivo-relevant conditions,” *Nanoscale*, vol. 7, no. 15, pp. 6471–6480, 2015.

[18] D. E. Ehrlich and D. Schoppik, “A primal role for balance in the development of coordinated locomotion,” *bioRxiv*, 2019.

[19] X. Li *et al.*, “SiO2 nanoparticles change colour preference and cause Parkinson’s-like behaviour in zebrafish,” *Sci. Rep.*, vol. 4, pp. 1–9, 2014.

[20] R. C. MacPhail, J. Brooks, D. L. Hunter, B. Padnos, T. D. Irons, and S. Padilla, “Locomotion in larval zebrafish: Influence of time of day, lighting and ethanol,” *Neurotoxicology*, vol. 30, no. 1, pp. 52–58, 2009.

[21] E. V. Kysil *et al.*, “Comparative Analyses of Zebrafish Anxiety-Like Behavior Using Conflict-Based Novelty Tests,” *Zebrafish*, vol. 14, no. 3, pp. 197–208, 2017.

[22] A. M. Valentim, “Behavioral Profiling of Zebrafish (Danio rerio) Larvae Following Teratogen Exposure,” *Teratog. Test. Methods Protoc. Methods Mol. Biol.*, vol. 1797, pp. 208–221, 2018.

[23] X. Li *et al.*, “Developmental neurotoxicity fingerprint of silica nanoparticles at environmentally relevant level on larval zebrafish using a neurobehavioral-phenomics-based biological warning method,” *Sci. Total Environ.*, vol. 752, p. 141878, 2021.

[24] M. Benavides, J. Fernández-Lodeiro, P. Coelho, C. Lodeiro, and M. S. Diniz, “Single and combined effects of aluminum (Al2O3) and zinc (ZnO) oxide nanoparticles in a freshwater fish, Carassius auratus,” *Environ. Sci. Pollut. Res.*, vol. 23, no. 24, pp. 24578–24591, 2016.

[25] K. Singh, A. Raghav, P. K. Jha, and S. Satapathi, “Effect of size and charge asymmetry on aggregation kinetics of oppositely charged nanoparticles,” *Sci. Rep.*, vol. 9, no. 1, pp. 1–8, 2019.

[26] V. K. Sharma, T. J. McDonald, M. Sohn, G. A. K. Anquandah, M. Pettine, and R. Zboril, “Assessment of toxicity of selenium and cadmium selenium quantum dots: A review,” *Chemosphere*, vol. 188, pp. 403–413, 2017.

1. Final Considerations and Future Directions

In chapter 1, a detailed review on environmental pollution and on the use of MNPs and SiO_2 NPs as adsorbents was performed. Environmental pollution has been a great concern in the past decades, being responsible for compromising entire ecosystems, for a great loss of biodiversity and paisagistic value of many locations as well as for many implications in human health. As part of these pollutants, one might find PTME, including elements such as cadmium, mercury and lead; and organic pollutants, that include, for example, POPs, pharmaceutical drugs, dyes and organic solvents. In fact, both groups have already reported to have devastating effects in the environment and human life in general.

A strategy to overcome this situation is by imposing and legislating limits regarding the PTME and organic pollutants concentrations in many environmental compartments. However, this approach has been insufficient to contain this threat and additional measures have been proposed. Many authors have proposed environmental remediation through adsorption to remove several types of pollutants in water and soil. In fact, remediation through adsorption using NPs has great potential because of its high efficiency and recovery, ease of handling, rapid speed and low cost. Its value is even more evident when compared to other conventional extraction methods, which often use large volumes of solution, produce chemical residues and that are inefficient in the presence of low concentrations of pollutants. Thus, materials such as activated carbons, carbon nanotubes, biochar, carbon fibres and graphene oxides, but also zeolites, silica, magnetic nanoparticles, clay-based nanocomposites, among others, have already been studied to be used as adsorbents. Notwithstanding, few have the potential of SiO_2 NPs and MNPs. Their good dispersion in solution, very high specific surface area, ability to be functionalized and become specific to the target pollutants, biocompatibility, in the case of the SiO_2 NPs, and magnetic properties, in the case of the MNPs, are some of the features that makes them so attractive to be used in this area. Furthermore, many studies have already been performed on the removal of pollutants with SiO_2 NPs and MNPs based adsorbents, being that they usually have an efficiency of more than 90%, can be reusable in several consecutive cycles without losing said efficiency, and have the ability to remove a wide variety of pollutants.

There are some limitations for the practical application of NPs as adsorbents, especially when applied in large-volume water samples. These limitations, are related to the possible residue of the NPs in the adsorption process, aggregation and dispersibility. Also, their small size might increase the risk that reacted pollutants will be transported to different locations rather than being safely controlled, existing also the concern regarding the leaching of internal components. That is why their toxicity needs to be further analysed.

Chapter 2 aimed to review the toxicity of SiO_2 NPs and MNPs both *in vitro* and *in vivo*, and showed that they cannot be used in environmental and biomedical applications without proper treatment. The formation of ROS leading to oxidative stress is thought to be the main mechanism of toxicity of these NPs. For example, *in vitro*, MNPs have shown effects such as inhibition of cell proliferation, reduction in cell viability, loss of membrane integrity, cell apoptosis, increased cell stiffness and the reduction in motility. *In vivo* effects include malformations, delay in hatching cycles, alteration in behaviour, DNA lesions and death in *D. rerio* embryos, inhibition in growth and reproduction in *C. silvestrii*, reduction in fertility and locomotion in *C. elegans*, and inhibition of growth and photosynthesis in *C. reinhardtii*. Regarding SiO_2 NPs, they are supposed to be biocompatible. However, *in vitro*, inhibition of cell differentiation, reduction in viability, loss of membrane integrity, induced cell apoptosis and compromised mitochondrial function, have been reported, while, *in vivo*, effects related to hepatic damage, disruption of axonal integrity, dysfunction of endothelial cells, inhibition of angiogenesis, developmental defects, delayed hatching and mortality were reported for *D. rerio*, while undeveloped and anomalous embryos, skeletal anomalies, delayed hatching and decrease of AChE expression was already found for *P. lividus*. However, very few studies were made regarding behaviour, which is a very powerful and sensitive tool to study sublethal effects in organisms.

The last chapter highlighted the need for a better understanding regarding the toxicity of these NPs. In Chapter 3 the effects of SiO_2 NPs regarding behaviour alterations of individuals was studied. This is a promising and very sensitive approach, making possible to assess the neurotoxicity of these NPs and to reveal the effects at the whole organism level. Thus, this chapter evaluated the toxicity according to the size (80 and 150 nm) and concentration (0, 0.1, 1, 10, 100, 1000 $\mu g.L^{-1}$) of SiO_2 NPs in *D. rerio* embryos with a focus in embryonic development and behavioural parameters. Interesting data was observed, especially regarding 80 nm sized NPs, as a non-significant tendency for early hatching, loss of equilibrium and an anxiety-like behaviour (similar to those induced by anxiogenics) were observed, especially in the group exposed to 10 $\mu g.L^{-1}$ SiO_2 NPs. The effects were higher at low concentrations, suggesting that there is an aggregation phenomenon occurring at higher concentrations. Also, the results where significantly more severe for 80 nm NPs than for the 150 nm ones, which might be due to the size, as smaller NPs are reported to be able to induce more severe effects than larger ones. However, even though it is clear that there is a risk regarding exposure to this NPs, their toxicity still needs to be further studied. Combining behaviour and biochemical endpoints while also studying the effects of functionalization and surface charge, might prove valuable to this end. In addition, the protective role of the chorion against these NPs and the aggregation tendency over time, according to NP size and concentration in solution, are other aspects that need to be further addressed to better comprehend the dynamics and behaviour of SiO_2 NPs in aqueous media, and its relation to their toxicity.

SiO_2 based adsorbents have proven to be very valuable and to possess great potential in environmental remediation. However, a more complete toxicological profile is needed. Future studies should also address the toxicity in terms of behaviour and development of MNPs as, along with the SiO_2 ones, they are the ones with the greater potential in these kinds of applications.